Exploring the Therapeutic Potential and Molecular Mechanisms of Targeting mTOR Kinases in Cancer

Thesis submitted in accordance with the requirements of the University of Liverpool for the degree of Doctor in Philosophy

By Ahoud Alotibi

June 2021

DECLARATION

This thesis is the result of my own work. The material contained within this thesis has not been presented, nor is currently being presented, either wholly or in part for any other degree or qualification.

Ahoud Alotibi

This research was carried out in the Institute of Systems, Molecular and Integrative Biology, University of Liverpool, UK.

Thesis contents

Acknowledgements

I would like to express my sincere gratitude to my supervisor, Dr. Varadarajan for his assistance, insightful comments and suggestions as well as invaluable advice during my PhD. I would also like to thank Varadarajan's lab members for their kind help and support in the lab and for an unforgettable social setting. My gratitude extends to Prince Sattam University- Saudi Arabia, for sponsoring my PhD and for giving me the opportunity to complete my doctorate degree. A special thank you goes to my family for their continuous encouragement and support at every step of my study.

List of Publications

1. **Alotibi A**., Carter RJ., Basabrain A. and Varadarajan S. Exploring the therapeutic potential and molecular mechanisms of targeting mTOR kinases in head and neck cancer. ***Manuscript in preparation***.

2. Al-Zebeeby A., Vogler M., Milani M., Richards C., **Alotibi A**., Greaves G., Dyer MJS., Cohen GM. and Varadarajan S. Targeting intermediary metabolism enhances the efficacy of BH3 mimetic therapy in haematological malignancies. **Haematologica**, doi:10.3324/haematol.2018.204701.

3. Carter RJ., Milani M., Butterworth M., **Alotibi A.,** Harper N., Yedida G., Greaves G., Al-Zebeeby A., Jorgensen AL., Schache AG., Risk JM., Shaw RJ., Jones TM., Sacco JJ., Hurlstone A., Cohen GM. and Varadarajan S. Exploring the potential of BH3 mimetic therapy in squamous cell carcinoma of the head and neck. **Cell Death and Disease**, 10(12):912. doi: 10.1038/s41419-019-2150-8.

Abstract

Until a few decades ago, mechanisms that control cellular growth through the availability of nutrients remained unknown. A major breakthrough came with the discovery of the mammalian target of rapamycin, also known as mTOR. This highly conserved serine/threonine protein kinase was found to regulate cell proliferation, survival and autophagy by coordinating the availability of environmental resources, such as nutrients and growth factors. Dysregulation in mTOR signalling cascade has been implicated in many diseases, including cancers. Due to the prevalence of mTOR activation in human cancers, there has been an on-going interest in exploring the therapeutic potential of drugs targeting mTOR kinases, in the context of cancer. However, targeting mTOR kinases with small molecule inhibitors in cancer has largely been unsuccessful, with most clinical trials resorting to the use of mTOR inhibitors as a combination treatment with other conventional chemotherapeutic agents. This thesis is primarily focused on mTOR signaling pathway in head and neck squamous cell carcinoma (HNSCC). In this cancer, mTOR is active and commonly found in two distinct complexes - mTORC1 and mTORC2. Therefore, this study is aimed at assessing whether modulating the mTOR signaling pathway by using Torin-1, a dual inhibitor of mTORC1 and mTORC2, could lead to cellular proliferative defects and/or increased cancer cell death, thus enhancing therapy in HNSCC.

Using cell lines derived from specific anatomical subsites of the head and neck, such as oral cavity, oropharynx, larynx, and hypopharynx, the ability of Torin-1 to affect clonogenicity, as a measure of cell proliferation was assessed. Inhibition of mTOR decreased colony formation in a concentration dependent manner, both in 2D and 3D spheroid models of the HNSCC cell lines. Torin-1-mediated defects in clonogenicity did not accompany enhanced cell death and occurred independent of autophagy. To assess whether Torin-1, when used in combination with other chemotherapeutic agents, could enhance the antiproliferative effects, studies were performed in conjunction with standard therapies (Cisplatin and Irradiation), as well as novel therapies (PARP inhibitor-Olaparib, BCL-X_L inhibitor- A-1331852, MCL-1 inhibitor- S63845, Wee1 kinase inhibitor – AZD1755, protein kinase A inhibitor – H-89 and PP2A activators –FTY720 and DT-061). The findings from these studies revealed that co-administration of Torin-1 with these agents exhibited little or no synergy, with some combinations revealing mild additive effects. This is in stark contrast to the studies that have reported the efficacy of these combinations in other cancers.

Since efforts to identify a promising drug that could be combined with Torin-1 to enhance HNSCC therapy were largely discouraging, the final part of this thesis was dedicated to understanding the cellular effects of Torin-1, as an attempt to assess whether the effect of Torin-1 on mitochondrial dynamics and apoptosis could be exploited in a therapeutic context. Torin-1 caused mitochondrial hyperfusion, which accompanied changes in the phosphorylation status of Drp-1, a mitochondrial fission GTPase, even though no changes with Drp-1 translocation were observed. However, Torin-1 exhibited contrasting responses to two distinct apoptotic stimuli, BH3 mimetics (inhibitors of the anti-apoptotic BCL-2 family of proteins) and BAY-2402234 (inhibitor of the enzyme, Dihydroorotate Dehydrogenase), in the context of mitochondrial fragmentation as well as apoptosis induction, thus revealing the complex interplay between mitochondrial dynamics and apoptosis. How this can be exploited in a therapeutic context remains to be charaterised.

Abbreviations

α-KG	α-Ketoglutarate
ALL	Acute lymphoblastic leukaemia
AML	Acute myeloblastic leukaemia
ANOVA	Analysis of variance
APAF-1	Apoptotic protease activating factor-1
BAD	Bcl-2-associated death promoter
BAK	Bcl-2 homologous antagonist killer
BAX	Bcl-2-associated X protein
BCL-2	B-cell lymphoma 2
BCL-2A1	Bcl-2-related protein A1
BCL-W	Bcl-2-like protein 2
BCL-X_L	B-cell lymphoma-extra large
BFL-1	Bcl-2-related protein A1
BH	Bcl-2 homology domain
BID	BH3 interacting-domain death agonist
BIK	Bcl-2-interacting killer
BIM	Bcl-2-like protein 11
BMF	Bcl-2-modifying factor
BSA	Bovine Serum Albumin
CCCP	Carbonyl cyanide m-chlorophenyl hydrazone
CDK	Cyclin-dependent kinase
DMEM	Dulbecco's Modified Eagle's Medium
DNA	Deoxyribonucleic acid
DRP-1	Dynamin-1-like protein
ECL	Electrochemiluminescence
EGFR	Epidermal growth factor receptor
EMEM	Eagle's minimal essential medium
FACS	Fluorescence-activated cell sorting
GAPDH	Glyceraldehyde 3-phosphate dehydrogenase
GLS	Glutaminase
H	Hour
HNSCC	Head and neck squamous cell carcinoma
HPV	Human papillomavirus
HRK	Harakiri
ICC	Immunocytochemistry
IHC	Immunohistochemistry
IMM	Inner mitochondrial membrane
MCL-1	Myeloid cell leukaemia 1
MFF	Mitochondrial fission factor
MFN1	Mitofusin 1

MFN2	Mitofusin 2
MiD49	Mitochondrial elongation factor 2
MiD51	Mitochondrial elongation factor 1
NF-κB	Nuclear factor kappa-light-chain-enhancer of activated B cells
NOXA	Phorbol-12-myristate-13-acetate-induced protein 1
OMM	Outer mitochondrial membrane
OPA-1	OPA1 mitochondrial dynamin like GTPase
PARP	Poly (ADP-ribose) polymerase
PI	Propidium iodide
PS	Phosphatidylserine
PUMA	BCL-2 binding component 3
WB	Western blots
Z-VAD.FMK	N-Benzyloxycarbonyl-Val-Ala-Asp(O-Me) fluoromethyl ketone

Chapter 1

General Introduction

1.1 mTOR kinases - Complexes 1 and 2

mTORC (mechanistic target of rapamycin Complex) previously known as (mammalian target of rapamycin) belongs to the phosphoinositide 3-kinase (PI3K)-related kinase family. An antifungal compound called rapamycin was first discovered from bacterium *Streptomyces hygroscopicus* found on the island of Rapa Nui [1]. Subsequent analysis of rapamycin exhibited immunosuppressive activity and therefore it was used to prevent organ rejection during organ transplants. Beside its immunosuppressive properties, rapamycin was found to exhibit antitumour activity in a screen [2] and inhibited the growth of several tumour cell lines, which led to the approval of rapamycin as an anticancer drug. This has been independently verified by other research groups [3]. The mechanism by which rapamycin exerts its inhibitory effect is through binding to an intracellular protein called FK506/rapamycin-Binding Protein (FKBP-12). This drug-protein complex further interacts with a target protein, later identified as mTOR, and suppresses its function [4]. Simultaneously, mTOR was discovered to be a direct target of rapamycin by three different research groups (of Prof. David Sabatini, Prof. Stuart Schreiber and Prof. Robert Abraham) in 1994 [4, 5, 6]. While Prof. Sabatini called it RAFT1 (rapamycin and FKBP-12 Target1) [4], Prof. Schreiber identified it as mTOR [5], and Prof. Abraham called it FKBP–rapamycin associated protein (FRAP) [6] . Nonetheless, all three research groups arrived at the same conclusion: rapamycin binds to and inhibits mTOR via its interaction with FKBP-12.

mTOR is a highly conserved serine/threonine kinase complex with a molecular weight of 289 kDa and considered as a master regulator of a diverse array of physiological processes that can be initiated by different metabolic signals [7].

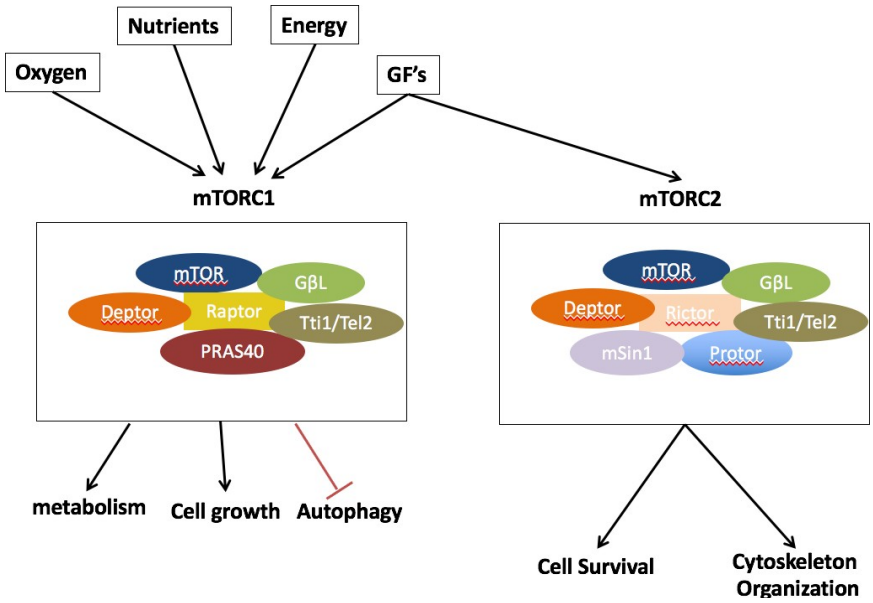

Figure 1.1: Components of mTORC1 and mTORC2. mTOR can form two distinct complexes - mTORC1 containing Raptor and mTORC2 containing Rictor. Both complexes contain Deptor, as inhibitory subunit and GβL to stabilise the domains. mTORC2 includes two regulatory subunits mSin1 and Protor. These complexes integrate a wide range of signals to promote cellular functions, such as cellular metabolism, growth and autophagy.

mTOR exists in two functionally distinct complexes, mTOR complex 1 (mTORC1) and mTOR complex 2 (mTORC2). mTORC1 consists of 6 subunits, whereas mTORC2 consists of 7 subunits (Figure 1.1). Both complexes share some of these subunits: mTOR, mLST8 (mammalian lethal with sec13 protein8, also known as GβL), Tti1/Tel2 complex and Deptor (dep domain containing mTOR interacting protein) [8, 9]. In addition, mTORC1 contains Raptor (regulatory associated protein of mTOR) and PRAS40 (proline rich Akt substrate 40 kDa) [10, 11], whereas mTORC2 contains Rictor (rapamycin insensitive companion of mTOR), Protor1/2 (protein observed with Rictor-1) and mSin1(mammalian stress-activated map kinase-interacting protein 1) [12, 13, 14]. A description of each subunit is summarised in Table 1.1.

mTOR is the key regulator of cellular metabolic homeostasis and it can sense changes from a variety of signals, such as nutrients, growth factors and oxygen levels. mTORC1 and mTORC2 act in parallel and have different upstream signals and downstream effectors. There are many downstream consequences of mTORC1 activity, and this can be grouped into anabolic (like lipid and protein biosynthesis) or catabolic processes, for example, autophagy [7]. mTORC2 senses the availability of growth factors to promote cell survival through lipid and glucose metabolism [15].

mTORC1		mTORC2	
mTOR	The catalytic subunit of the complex	**mTOR**	The catalytic subunit of the complex
Raptor	Regulates substrate binding to active site of mTOR	**Rictor**	Regulates substrate binding to active site of mTOR
PRAS40	Inhibitor of Raptor	**mSin1**	Regulates substrate binding of mTORC2
		Protor1/2	Regulates downstream signalling of mTORC2
Deptor	Endogenous inhibitor of mTOR	**Deptor**	Endogenous inhibitor of mTOR
mLST8	Stabilises kinase domain	**mLST8**	Stabilises kinase domain
Tti1/Tel2	Stabilises mTORC1	**Tti1/Tel2**	Stabilises mTORC2

Table 1.1: Components of mTORC1 and mTORC2 and their functions.

1.2 mTOR structure/domains

mTOR protein is composed of 2549 amino acids (NG_033239.1) with different functional domains. In the N-terminus, mTOR contains multiple HEAT (Huntingtin, Elongation factor 3, a subunit of protein phosphatase-2A and TOR1) repeats that ensure protein-protein interactions [16], followed by a FAT (FKBP12-rapamycin-associatedprotein, ataxia-telangiectasia and transactivation/transformation domain-associated protein) domain, which is hypothesised to promote mTOR kinase activity. This is followed by FRB (FKBP12/rapamycin-binding domain), which binds to FKBP12/ rapamycin complex [17]. The kinase domain of mTOR shares a sequence similar to that of the catalytic domain of PI3K and contains the phosphorylation site that is responsible for the kinase activity of mTOR complex. Adjacent to the kinase domain, is a negative regulatory domain (NRD), followed by a FATC domain, which is another FAT domain at its C-terminus [9].

Raptor and Rictor bind to the HEAT repeats; thus, dictating whether the complex formed is that of mTORC1 or mTORC2. As previously mentioned, PRAS40 binds and inhibits Raptor, whereas Protor and mSin1 bind mTORC2 [13, 14, 18]. Deptor binds and inhibits the FAT domains of both mTORC1 and mTORC2 [19]. rapamycin/FKBP-12 complex binds to the FRB domain of mTORC1 and not mTORC2 [20]. However, chronic exposure of rapamycin can inhibit the assembly of mTORC2 [21]. The expression level of FKBP-12 can determine the sensitivity of mTORC2 towards rapamycin [22]. Although mLST8 binds the kinase domain of both mTORC1 and mTORC2, its function in mTORC1 is not known. A knockdown of mLST8 affected both the function and stability of mTORC2 but not mTORC1[23]. Each interaction has been illustrated in Figure 1.2.

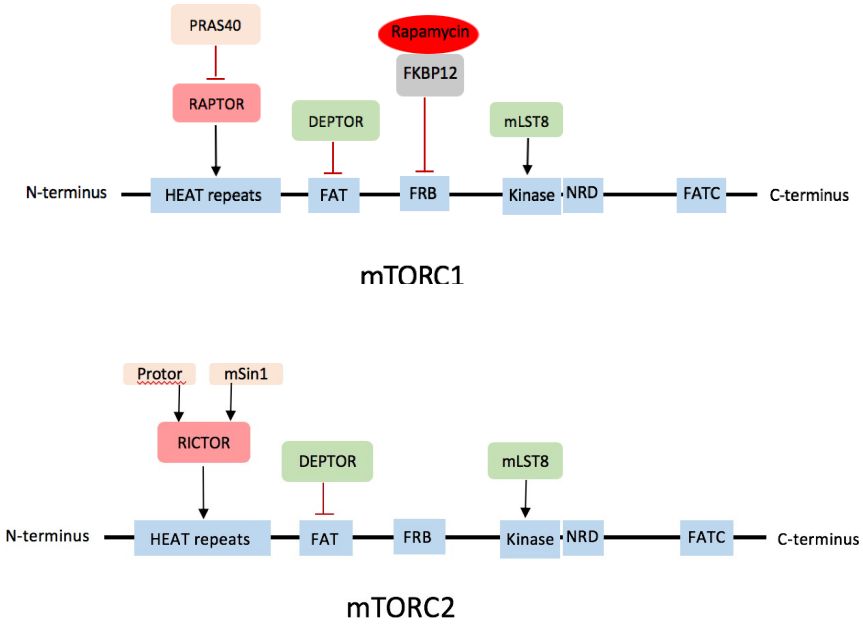

Figure 1.2: mTORC1 and mTORC2 structure. A schematic diagram shows the different functional domains of mTOR complex1 and 2. Both mTORC1 and mTORC2 incorporate the following: HEAT repeats, FAT, FRB, kinase and FATC domains. HEAT repeats bind to either Raptor or Rictor and thus determine whether the complex formed is mTORC1 or mTORC2. FRB region of mTORC1 is where the FKBP12/rapamycin drug complex binds to and exert its inhibitory action. However, this binding does not occur in mTORC2.

1.3 mTOR signalling pathways

mTORC1 and mTORC2 act in parallel with different upstream signals and downstream effectors. mTORC2 is part of a traditional growth factor pathway, as it is downstream of insulin and its main downstream effector is Akt kinase which involves in lipid and glucose homeostasis [24]. Thus, mTORC2 is considered as part of the insulin signalling pathway. mTORC1 on the other hand, positively regulates many processes, including lipid and nucleotide synthesis, ribosome biogenesis, whilst supressing catabolic pathways, such as autophagy [7]. mTORC1 in response to environmental factors strikes a balance between anabolic and catabolic processes within the cell.

1.3.1 Upstream of mTORC1

mTORC1 is regulated by a variety of signals, such as nutrients, growth factors, energy levels and stress [25]. For instance, exposure to insulin growth factor (IGF-1) results in the activation of PI3K which leads to the phosphorylation and activation of Akt [26] (Figure 1.3). Akt, in turn, inhibits TSC (Tuberous Sclerosis Complex) complex, which is a negative regulator of mTORC1 [27]. TSC complex has two components- TSC1 and TSC2. When TSC1/2 is inactivated by Akt, RHEB (Ras homolog enriched in brain) converts from a GDP-bound (inactive) form to GTP-bound (active) form, which results in the translocation of mTOR from the cytosol onto the lysosomal membrane [28] (Figure 1.3). Lysosomal translocation of mTOR activates the protein to perform several downstream functions.

During stress conditions, such as low energy levels, hypoxia, DNA damage and nutrient deprivation, AMP-activated protein kinase (AMPK), which is a stress

responsive protein becomes activated. Thus, activated AMPK inhibits mTOR activity indirectly by phosphorylating and activating TSC1/2 complex or directly by phosphorylating and inhibiting Raptor within mTORC1 complex [29]. Hypoxia can also regulate mTORC1 independently of AMPK via an upregulation of REDD1 (regulated in development and DNA damage responses 1) that also activates TSC1/2 complex to suppress mTORC1 activity [30].

1.3.2 Upstream mTORC2

In comparison to mTORC1, less is known about the upstream signals of mTORC2. Upon the binding of insulin to its receptor, PI3K gets phosphorylated, which can activate mTORC2 (Figure 1.3). This can be antagonised by a signalling kinase called S6K1, which provides a negative feedback loop towards insulin receptor1 (IRS1) (Figure 1.3) and facilitate the degradation of this receptor and thereby negatively regulating mTORC2 [31]. In addition, stress - activated AMPK can directly phosphorylate mTORC2 and promote its activity [32] (Figure 1.3).

1.3.3 Downstream processes of mTORC1

Protein synthesis is one of the cellular processes that is regulated by mTORC1. It is regulated through the phosphorylation of two key effectors, p70 ribosomal S6 kinase 1 (S6K1) and the Eukaryotic Initiation Factor 4E (eIF4E)- Binding Protein 1 (4E-BP1) [33]. mTORC1 directly phosphorylates S6K1 on Thr389 residue, which stimulates its activity and promotes mRNA translation. Similarly, mTOR phosphorylate 4E-BP1 on Thr 37/46 [34]. However, unlike the activating phosphorylation of S6K1, mTORC1 - mediated phosphorylation of 4E-BP1 results in

the inactivation of 4E-BP1. 4E-BP1 inhibits mRNA translation by preventing the assembly of eIF4E (Eukaryotic Translation Initiation Factor 4E) complex. Therefore, mTORC1 - mediated inactivation of 4E-BP1 results in protein translation. Thus mTORC1 promotes protein synthesis by phosphorylating both S6K1 and 4EBP-1 [35] (Figure 1.4).

Besides protein synthesis, mTORC1 has a role in lipid biogenesis, which is required for cellular growth and proliferation. mTORC1 can regulate lipogenesis through the Sterol Responsive Element Binding Protein (SREBP). mTORC1 can sense low levels of sterols and as a result, directly activate SREBP or independently through the phosphorylation of S6K1 [36] or Lipin1[37]. Similarly, in response to starvation or low energy levels, mTORC1 can activate a cellular mechanism called autophagy. Autophagy is a self-degrative mechanism, initiated during stress to promote survival. Several members of Atg (genes critical for the induction and execution of autophagy) gene family have been characterised so far. Of these, Atg13 is a primary player that is phosphorylated by mTORC1[38]. mTORC1 inhibition prevents the phosphorylation of Atg13, which allows it to bind Ulk1/2 to form the autophagy initiation complex [39] (Figure 1.5). This expands further with the help of Atg5, Atg7, Atg10, Atg12 and Atg16 to form an autophagosome, which engulfs the intracellular cargo (Figure 1.5). The selection of intracellular cargo for degradation is achieved by Atg8 or LC3B-I, which undergoes lipidation to form LC3B-II. Taken together, mTORC1 regulates a wide variety of functions, such as protein and lipid synthesis as well as autophagy induction.

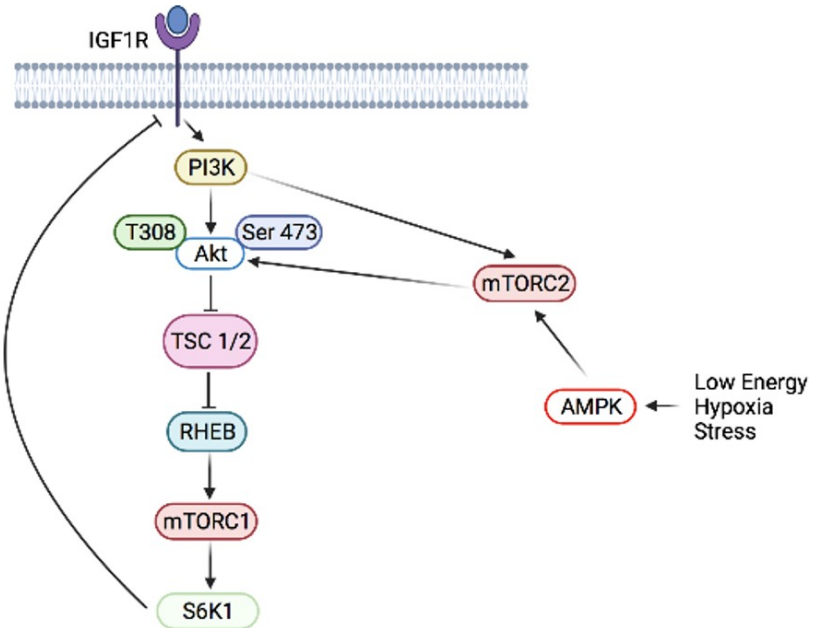

Figure 1.3: Schematic diagram of the upstream signalling events of mTORC1 and mTORC2. Upon activation by growth signals, PI3K phosphorylates Akt at T308 and promotes its activity, which in turn inhibits TSC1/2 complex and eventually activates mTORC1, via RHEB. During stress, mTORC2 is activated through AMPK.

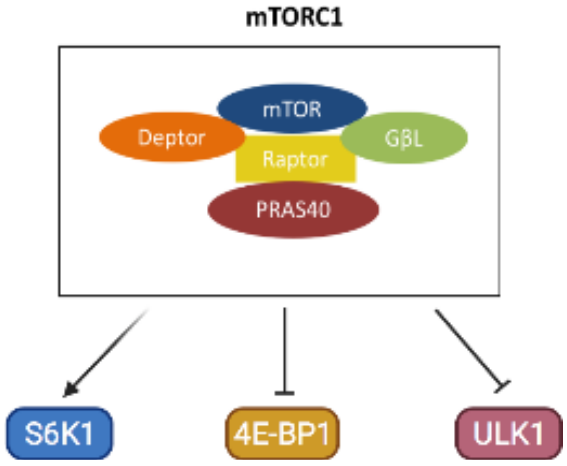

Figure 1.4: Schematic diagram of mTORC1 downstream effectors. mTORC1 regulates protein synthesis through phosphorylation of S6K (activation) and 4E-BP1 (inhibition), as well as inhibition of autophagy to promote cellular growth and metabolism.

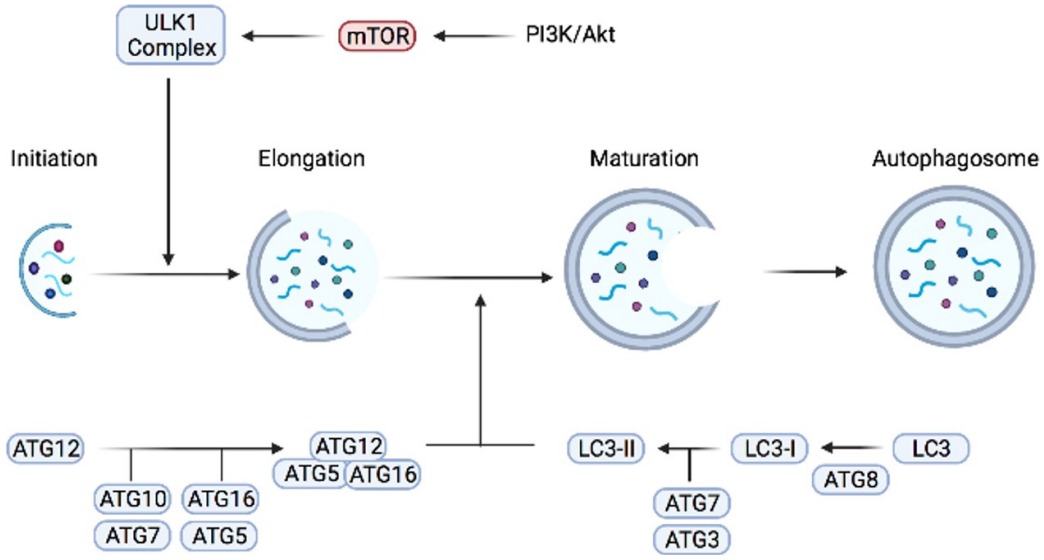

Figure 1.5: Schematic diagram of autophagy induction downstream of mTOR inhibition. Upon mTOR inhibition, autophagy is initiated by the formation of autophagy initiation complex, followed by formation of autophagosomes through the assembly of multiple Atg proteins. Autophagosomes fuse with the lysosomes as a final step to degrade and release its contents into the cytosol.

1.3.4 Downstream processes of mTORC2

The physiological functions of mTORC1 include regulation of cellular growth and metabolism. mTORC2, on the other hand, is responsible for cellular proliferation, survival and cytoskeleton organisation [7]. These processes occur through the phosphorylation of its downstream effectors, including the protein kinase C (PKC) family of proteins. This family consists of at least 10 different members, including PKCα, PKCβi, PKCβii, PKCγ, PKCδ, PKCε, PKCη and PKCθ [40]. Of these, PKCα, a regulator of the actin cytoskeleton, was the first mTORC2 substrate discovered [41]. Similarly, mTORC2 phosphorylates other members, including PKCε and PKCγ, which in turn influence cytoskeletal remodelling [42, 43].

The phosphorylation and activation of Akt is one of the important roles of mTORC2 complex. Akt becomes phosphorylated by mTORC2 in insulin-PI3K signalling pathway, and upon activation, it promotes the phosphorylation of its substrates (forkhead transcription factors, Foxo), which are responsible for transcription of various enzymes involved in glycolysis and pentose phosphate pathway (PPP) [44]. Moreover, as previously mentioned, Akt also inhibits TSC1/2 complex [45] and as a result, relieve its inhibition of mTORC1 . Thus, Akt serves as an important crosstalk signalling kinase between mTORC1 and mTORC2.

Finally, mTORC2 activation is also linked to the phosphorylation and activation of a Serum and glucocorticoid-induced protein kinase 1(SGK1) at Ser422 [46], which in turn results in regulating ion transport and cell survival. Although mTORC2 promotes cell survival and cytoskeleton rearrangement, its role in cancer progression has yet to be characterised.

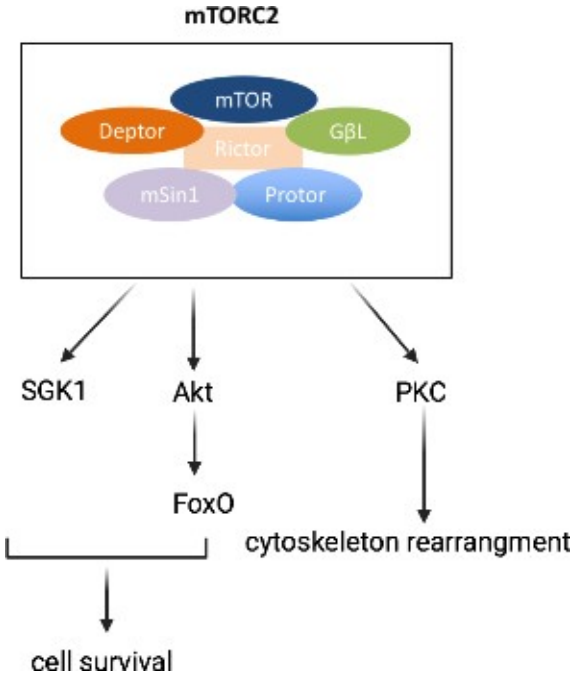

Figure 1.6: Schematic diagram of mTORC2 downstream effectors. mTORC2 regulates cytoskeleton remodelling through the phosphorylation of PKC proteins. mTORC2 promotes cellular proliferation and survival through the activation of its downstream effectors, SGK1 and Akt, respectively.

1.4 mTOR inhibitors

As previously mentioned, rapamycin, one of the best known mTORC1 inhibitors, exhibited not only antifungal characteristics but also immunosuppressive properties and anti-tumour effects [47]. rapamycin binds to mTORC1 but not mTORC2, which makes mTORC2 unresponsive to its effect. Moreover, rapamycin does not directly bind and inhibit the kinase domain of mTOR protein and exhibits a limited effect on its substrate/target phosphorylation. For instance, rapamycin can fully phosphorylate S6K-1, and exhibit little/no effects in phosphorylating 4EBP-1 [48]. rapamycin is one of the first-generation allosteric inhibitors of mTOR. Other drugs in this category are temsirolimus(CCI-779), everolimus (RAD-001) and deforolimus, all of which share the same mechanism of action with rapamycin and therefore, are referred to as rapamycin analogs or rapalogs [49]. Rapalogs overcome the poor bioavailability of rapamycin (due to its low water solubility) and possess better pharmacokinetics and low immunosuppressive properties [50]. Temsirolimus, in particular, has a higher solubility and hence can be administered orally, as well as intravenously [51]. It was the first rapalog to be approved in 2007 as an anti-cancer drug, as it has demonstrated anti-tumour activity in phase II clinical trials of patients with advanced renal cell carcinoma, mantle cell lymphoma and metastatic breast cancer [52, 53, 54]. Another orally available rapamycin analog, everolimus, has demonstrated antitumour effect in patients with advanced pancreatic neuroendocrine tumours, breast cancer and renal cell carcinoma [55]. Similarly, deforolimus, which also has better pharmacological properties, including high solubility and chemical stability in comparison to rapamycin, has been used in the treatment of a variety of solid tumours [56].

Despite exhibiting promise in clinical trials, these inhibitors were accompanied with a wide range of adverse effects, ranging from fatigue, depression to Thrombocytopenia [57] and Mucositis [58]. In addition, these inhibitors target mTORC1 and not mTORC2, which could potentially retain its ability to activate Akt and promote survival. Moreover, mTORC1 inhibition using these first-generation inhibitors can induce a stress response, such as induction of autophagy that can promote cell survival under stress [59].

To overcome these limitations, two strategies have been explored: (1) Combination therapies of rapalogs with other chemotherapeutic agents, such as sorafenib in treatment of lymphoma [60], and paclitaxel + carboplatin for advanced ovarian cancer [61]; and (2) development of specific inhibitors (dual inhibitors) that target the kinase domain of mTOR, thus enabling the simultaneous inhibition of both mTOR and PI3K [62]. This is due to the similarity in the kinase domains of these proteins. Among these dual inhibitors, NVPBEZ235 is in clinical trials for metastatic breast cancer and advanced solid cancers, either as single agent or in combination with other chemotherapeutic agents [63, 64]. Although simultaneously targeting PI3K and mTOR overcomes the limitations of rapalogs in blocking PI3K/AKT signalling, the possible toxicity of these inhibitors is a major concern, especially given the diverse cellular functions of PI3K. Therefore, inhibitors that are more selective for mTORC1 and mTORC2 have been developed, which are thought to be better tolerated than mTOR/PI3K dual inhibitors [65]. Such inhibitors that selectively target mTORC1 and mTORC2 include PP242 [66], AZD2014 [67], INK128 [68] and Torin-1[69].

Torin-1, known as 1-[4-[4-(1-oxopropyl)-1-piperazinyl]-3-(trifluoro-methyl) phenyl]-9-(3-quinolinyl) benzo[h]-1,6-naphthyridin-2(1H)-one, is a selective and potent mTOR inhibitor that was originally identified by the research group of Prof. Nathanael Gray, in a compound library screen containing kinase inhibitors as well as heterocycles that can bind the ATP-binding site of mTORC1 or mTORC2 kinases [70, 71]. In addition to enhanced binding affinity (at low nM concentrations), Torin-1 also exhibited a higher selectivity for mTORC1 and mTORC2 relative to PI3K. However, Torin-1 was found to have a short half-life *in vivo* and relatively low oral bioavailability, albeit to a greater degree in comparison to rapamycin [71, 72]. Torin-1 has been shown to impair growth and proliferation in a wide variety of cancer cells, as well as xenografts models [72, 73]. Moreover, Torin-1 inhibits the downstream effectors of mTORC1, such as S6K and 4E-BP1, as well as the downstream effector of mTORC2, Akt (phosphorylation at Ser473) [70, 71]. An improved version named Torin-2, retains its ability to inhibit both mTORC1 and mTORC2 in an ATP-competitive manner at low nM concentrations [74]. In the context of mTOR inhibition, Torin-1 has been reported to sustain the inhibition of S6K1 for 16 h, even after the drug has been removed. In marked contrast, the cellular inhibitory effects of Torin-2 last only for 4 h [71]. This could be attributed to the strong conformational changes to the kinases that are mediated by Torin-1 but not Torin-2 [74]. Despite numerous studies demonstrating the efficacy of these inhibitors *in vitro*, no clinical trials have been reported with these drugs to date.

Some of the mTOR inhibitors and their clinical trial studies have been listed below in Table 1.2.

Compound	Target	I	II	III	Patients
rapamycin (sirolimus)	mTORC1	X	X	X	Solid tumours
RAD001 (everolimus)	mTORC1	X	X	X	Renal cell carcinoma, pancreatic, breast, gastric cancers, lymphoma
CCI-779 (temsirolimus)	mTORC1	X	X	X	Renal cell carcinoma, pancreatic, breast, gastric cancers, lymphoma
NVPBEZ235	Dual PI3K/mTOR	X	X		Advanced solid tumours, endometrial cancer, breast cancer
GSK2126458	Dual PI3K/mTOR	X	X		Advanced solid tumours, lymphoma
PF4691502	Dual PI3K/mTOR	X			Solid tumours
PF05212384	Dual PI3K/mTOR	X			Solid tumours
OSI027	mTORC1/mTORC2	X			Solid tumour, lymphoma
Torin-1	mTORC1/mTORC2				Preclinical breast, colon and prostate cancers
AZD2014	mTORC1/mTORC2	X			Solid tumours
AZD8055	mTORC1/mTORC2	X	X		Liver cancer, solid tumours
INK128	mTORC1/mTORC2	X			Solid tumour, multiple myeloma
PP242	mTORC1/mTORC2	X			Solid tumours
WAY-600	mTORC1/mTORC2				Preclinical breast, colon, prostate cancers and renal cell carcinoma

Table 1.2: Examples of mTOR inhibitors currently used in pre-clinical studies or clinical trials.

1.5 Apoptosis

The term Apoptosis was first used by Kerr, Wyllie, and Currie in 1972 and it is defined as a form of highly organised cell death, which is characterized by morphological and biochemical changes [75]. Apoptosis is important for cell development and to maintain cell population within tissues. It can also act as a defence mechanism in immune reactions [76]. It is a conserved programmed cell death pathway that is enabled to maintain normal cellular homeostasis. Cells undergo apoptosis to regulate the clearance of damaged or dysfunctional cells. Apoptosis is characterised by morphological changes, such as cell shrinkage, chromatin condensation, blebbing of cell membrane and formation of apoptotic bodies [77]. Apoptotic bodies are tightly packed with cellular and nuclear fragments, which are eventually engulfed by the macrophages [76].

There are two main pathways of apoptosis, intrinsic that act on mitochondrial level and extrinsic that act on cell surface. Both pathways undergo three main steps: firstly, initiation by damaged cells or stress stimuli, followed by signal transduction for apoptosis and finally cell dismantling and death. Both pathways share similarity in the final step, which involves caspase activation. On the other hand, they differ in their location and response to stimuli. Extrinsic pathway, as specified above, occurs at the level of the cell membrane and respond to external signals. It involves the recruitment of death ligands to death receptors, which subsequently recruits DISC (Death Inducing Signalling Complex) to activate caspase 3/7. In contrast, the intrinsic pathway occurs at the mitochondrial level and perturbs mitochondria integrity (Figure 1.7).

Mitochondria are the powerhouse of cells that meets the cellular demands for energy through oxidative phosphorylation. Mitochondria consists of 4 main compartments: an outer mitochondrial membrane (OMM) that is permeable to certain ions and small molecules, inner mitochondrial membrane (IMM) in the form of folded cristae that contains the respiratory proteins, and a space between OMM and IMM called the inner mitochondrial membrane space (IMS). Each of these compartments play an important role in apoptosis. Cytochrome c is one of the important proteins within the mitochondria and has a vital role in apoptosis. it is located in IMM impounded within the cristae by a protein called OPA1 (Optic Atophy1) [78]. During apoptosis, cristae folds go through reshaping by a process called cristae remodelling, which accompanies the proteolysis of OPA1[78, 79]. This results in the redistribution of cytochrome c into IMS. In order for cytochrome c to be released out of the mitochondria, pores need to be formed in OMM and that is facilitated by BAX and BAK, which belong to the BCL-2 family of proteins. Thus, Cytochrome c released into the cytosol initiates the final step of apoptosis, which involves the formation of apoptosome [80, 81]. Apoptosome is formed by the binding of cytochrome c to apoptotic activating factor1 (APAF1) and pro-caspase 9, which eventually results in the activation of caspase 3 and 7 (Figure 1.7).

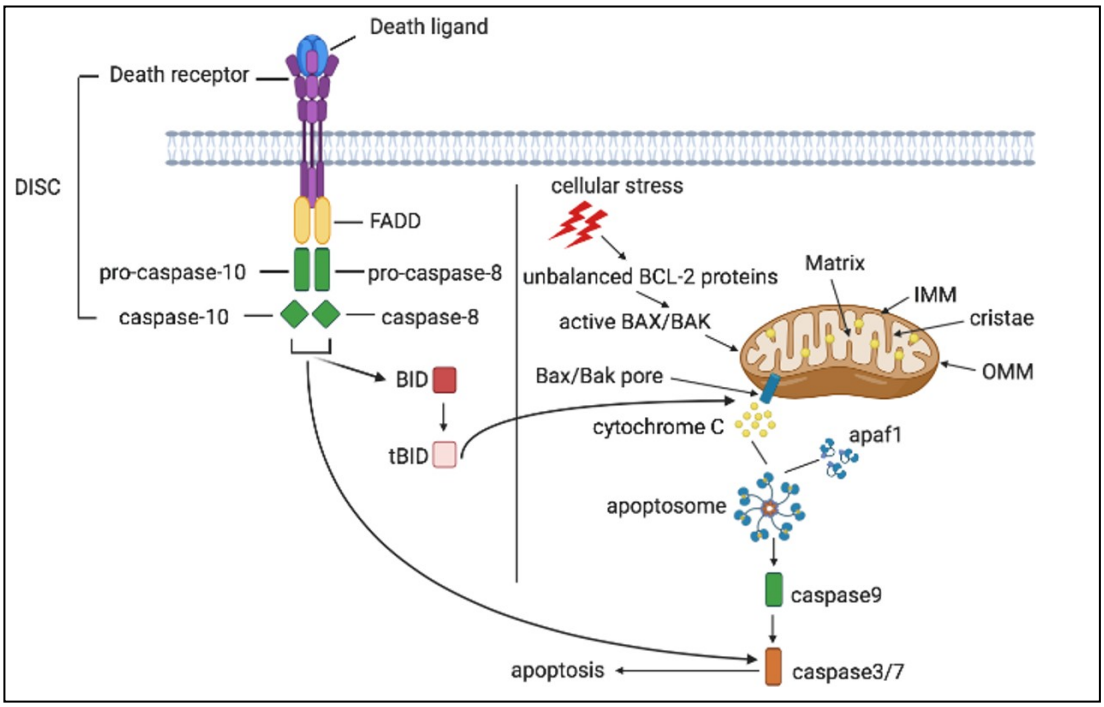

Figure 1.7: Pathways of apoptosis. Intrinsic pathway occurs at the mitochondrial level. It is initiated by a cellular stress, which leads to BAX/BAK oligomerisation and release of cytochrome c from the IMM into the cytosol, followed by the formation of apoptosome and activation of pro-caspases 9, 3, and 7, all of which result in apoptosis. Extrinsic pathway, on the other hand, is initiated when a death ligand binds to a death receptor on the plasma membrane. This binding result in the formation of DISC and activation of pro-caspases 8 and 10. Caspases 8 and 10 convert BID to tBID which translocate to the mitochondria to facilitate BAX/BAK mediated release of cytochrome c. Active Caspases 8 and 10 cleave pro-caspases 3 and 7 leading to apoptosis.

1.6 BCL-2 family of proteins

BCL-2 family of proteins share BH (BCL-2 Homology) domains, including BH1, BH2, BH3 and BH4. These domains are composed of a short (~20 amino acids) sequence [82]. BCL-2 proteins can be divided into two groups depending on their mechanism of action: pro-apoptotic and anti-apoptotic. Anti-apoptotic proteins including BCL-2, BCL-XL and MCL-1 promote cell survival and prevent apoptosis, whereas pro-apoptotic proteins perform the opposite function [83]. Pro-apoptotic proteins can be divided further into three subgroups: activators (BIM, PUMA and BID), sensitisers (NOXA, HRK, BMF, BAD and BIK) and effectors (BAX and BAK), all of which regulate apoptotic pathway. The fate of a cell is dependent on the expression levels and balance between the anti- and pro-apoptotic BCL-2 family of proteins [84]. The anti- and pro-apoptotic BCL-2 family of proteins share certain degree of similarity in their BH domains. For example, BAK and BAX, as well as anti-apoptotic proteins, contain BH1-4 domains, whereas the other pro-apoptotic members contain only BH3 domains, and hence are called BH3-only proteins.

The primary purpose of the anti-apoptotic members belonging to BCL-2 group during apoptosis is to bind and inhibit the function of pro-apoptotic factors and thus antagonising apoptosis. Overexpression of BCL-2 family members has been commonly observed in various kinds of cancers. Moreover, cancer cells depend on BCL-2 family members for survival and proliferation [85]. Due to this, the anti-apoptotic group has been recognised as promising agents for cancer treatment. Inhibitors designed to target these members are called BH3 mimetics and some of them are already approved for use in patients or being investigated in clinical trials [86].

1.6.1 BCL-2

BCL-2 was the first protein identified in this family [87]. High levels of BCL-2 have been found to play significant survival roles in various solid tumours, such as brain, colorectal, bladder, lung, breast, and prostate cancer, as well as in haematological malignancies, for instance, chronic lymphocytic leukaemia (CLL), acute myeloid leukaemia (AML), and non-Hodgkin's lymphoma [88, 89, 90, 91, 92, 93]. BCL-2 is found in two isoforms: BCL-2α, is the well-characterised BCL-2 protein with anti-apoptotic properties, and BCL-2β, which is found in the bone marrow cells and blood cells of chronic myeloid leukaemia (CML) patients [94]. The function of BCL-2β has not yet been characterised. BCL-2 is mainly localised within the OMM and membranes of the endoplasmic reticulum (ER) and does not redistribute from these locations during apoptosis [84]. In addition to its role in apoptosis, BCL-2 has been found to play a role in autophagy, through its interface with Beclin-1 [95]. Out of the effector proteins, BAK but not BAX interacts with BCL-2. Similarly, BCL-2 can bind and sequester all the activator proteins and some of the sensitiser proteins, such as HRK, BMF and BAD (Figure 1.8).

1.6.2 BCL-X_L

B-cell lymphoma extra-large or BCL-X_L has a 44% similar amino acid identity to BCL-2 and has been associated with various tumours, such as head and neck, CML, colorectal and prostate cancer [96, 97, 98, 99]. It has another isoform, BCL-X_S, that is generated through alternative splicing. While BCL-X_L has anti-apoptotic properties, BCL-X_S has been reported to possess pro-apoptotic functions [100]. BCL-X_L is generally restricted to the cytosol and to some degree, the OMM. Most cytosolic BCL-X_L is translocated to the OMM and ER during apoptosis [101]. Within cytosol, BCL-X_L applies

its anti-apoptotic properties, by regulating BAX re-translocation from the mitochondria to cytosol, thus preventing BAX activation followed by anchoring to the OMM [101]. In addition, BCL-X_L is also known to mediate autophagy through binding with Beclin-1 [95]. Both the effector proteins, BAK and BAX interact with BCL- X_L. Similarly, BCL- X_L can bind and sequester all the activator proteins and some of the sensitiser proteins, such as HRK, BMF and BAD (Figure 1.8).

1.6.3 MCL-1

Myeloid cell leukaemia 1 (MCL-1) was initially founded as a proliferation inducer in myeloid leukaemia cells [102]. Having oncogenic potential in various cancers, MCL-1 is found to be one of the most overexpressed genes in most cancers. It is mostly mutated or overexpressed in solid tumours of lung, breast, head and neck, thyroid, ovaries, prostate and pancreas cancer, as well as in haematological malignancies, for instance, AML and multiple myeloma [103, 104, 105, 106, 107, 108]. Moreover, it is also likely to cause resistance to cisplatin during chemo- and radiotherapy [106, 109]. MCL-1 possesses three isoforms: MCL-1L or Long isoform, which is deemed to be the classic pro-survival/ anti-apoptotic isoform; MCL-1ES or extra short and MCL-1S or short isoform. The short and extra short isoforms have not yet been studied in detail [94]. The N-terminus of MCL-1 has a motif that is rich in proline (P), glutamic acid (E), serine (S) and threonine (T), hence named PEST. This has mostly been observed in short-lived proteins and contributes to the labile characteristic of such proteins, and in this case, MCL-1 [110]. The fast turnover of MCL-1 (attributed to post-translational modifications, ubiquitination and proteasomal degradation) can be exploited in cancer treatment by transcriptional/translational suppression of MCL-1 [111, 112]. Both effector proteins, BAK and BAX interact with MCL-1. Similarly, MCL-1 can bind and

sequester all the activator proteins and out of sensitiser proteins it only interacts with NOXA (Figure 1.8).

1.6.4 BCL-w and BCL-2A1

Besides the aforementioned BCL-2 family members, other anti-apoptotic proteins, such as BCL-w and BCL-2A1 (BCL-2 linked protein A1) have been identified in various cancers. Overexpression of BCL-w has been observed in the cancers of breast, colorectal, melanoma, and B cell malignancies[113, 114, 115], whereas BCL-2A1 is generally linked to stomach and breast cancers, CLL and acute lymphoblastic leukaemia (ALL) [116, 117]. Out of the effector proteins, BAX but not BAK interacts with BCL-w and BCL-2A1. Similarly, BCL-w can bind and sequester all the activator proteins and some of the sensitiser proteins, such as BMF and BAD. (Figure 1.8). BCL-2A1 can interact with some activator proteins, such as BIM and BID, as well as some of the sensitiser proteins, such as BIK and NOXA.

1.6.5 Pro-apoptotic BCL-2 family members (the effectors)

The effector proteins have a critical role in the intrinsic apoptotic pathway and their role has been broadly studied. During apoptosis, BAX (BCL-2 associated X) and BAK (BCL-2-homologous antagonist killer) oligomerise to form pores on the mitochondrial membrane to promote cytochrome c release from IMM to OMM [118]. Mutations in BAX and BAK have been shown to enhance cell survival in gastric and colon cancers [119]. BAX was originally discovered as a BCL-2 associated protein, and the molecular mechanisms behind its activation, pore formation and cytochrome c release were characterised much later. Soon after the discovery of BAX, BAK was

also identified to possess similar characteristics to BAX. Both BAX and BAK can interact and bind to BCL-2 family of proteins including, BCL-2, BCL-X_L and MCL-1 (Figure 1.8). Apoptosis and mitochondrial outer membrane permeabilization (MOMP) are kept under control through the prevention of BAX activation. BAX, with the help of proteins such as BCL-$X_{L,}$ transports between the cytosol and the mitochondria, thus aid in preventing BAX activation [120, 121]. BAK, on the other hand is found inserted within the OMM due to its minimum movement between the cytosol and the mitochondria [122]. In contrast to BAX and BAK, another member of this group, Bcl-2-related ovarian killer (BOK), is less explored and its mechanism of action in the intrinsic apoptotic pathway is not fully understood. However, it has been shown that BOK overexpression can result in cell death [123].

1.6.6 Pro-apoptotic BH3-only proteins

As previously mentioned, the BH3-only proteins display a great degree of promiscuity in binding to different anti-apoptotic counterparts, and there are certain instances of specificity as well. For example, NOXA exclusively binds MCL-1, whereas BAD does not exhibit any affinity towards MCL-1 [124]. Nevertheless, activation of BAK and BAX can occur through two distinct mechanisms: (1) by the direct binding and activation of the activator (BIM, PUMA and BID) to the effector proteins (BAK and BAX); and (2) by the indirect displacement, mediated by BH3-only members, of BAX and BAK from the anti-apoptotic proteins [125, 126, 127] (Figure 1.8).

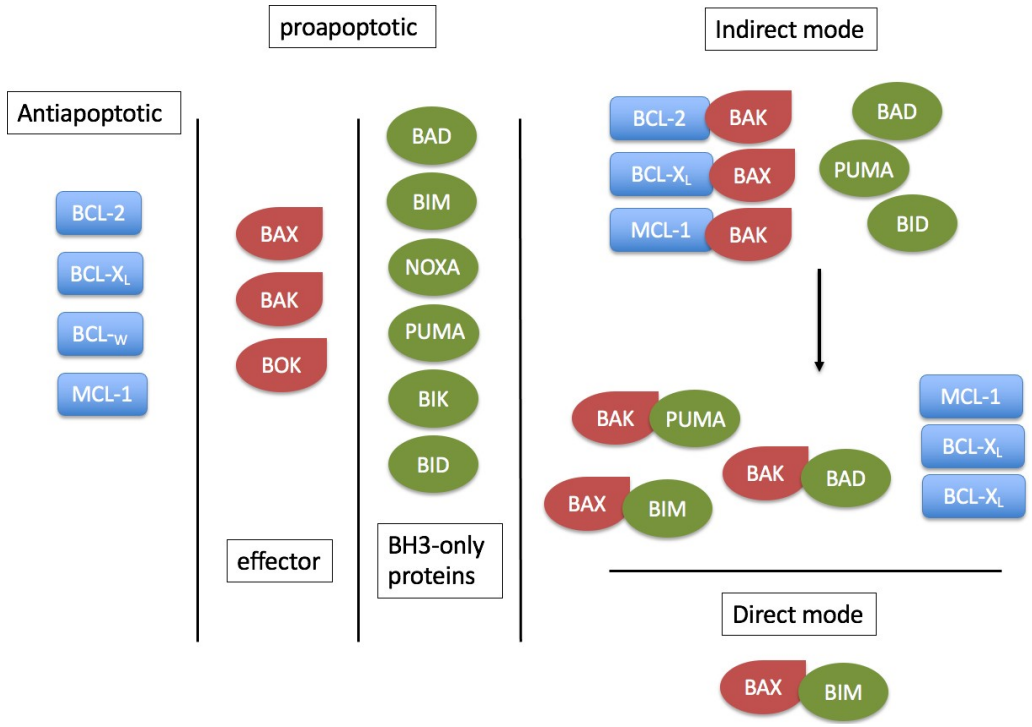

Figure 1.8: Schematic diagram of BCL-2 family of proteins and their mode of action to induce apoptosis. BCL-2 family of proteins can be divided into antiapoptotic members (BCL-2, BCL-xL, BCL-w and MCL-1), proapoptotic effectors (BAX, BAK and BOK) and BH3-only proteins (BAD, BIM, NOXA, PUMA, BIK and BID). Within a cell, it is suggested that effector proteins interact with BH3-only proteins to facilitate apoptosis directly, when BAX or BAK bind to the activators, or indirectly when BH-3 only proteins displace BAX or BAK from anti-apoptotic proteins.

1.7 BH3 mimetics in cancer therapy

With the discovery of BCL-2 family of proteins and their major role in regulating apoptosis, studies have been conducted to target these proteins as cancer therapies. To induce cell death in cancer cells, scientists explored ways to disrupt the interaction between anti and pro-apoptotic proteins. For apoptosis to occur, anti-apoptotic proteins will have to be displaced from BAX and BAK by BH3-only proteins. This can be achieved by small molecules that can mimic the action of BH3-only proteins; hence named BH3 mimetics (Figure1.9). The first BH3 mimetic inhibitor synthesised was ABT-737. This inhibitor mimics the structure of the BH3-only protein, BAD, and thus, can bind and inhibit BCL-2, BCL-X_L and BCL-w [127]. At low concentrations, ABT-737 has shown to induce apoptosis in haematological and solid tumours both *in vivo* and *in vitro* [127]. However, this inhibitor presented with poor pharmacokinetics (low bioavailability and solubility), which led to the design of its derivative, ABT-263 (or Navitoclax), with better pharmacokinetics [128]. Later, an inhibitor that specifically targeted BCL-2 was developed. This drug, ABT-199, also called Venetoclax, has been now been approved for use in CLL patients [129], and being trailed in other malignancies, such as AML, multiple myeloma and non-Hodgkin's lymphoma [129]. Similarly, BCL- X_L inhibitors, such as A-1331852 and WEHI-539 were reported to induce apoptosis *in vitro* [130, 131] but no clinical trials have been reported with these drugs as of now. MCL-1 was the next protein to be targeted for therapy and the first inhibitor, A-1210477 was successfully developed by AbbVie [132]. Since A-1210477 targeted MCL-1 only at micromolar concentrations, S63845 has been developed to induce rapid apoptosis at low nanomolar concentrations both *in vivo* and *in vitro* [133].

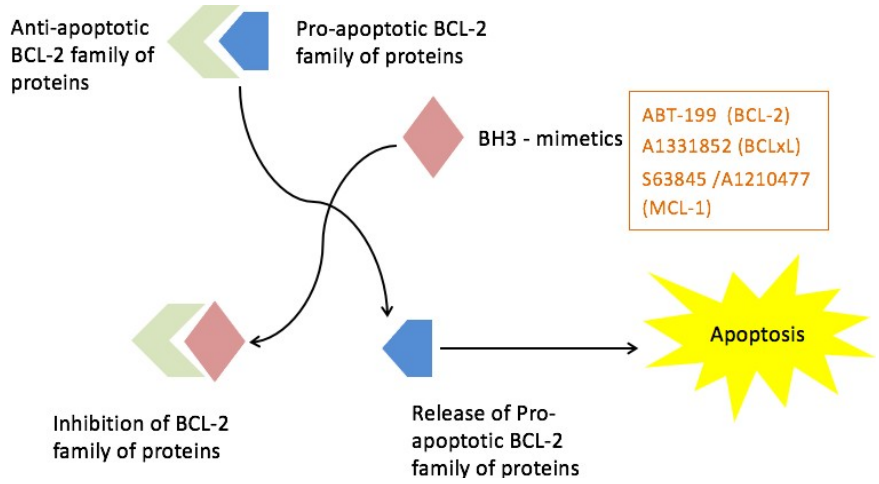

Figure 1.9: Illustration of the mechanism by which BH3 mimetics exerts their actions. BH3 mimetics, small molecule inhibitors of the anti-apoptotic proteins, bind to BCL-2, BCL-xL or MCL-1 to prevent their interaction with pro-apoptotic proteins, thus resulting in apoptosis.

1.8 Aims of the study:

As mTOR signaling pathway is activated in HNSCC, it made it a suitable target for therapy. However, until now targeting this pathway with small molecule inhibitors was unpromising. The aim of this study is to identify a combination of Torin-1, an inhibitor of both mTOR complexes 1 and 2, with other conventional therapies such as, IR and Cisplatin and other novel therapies such as, DT-061 and CB-839 and whether it can modulate this pathway by causing cellular proliferation defect or increased cancer cell death in HNSCC cell lines. A second aim of this study is to assess the crosslink between mTOR inhibition and mitochondrial dynamics in the cell lines tested. Can mTOR inhibition regulate mitochondrial functions by altering the translocation and phosphorylation levels of Drp-1, an integral protein for mitochondrial dynamics.

This work has been conducted during a COVID-19 pandemic which had an impact on the research. During that time laboratories were inaccessible and as a result productivity was reduced and priorities in regard to some experiments were rearranged to meet the deadline of submitting the thesis.

Chapter 2

Materials and Methods

Chapter contents

2.1 Cell lines

The cell lines used in the study are shown in the table below.

Cell line	Origin of tumour	Culture media	Source
UM-SCC-1	Oral cavity SCC	DMEM + 1%NEAA	Prof. T. Carey (University of Michigan, USA)
UM-SCC-11B	Larynx SCC		
UM-SCC-17A	Larynx SCC		
UM-SCC-74A	Oropharynx SCC		
UM-SCC-81B	Oropharynx SCC		
Detroit 562	Hypopharynx SCC	EMEM +1% NEAA +1% Sodium Pyruvate +1% L-Glutamine	ATCC
FaDu	Hypopharynx SCC		
A253	Oral cavity SCC	McCoy's 5A	
K562	Chronic myeloid leukaemia	RPMI 1640	ATCC

Table 2.1: Cell lines used along with information on their media, supplementations and sources. "SCC" stands for squamous cell carcinoma, "DMEM" stands for Dulbecco's modified Eagle Medium, "EMEM" stands for Eagle's minimum essential medium, "NEAA" stands for non-essential amino acids. "ATCC" stands for American Type Culture Collection. 10% FBS (Gibco, ThermoFisher Scientific) was added to all culture media.

2.2 Cell Culture

Cells were purchased from American Type Culture Collection (ATCC, Manassas, VA, USA) or from *Deutsche Sammlung von Mikroorganismen und Zellkulturen* (DSMZ, Braunschweig, Germany), unless stated otherwise in Table 2.1. Cells were grown at 37 °C and 5 % CO_2 in their corresponding cell culture media, which were obtained from Life Technologies Inc (Paisley, UK). The media were supplemented with 10 % foetal bovine serum (FBS) and other components, as detailed in Table 2.1. Cells were left to grow until they reached 80 % confluence. Sub-culturing of adherent cells was carried out, after cells reached the desired confluence, by first aspirating the media, a quick wash with warm PBS (ThermoFisher Scientific, MA, USA), followed by incubation with 0.05 % trypsin-EDTA (Gibco, ThermoFisher Scientific) at 37 °C for approximately 5 min. After that, cells were collected and re-seeded in a new plate.

For 3D Spheroid culture, two HNSCC cell lines (UM-SCC-17A and FaDu) were seeded at 500/300 cells/well, respectively, in 96-well polystyrene ultra-low attachment microplates (Cell carrier spheroid ULA, PerkinElmer, UK), incubated in humidified incubators at 37 °C with 5% CO_2 for 3 days, the desired treatment then was added, and growth monitored by taking images of the spheroids every 3 days for 9 days in total using EVOS FLoid Cell Imaging Station (Life Technology, UK). The changes in volume of the spheroids were measured using a plug-in for imageJ (public software, National Institutes of Health, Maryland, USA) and the volume was calculated using the equation below:

$$\textit{Volume} = (4/3) \times \pi(\textit{diameter}/2)^3 \ (\textit{unit: } \mu m^3)$$

2.3 Reagents

All reagents, chemicals and buffers were supplied by Sigma-Aldrich/Merck (Darmstadt, Germany) or Thermo Fisher Scientific (MA, USA) unless stated otherwise.

Reagent	Target	Supplier
A-1331852	BCL-X_L (inhibitor)	Abbvie
S63845	MCL-1 (inhibitor)	Selleck
Z-VAD.FMK	Caspases (inhibitor)	Selleck
Cisplatin	DNA (alkylating agent)	Selleck
MG-132	Proteasome (inhibitor)	Active Biochem
Torin-1	mTOR complex 1&2 (inhibitor)	Sigma
rapamycin	mTOR complex 1 (inhibitor)	Selleck
everolimus	mTOR complex 1 (inhibitor)	Selleck
Chloroquine	Lysosomotropic agent	Selleck
3-MethylAdenine (3-MA)	PI3K (inhibitor)	Selleck
DT-061	PP2A (activator)	Selleck
FYT720	PP2A (activator)	Sigma
H-89	PKA (inhibitor)	Sigma
AZD1775	Wee1 kinase (inhibitor)	Selleck
Olaparib	PARP (inhibitor)	Selleck
CB-839	Glutaminase1 (GLS1) (inhibitor)	Selleck
BAY-2402234	DHODH (inhibitor)	Selleck

Table 2.2: Reagents used along with information on their target and sources. Abbvie stands for Abbvie (Chicago, IL, USA), Selleck stands for Selleck Chemicals Co (Houston, TX, USA), Sigma stands for Sigma-Aldrich/Merck (Darmstadt, Germany) and Active Biochem stands for Active Biochem LTD (Hong Kong).

2.4 siRNA Transfection

siRNAs (small interfering RNA oligoduplexes), obtained from Qiagen (Cambridge, UK), were reconstituted in RNAse-free water to a final concentration of 10 μM. A final concentration of 10 nM was transfected into the cells using OptiMEM Reduced Serum Media (Life Technologies) and Interferin transfection reagent (Polyplus, Illkirch, France), according to manufacturer's protocol.

Protein target	Sequence	Catalogue no.
ATG5	CTAGGAGATCTCCTCAAAGAA	SI02633946
ATG7	CACTAGAGTGTGCATATGATA	SI04344830
Non-targeting control	AACTGGGGGAGGATTGTGGCC	1027310
Raptor	GACACGGAAGATGTTCGACAA	SI05182212
Rictor	ATGACCGATCTGGACCCATAA	SI03151379
Sin-1	AAGGGTCATGTAGGTACAACA	SI03036103

Table 2.3: siRNAs targets, sequence and catalogue numbers. all siRNA used were obtained from Qiagen (Cambridge, UK) in the table below it shows their targets and sequences.

2.5 Immunoblotting

a) Protein sample preparation

Cells were harvested and pellets were lysed by radioimmunoprecipitation assay (RIPA) buffer (10 mM Tris-Cl (pH 8.0), 1 mM EDTA, 0.5 mM EGTA, 1 % Triton X-100, 0.1 % sodium deoxycholate, 0.1 % SDS, 140 mM NaCl) with 20 μM MG-132 and one protease inhibitor tablet cOmplete Mini protease inhibitor cocktail (Roche, Basel, Switzerland). After adding the buffer, cells were kept on ice for at least 15 minutes, sonicated with a Bandelin SONOPULS ultrasonic homogeniser (Bandelin, Berlin, Germany). Samples were centrifuged and supernatants were collected. Proetein concentration in every cell lysate was determined using

Colorimetric Bradford assay (BioRad Protein Assay Dye Reagent, BioRad, CA, USA) using a spectrophotometer (Eppendorf, Hamburg, Germany). Pre-determined concentrations of Bovine serum albumin (BSA) was used to standardised and calculate the protein concentration in each sample. A range between (20-50) μg of protein was used and 4 x NuPAGE LDS sample buffer (Life Technologies) was added to the protein lysate, followed by 5 min boiling at 70 °C (ThermoFisher Scientific), before loading the samples in gels.

b) Gel electrophoresis and transfer

Desired percentages of Acrylamide gels were made in the lab by following table 2.4 below. Normalised and uniform concentrations of samples were loaded onto the gels alongside 7 μl of protein ladder SeeBlue™ Plus2 Pre-stained Protein Standard (ThermoFisher Scientific). Gels were run at a constant voltage of 120 V for 90 mins in electrophoresis buffer (25 mM Tris-HCL, 192 mM glycine, 10 % SDS). Nitrocellulose membranes (VWR, Radnor, PA, USA) were used to transfer proteins in a chamber containing transfer buffer (25 mM Tris-HCL, 192 mM glycine, 20 % methanol) at 100 V for 90 min. To evaluate efficiency of the proteins being transferred from the gels to the nitrocellulose membranes, the membranes were stained with Ponceau S solution (0.1% (w/v) in 5% acetic acid) for 1 min and excess stain was removed by a quick wash with TBS-T (Tris-buffered saline with 0.1 % Tween, 20 mM Tris-HCL, 150 mM NaCl, 0.1 % Tween-20). Membranes then were blocked in non-fat 5 % milk in TBS-T for 30 mins followed by overnight incubation at 4 °C with the designated primary antibodies described in table 2.5 below. Next day, membranes were washed twice in TBS-T followed with incubation with either anti-mouse or anti-rabbit IgG HRP-linked secondary antibodies (Cell Signalling Technology) for 1-2 h.

After that, membranes were washed in TBS-T for 10 mins and protein bands visualized by enhanced chemiluminescence reagent ECL (GE Healthcare, IL, USA) via ChemiDoc Imaging system (BioRad).

	7 %	10 %	15 %	**Stacking**
H_2O	15.3 ml	12.3 ml	7.3 ml	12.38 ml
30 % Protogel acrylamide	7 ml	10 ml	15 ml	2.5 ml
1.5 M Tris-HCL, 0.4 % SDS, pH 8.8	7.5 ml	7.5 ml	7.5 ml	-
0.5 M Tris-HCL, 0.4 % SDS, pH 6.8	-	-	-	5 ml
10 % ammonium persulphate (APS)	180 µl	180 µl	180 µl	180 µl
TEMED	24 µl	24 µl	24 µl	24 µl

Table 2.4: Resolving and stacking gel components required to fill a gel cassette. Volumes required to make up 4 gels.

Antibody	Epitope	Supplier	Catalogue no.
GAPDH (FL-335)	AA 1-335	SC	sc-25778
P70 S6 kinase	C-terminus	CST	9202
phospho P70 S6 kinase	Thr (389)	CST	9205
LC3II	N-terminus LC3B	CST	3868
mTOR	Around Ser2481	CST	2972
p-mTOR	Ser (2448)	CST	2976
Raptor	Full length	CST	2280
Rictor	Around Lys1125	CST	2140
Sin-1	C-terminus	CST	12860
AKT	PH domain	Upstate	14-276
p-AKT	Thr (308)	Upstate	05-802
p-AKT	Ser (473)	CST	9271
AMPK	Full length	CST	5832S
p-AMPK	Thr (172)	CST	500815
Caspase-3	N/A	CST	9662
Cleaved PARP (D64E10)	Around Asp214	CST	5625
Beta-actin	C-terminus	SC	sc-1616R
OPA-1	AA 708-830	BD	612607
Drp-1	AA 601-722	BD	611113
p-DRP-1	Ser (616)	CST	3455
p-DRP-1	Ser (637)	CST	4867
MTFP1	N/A	Sigma	SAB4301167
Cytochrome c	Around AA 62	BD	556432
HSP70	AA 661-679	Abcam	ab2799

Table 2.5: Primary antibodies used in this study. The vendors were Santa Cruz Biotechnology (SC, CA, USA), Cell Signalling Technology (CST, MA, USA), BD BioSciences (BD,California, USA), “Upstate” stands for Upstate USA Inc (NY, USA), Sigma-Aldrich (Darmstadt, Germany), Abcam (Cambridge, UK).

2.6 Clonogenic assay

Cells were seeded at low density as mentioned in Table 2.6. The following day, cells were subjected to the required treatment and left to grow and form colonies (~ 50 cells per colony), which usually takes between 7 to 10 days. Upon colony formation, cells were washed with PBS, fixed for 5 mins with fixing solution (1:7 v/v ratio acetic acid to methanol) at room temperature and stained with (0.5 % crystal violet in 20 % methanol) for 1 h. The stain then was removed, and cells washed under running water and left to dry for 1 day. Colonies were counted using an automated counting machine (GelCount -Oxford Optronix, Oxford, UK). The following equation was used to determine the surviving fraction:

$$Surviving\ fraction = \frac{number\ o*\ colonies}{seedin0\ density}\ \text{X } 100$$

Cell line	6 well plate	12 well plate
A253	2000-4000	1000-2000
UM-SCC-1	500-1000	250-500
UM-SCC-11B	500-1000	250-500
UM-SCC-17A	2000-4000	1000-2000
UM-SCC-81B	500-1000	250-500
UM-SCC-74A	500-1000	250-500
FaDu	1000-2000	500-1000
Detroit 562	1000-2000	500-1000

Table 2.6: Seeding density (per well) for cell lines used in the study.

2.7 Flow Cytometry- Phosphatidylserine (PS) externalisation assay

Suspension cells were collected into tubes whereas adherent cells were trypsinised, washed with PBS and centrifuged to get a pellet. This was then resuspended in 500 µl of 1x Annexin Binding Buffer (10 mM HEPES, 140 mM NaCl, 2.5 mM $CaCl_2$, pH 7.4) with Annexin-V-FITC (1:20,000 dilution, prepared in the lab) and incubated at room temperature for 8 min. Just before analysis, 5 µl of propidium iodide (PI; 1 mg/ml) (Sigma-Aldrich/Merck, Darmstadt, Germany) was added to cell suspension. Cells then were run through an Attune NxT flow cytometer (ThermoFisher) to measure the extent of Annexin-V/PI staining.

2.8 Immunocytochemistry

Cells were seeded on sterile coverslips, which were placed on a 24 well plate to reach 70 % confluence. Following different treatments, the media was discarded, and coverslips were washed twice with PBS. Coverslips were then fixed with either 4 % (w/v) paraformaldehyde or ice-cold methanol, depending on the primary antibody used, for 10 mins at room temperature. Cells were permeabilised with 0.5 % (v/v) Triton X-100 in PBS for 10 min at room temperature. Primary antibodies were made in 3 % BSA in PBS and added onto the coverslips. Coverslips were kept in humidified chamber for 1 h followed by 1 h incubation with suitable AlexaFluor (Life Technologies) secondary antibody at 1:1000 which was made in 3 % BSA in PBS. Coverslips were then rinsed multiple times with dH_2O, dried and mounted on glass slide using Polymount (Polysciences, PA, USA) mounting solution. Images were taken using 3i Marianas spinning disk confocal microscope, fitted with a Plan-

Apochromat × 63/1.4 NA Oil Objective, M27 and a Hamamatsu ORCA-Flash4.0 v2 sCMOS Camera (Intelligent Imaging Innovations, GmbH, Gottingen, Germany).

2.9 Bright field microscopy

EVOS FLOID cell imaging system (ThermoFisher Scientific) was used to acquire bright field microscopy images of cells.

2.10 Statistics

Two-way ANOVA with multiple comparisons test was used for studies with two numerical variables while one-way ANOVA with multiple comparisons test was used for studies with single numerical variables. The asterisks depicted correspond to the following p values: * for $p \leq 0.05$, ** for $p \leq 0.01$ and *** for $p \leq 0.001$. GraphPad Prism version 7 was used to conduct these statistical analyses.

Chapter 3

Targeting mTOR kinases in head and neck squamous cell carcinoma

Chapter contents

3.1 Introduction

Head and Neck Squamous Cell Carcinoma (HNSCC) is the sixth leading cancer worldwide with annual incidence of more than 550,000 cases [134]. HNSCC includes malignancies arising in the mucosal layer beneath the epithelial cells that line the upper aerodigestive tract. The different subsites of this region are oral cavity, oropharynx, larynx and hypopharynx as shown in Figure 3.1.

Multiple factors can cause HNSCC development, such as genetic inheritance and environmental factors. Consumption of alcohol and tobacco are amongst the classical high-risk factors associated with HNSCC. Not all smokers and alcohol consumers develop HNSCC, which suggest a role of genetic variations in HNSCC disease progression. Minimizing alcohol intake can reduce the risk of developing HNSCC, as the risk of developing HNSCC is directly proportional to blood alcohol concentration [135], and this risk can increase by 40 -fold when combined with tobacco consumption. Despite the advances in treatment strategies of HNSCC, the survival rate has not improved and remains at approximately 50 % [136]. In recent years, infection with high risk-Human Papillomavirus (HPV) has been associated with HNSCC pathogenesis, especially in oropharyngeal carcinogenesis. HNSCC can be divided into HPV- negative and HPV-positive. Radiation and Chemotherapy are more effective and offer better outcomes in HPV-positive HNSCC patients [137]. Other factors that can be associated with HNSCC pathogenesis include diet. Recent studies show diets that contain less red meat and higher level of fibre and carotenoids can lower the risk of HNSCC [138]. In addition to these risk factors, chronic irritation of the lining of the mouth and poor dental hygiene can also play an important role in HNSCC disease progression [135].

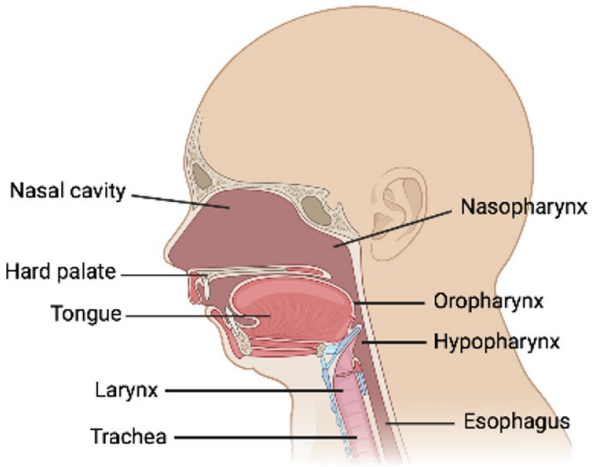

Figure 3.1: Head and Neck anatomical subsites. Illustrations of the different subsites where tumour can occur and that includes oral cavity, oropharynx, larynx and hypopharynx.

The therapeutic outcomes of HNSCC treatments are often limited by acquired resistance to chemotherapy or radiotherapy, as well as undesirable toxicity. Development of more personalised therapies that can selectively target cancer cells are currently been explored [139]. It has been found that several molecular signalling pathways in HNSCC are differentially regulated, thus making this cancer suitable for molecular targeted therapies. One such pathway is mTOR signalling that is highly active in HNSCC [140]. The efficacy of conventional therapies for HNSCC patients can be enhanced by blocking this pathway using different inhibitors, such as BEZ235, PF-04691502 (dual PI3K/mTOR inhibitors), everolimus, rapamycin and temsirolimus(mTOR complex1 inhibitors) and Torin-1 (mTOR complex 1 and 2 inhibitor).

In this chapter, the potential to target mTOR complexes in the context of HNSCC will be assessed. As part of this, the following questions will be addressed:

1. Could mTOR inhibition decrease the clonogenic survival of HNSCC cell lines?
2. Could mTOR inhibition decrease spheroid growth in 3D cultures of HNSCC cell lines?
3. Could mTOR inhibition cause apoptosis in HNSCC cell lines?
4. Could the effect of mTOR inhibition be attributed to the induction of autophagy?

3.2 Results

3.2.1 Characterisation of mTOR kinase signalling in HNSCC cell lines

To assess mTOR signalling in HNSCC, two different cell lines per subsite were used. Cell lines chosen were: A253 and UM-SCC-1 derived from oral cavity, UM-SCC-11B and UM-SCC-17A derived from larynx, UM-SCC-74A and UM-SCC-81B derived from oropharynx, and Detroit 562 and FaDu derived from hypopharynx. Cells were lysed and western blotting was carried out for the indicated proteins to characterise mTOR signalling. Endogenous levels of mTOR appeared to be highly expressed in 5 out of the 8 cell lines tested and it was irrespective of the origin (anatomical subsite) of the tumour (Figure 3.2.1). Phosphorylation of mTOR at Ser2448 could be observed in these cell lines and correlated with total mTOR expression (Figure 3.2.1). Since mTOR exists in two different complexes, mTORC1 and mTORC2, the individual components of mTOR complexes, namely Raptor and Rictor were assessed. Raptor was more widely expressed among the cell lines tested, with relatively higher expression levels in A253 and FaDu (Figure 3.2.1). In contrast, Rictor was highly expressed only in 5 of these 8 cell lines tested (Figure 3.2.1). The expression levels of downstream mTOR substrate, S6 kinase (both whole and phosphorylated form) were quite varied in the different HNSCC cell lines (Figure 3.2.1). Downstream kinases, AKT and AMPK, were highly expressed in 4 out of the 8 cell lines (Figure 3.2.1). Phosphorylation of AKT at S473 was high in UM-SCC-1 and UM-SCC-81B, whereas it was moderately expressed in 3 cell lines, A253, UM-SCC-11B and Detroit 562. Phosphorylation of AMPK at Thr172 was higher in 5 out of the 8 cell lines (Figure 3.2.1). Taken together, all 8 cell lines demonstrate varied expression levels of mTOR signalling proteins.

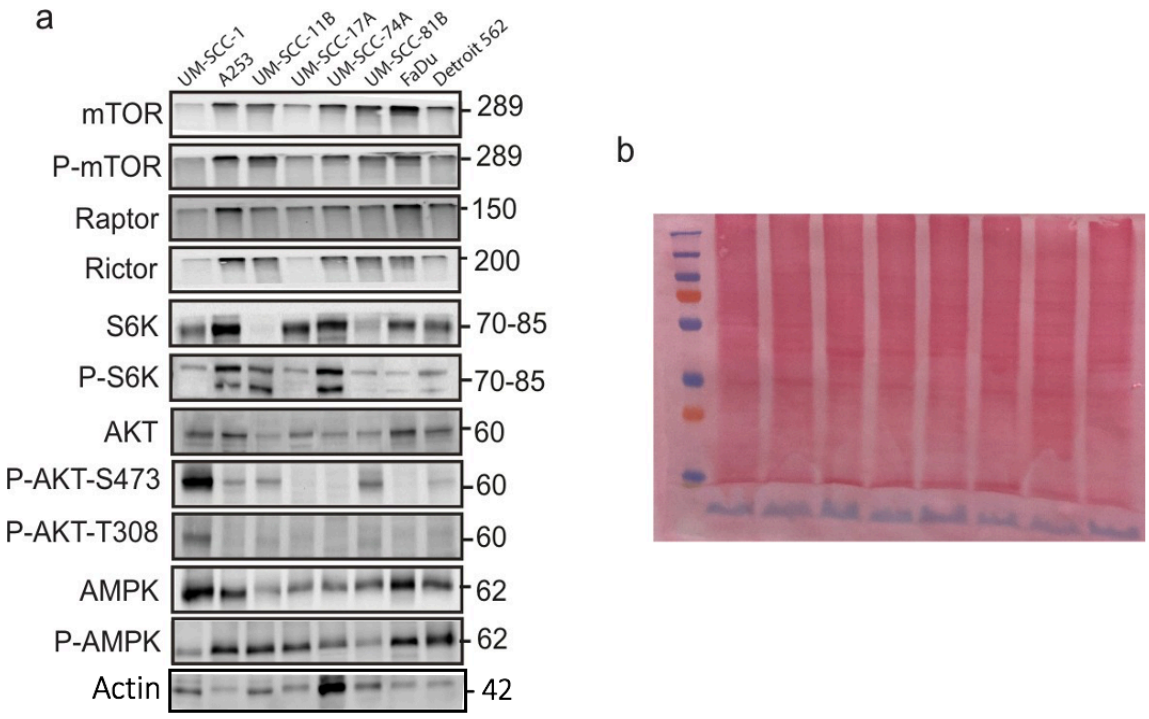

Figure 3.2.1: mTOR kinase signalling is prevalent in a wide variety of HNSCC cell lines. a) Western blot of proteins associated with mTOR and its signalling pathway were analysed in 8 different cell lines derived from 4 head and neck subsites. b) Ponceau S staining was used as loading control because the expression levels of housekeeping proteins, such as GAPDH, Actin and Tubulin hugely differed in these cell lines.

3.2.2 mTORC2 appears to play a more prominent role than mTORC1 in decreasing clonogenicity of HNSCC cell lines

Since mTOR signalling pathway is mediated by both mTOR complex 1 and complex 2, it was important to determine if mTORC1 and /or mTORC2 could inhibit tumour growth in HNSCC. This can be measured *in vitro* by assessing the clonogenic potential of the HNSCC cell lines. For this, cells were transfected with siRNAs against components of mTORC1 (namely Raptor) and mTORC2 (namely Rictor and mSin1), and clonogenic assays were performed. Silencing of Raptor resulted in a significant decrease in the colony formation of UM-SCC-1 cell line (Figure 3.2.2), whereas only a modest reduction was seen in UM-SCC-11B (Figure 3.2.2). In contrast, silencing of Raptor did not result in decreased clonogenicity of UM-SCC-81B and FaDu cell lines. In fact, there was a slight increase in the colony formation upon silencing of Raptor (Figure 3.2.2). This suggested that UM-SCC-1 and UM-SCC-11B are more dependent on mTORC1 than UM-SCC-81B and FaDu. To determine if mTORC2 played a significant role in UM-SCC-81B and FaDu, the four HNSCC cell lines were transfected with siRNA against Rictor. It is interesting to note that in UM-SCC-1, silencing of Rictor had a significant effect on clonogenicity suggesting that both mTORC1 and mTORC2 play important roles in the survival of this cell line (Figure 3.2.3). In contrast, in UM-SCC-11B, silencing Rictor had a significant effect compared to Raptor siRNA, suggesting that mTORC2 played a more prominent role in UM-SCC-11B (Figure 3.2.3). The same effect was also seen in UM-SCC-81B, which confirmed that these two cell lines are more dependent on mTORC2 than mTORC1 (Figure 3.2.3). In marked contrast, in FaDu, neither Raptor nor Rictor affected clonogenicity, suggesting redundant roles of mTORC1 and mTORC2 in this cell line (Figure 3.2.3).

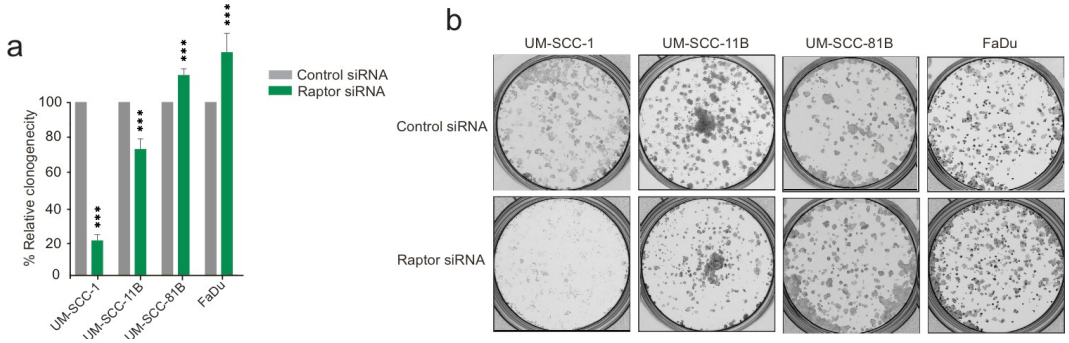

Figure 3.2.2: mTORC1 plays a significant role in the clonogenic survival of only UM-SCC-1 and UM-SCC-11B. UM-SCC-1, UM-SCC-11B, UM-SCC-81B and FaDu cells were seeded and transfected with either control siRNA or siRNA against Raptor. Cells were left to grow for ~ 7-10 days. Cells were then fixed and stained with crystal violet and counted using automated colony counter. (a) Represents the % survival factor in each cell line tested. (b) Represents bright field images of the colonies that were quantified in (a). Error bars represent standard error of the mean (S.E.M) from at least 3 independent experiments. ***$p \leq 0.001$.

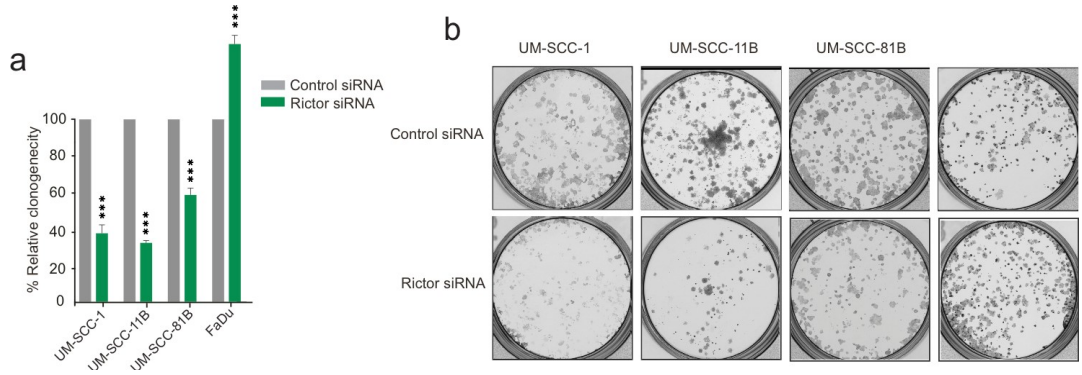

Figure 3.2.3: mTORC2 plays a significant role in the clonogenic survival of most HNSCC cell lines tested. UM-SCC-1, UM-SCC-11B, UM-SCC-81B and FaDu cells were seeded and transfected with either control siRNA or siRNA against Rictor. Cells were left to grow for ~ 7-10 days. Cells were then fixed and stained with crystal violet and counted using automated colony counter. (a) Represents the % survival factor in each cell line tested. (b) Represents bright field images of the colonies that were quantified in (a). Error bars represent standard error of the mean (S.E.M) from at least 3 independent experiments. ***$p \leq 0.001$.

As these findings were interesting, another component of mTORC2 (namely Sin-1) was chosen and the same experiment was repeated. mSin-1, similar to Rictor, resulted in a marked reduction in clonogenicity in UM-SCC-1, UM-SCC-11B and UM-SCC-81B cell lines (Figure 3.2.4). As previously observed, mSin-1 siRNA did not have an effect in FaDu cell line (Figure 3.2.4). Collectively, these results confirm that HNSCC cell lines seem to depend on mTORC2 more than mTORC1 for clonogenic survival.

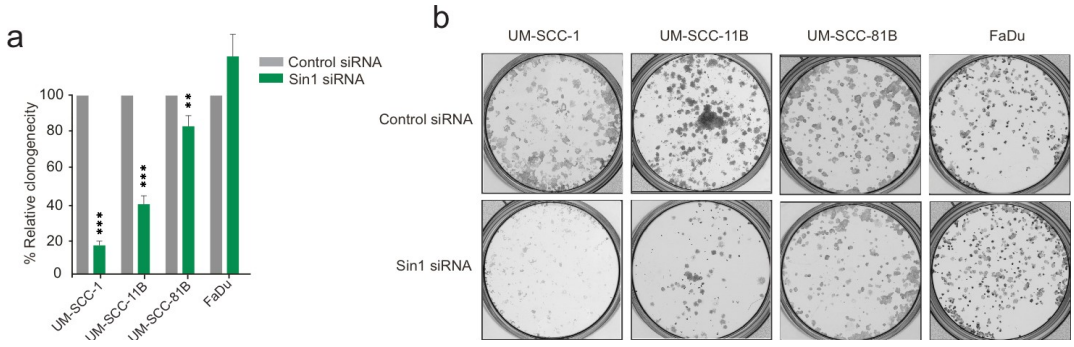

Figure 3.2.4: mTORC2 plays a significant role in the clonogenic survival of most HNSCC cell lines tested. UM-SCC-1, UM-SCC-11B, UM-SCC-81B and FaDu cells were seeded and transfected with either control siRNA or siRNA against Sin-1. Cells were left to grow for ~ 7-10 days. Cells were then fixed and stained with crystal violet and counted using automated colony counter. (a) Represents the % survival factor in each cell line tested. (b) Represents bright field images of the colonies that were quantified in (a). Error bars represent standard error of the mean (S.E.M) from at least 3 independent experiments. ***$p \leq 0.001$, ** $p \leq 0.01$.

3.2.3 Assessing the ability of Torin-1 to inhibit mTOR signaling in HNSCC cell lines

Inhibition of mTOR kinases can be achieved by using different inhibitors, including rapamycin, everolimus and Torin-1. rapamycin and everolimus inhibit mTOR complex 1, whereas Torin-1 inhibits both complexes 1 and 2. Since all HNSCC cell lines expressed differing levels of Raptor, Rictor, S6 Kinase, AKT and AMPK (Figure 3.2.1), it is probable that both mTOR complexes 1 and 2 are active in HNSCC cell lines. Moreover, HNSCC cell lines appear to depend more on mTORC2 for survival (Figures 3.2.3 and 3.2.4). Therefore, it was important to inhibit both mTORC1 and mTORC2 in this study. Torin-1 was chosen to target both mTOR complexes in this thesis.

Increasing concentrations of Torin-1 was used to treat the cells for 48 h, followed by western blotting to analyse the expression levels of mTOR signalling proteins. The levels of p-S6 kinase decreased with increasing concentrations of Torin-1 (Figure 3.2.5), which was in agreement with previous findings, supporting that Torin-1 inhibited mTOR activity by preventing the phosphorylation of its downstream effectors, S6K-1 [69]. There was no change in the phosphorylation levels of both AKT at T308 and AMPK at T172 (Figure 3.2.5). This could be because these phosphorylation events (of AKT at T308 and AMPK at T172) occur upstream of mTOR [24]. In contrast, exposure of cells to Torin-1 resulted in a decrease in the phosphorylation of AKT at S473 (Figure 3.2.5), supporting that this phosphorylation event occurs downstream of mTORC2 [24], which in turn can be efficiently inhibited by Torin-1. Furthermore, an increase in the level of LC3II processing was observed (Figure 3.2.5), which indicated that inhibition of mTOR resulted in the induction of autophagy.

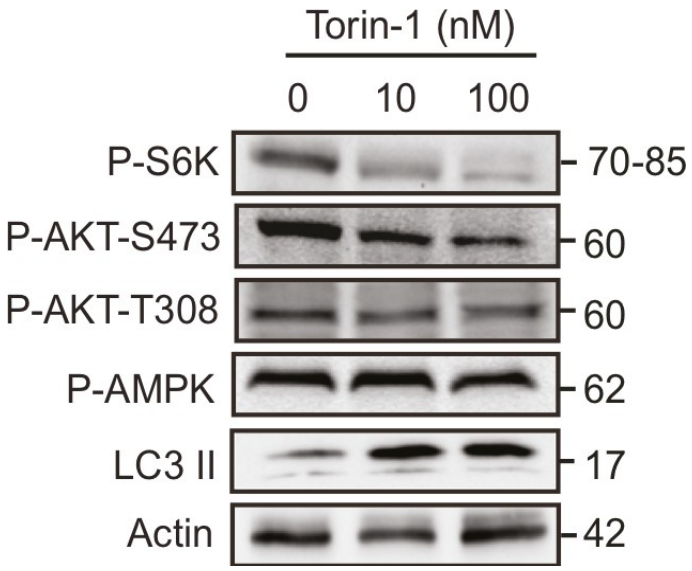

Figure 3.2.5: Torin-1 inhibits mTOR kinases signalling in the hypopharynx cell line, FaDu. FaDu cells were exposed to Torin-1 (0,10,100 nM) for 48h. After treatment cells were lysed and were probed for the indicated antibodies. Experiment was performed three times. Actin was used as a loading control**.**

3.2.4 Targeting mTOR kinases inhibits the clonogenic survival and spheroid growth of HNSCC cell lines

Since Torin-1 inhibits both mTOR complex 1 and complex 2, it could potentially inhibit tumour growth in HNSCC. This can be measured *in vitro* by assessing the clonogenic potential of the HNSCC cell lines. For this, HNSCC cell lines were exposed to increasing concentrations of Torin-1 and clonogenicity was assessed. As evident from Figures 3.2.6 - 3.2.9, at 5 nM Torin-1 concentration, the sensitivity to Torin-1 with respect to clonogenic potential can be ordered as follows:

1 > 81B > 17A > 11B = Detroit = 74A = FaDu > A253

At 10 nM Torin-1 concentration, the sensitivity to Torin-1 was largely similar: 1 = 81B > 17A = 11B = Detroit > 74A > FaDu > A253

Taken together, it can be concluded that Torin-1 is effective in reducing the clonogenic potential for all 8 cell lines at concentration as low as 5 -10 nM. Although clonogenic assays are indirect measures of tumour growth and survival, tumours *in vivo* occur in a 3D architecture. In comparison to two-dimensional culture system, 3D cell culture provides relevance to *in vivo* tumour through exhibiting cell-cell interaction, cell-matrix interactions, heterogeneity and structural complexity. Unlike 2D system, 3D cultures can utilise a single cell line or it can be a combination of variety of cell type, for instance breast cancer co-cultured with stromal fibroblast provided a good representation of ductal carcinoma. In terms of growth dynamics, cellular heterogeneity, signal pathway activity, and gene expression, is an appealing model because it closely mimics in vivo tumour cell properties and as it has been established that Torin-1 does affect cell proliferation it was reasonable to use 3D-spheroid model to study the effect of Torin-1.

In order to confirm the effect of Torin-1 in a 3D spheroid model, all 8 HNSCC cell lines were seeded, as detailed in the method section, for spheroid culture. Of these, only FaDu and UM-SCC-17A formed well-defined spheroids without the requirement of extra supplements (Figure 3.2.10). Since the addition of extra supplementation could interfere with mTOR signalling and potentially give false results, FaDu cell lines were used for the spheroid study in this thesis. Consistent with the results of the clonogenic assays, increasing concentrations of Torin-1 significantly decreased the volume of FaDu spheroids (Figure 3.2.11). Taken together, targeting mTOR kinases using Torin-1 inhibited not only the clonogenic survival but also the spheroid growth of the HNSCC cell lines tested.

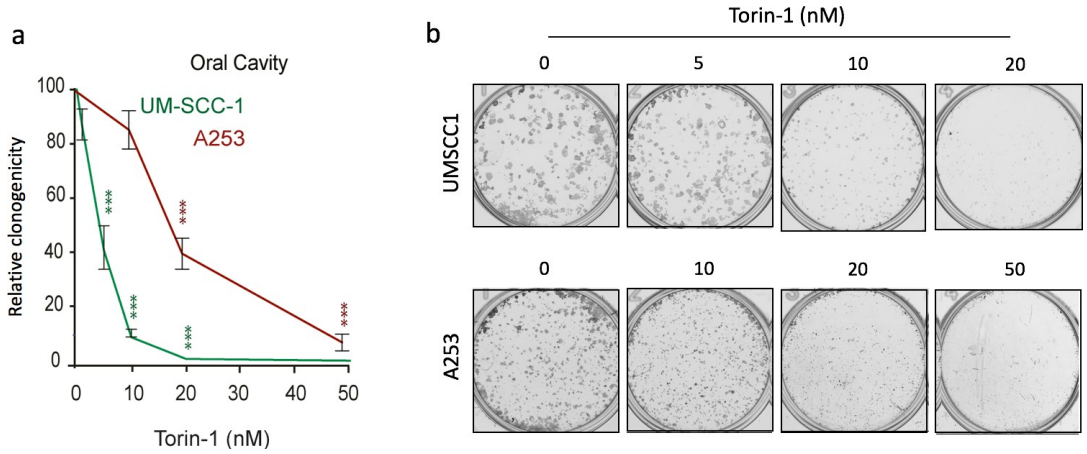

Figure 3.2.6: Inhibition of mTOR kinase by Torin-1 decreases clonogenic potential of oral cavity HNSCC cell lines. Cell lines derived from oral cavity, UM-SCC-1 and A253 were seeded at low density and treated with increased concentration of Torin-1 and left to grow for approximately 7-10 days. Cells were then fixed and stained with crystal violet and counted using automated colony counter. (a) Line graph represents the % relative clonogenicity of cells using colony formation assay. (b) Representative images of the colonies counted after treatment. Error bars represent standard error of the mean (S.E.M) from at least 3 independent experiments; ***$p \leq 0.001$.

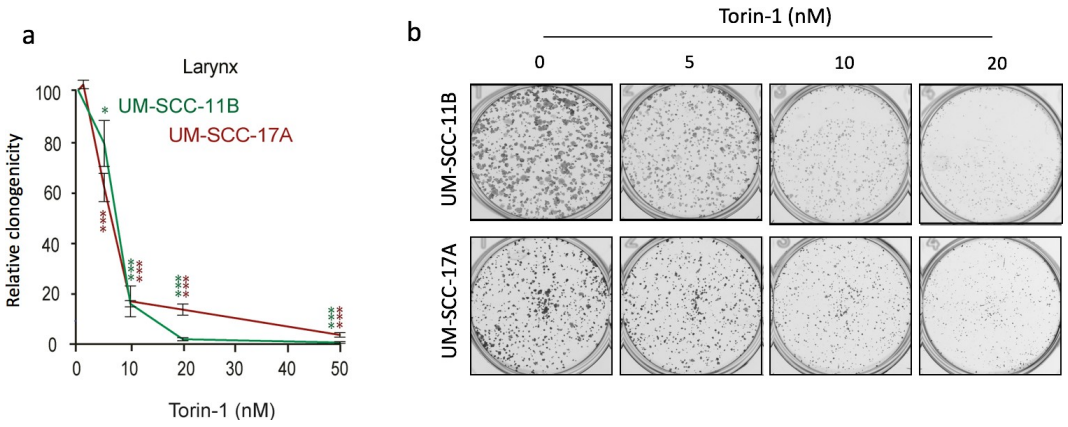

Figure 3.2.7: Inhibition of mTOR kinase by Torin-1 decreases clonogenic potential of laryngeal HNSCC cell lines. Cell lines derived from larynx, UM-SCC-11B and UM-SCC-17A, were seeded at low density and treated with increased concentration of Torin-1 and left to grow for approximately 7-10 days. Cells were then fixed and stained with crystal violet and counted using automated colony counter. (a) Line graph represents the % survival factor of cells using colony formation assay. (b) Representative images of the colonies counted after treatment. Error bars represent standard error of the mean (S.E.M) from at least 3 independent experiments; ***$p \leq 0.001$.

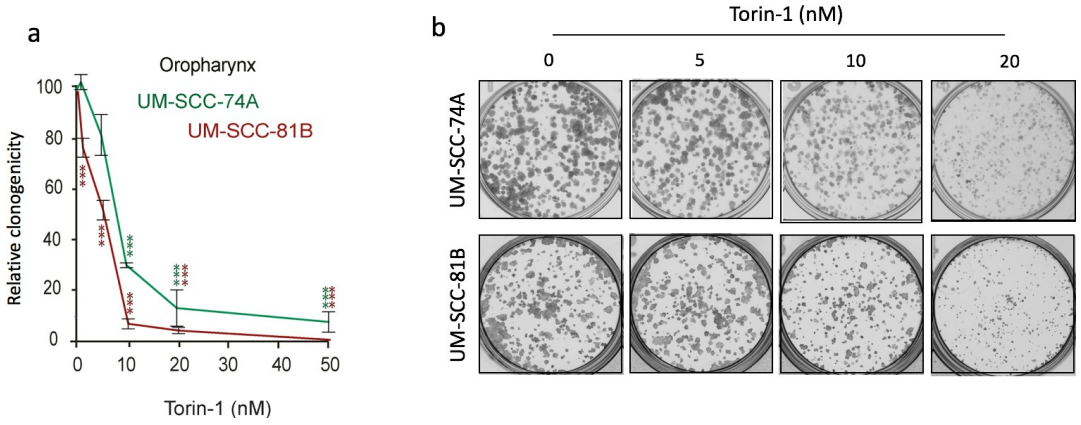

Figure 3.2.8: Inhibition of mTOR kinase by Torin-1 decreases clonogenic potential of oropharyngeal HNSCC cell lines. Cell lines derived from oropharynx, UM-SCC-74A and UM-SCC-81B, were seeded at low density and treated with increased concentration of Torin-1 and left to grow ~ 7-10 days. Cells then fixed and stained with Crystal violet and counted using automated colony counter. (a) Line graph represents the % survival factor of cells using colony formation assay. (b) Representative images of the colonies counted after treatment. Error bars represent standard error of the mean (S.E.M) from at least 3 independent experiments; ***$p \leq 0.001$.

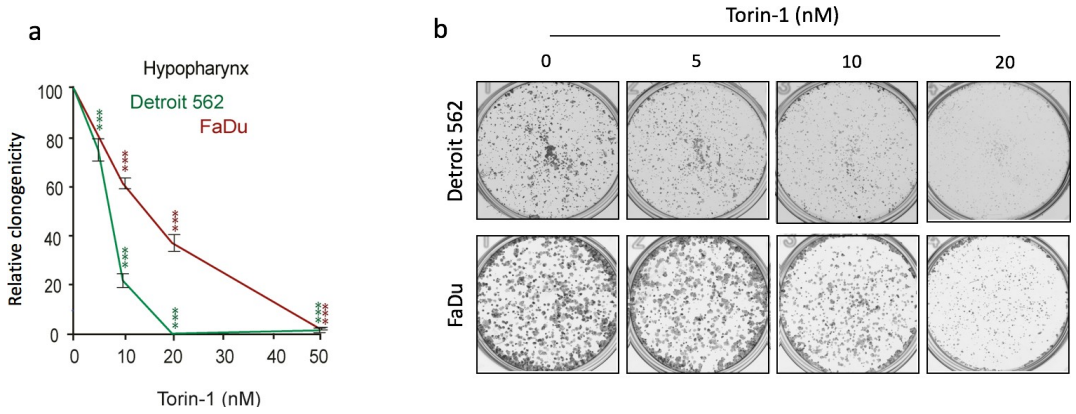

Figure 3.2.9: Inhibition of mTOR kinase by Torin-1 decreases clonogenic potential of hypopharyngeal HNSCC cell lines. Cell lines derived from Hypopharynx, Detroit 562 and FaDu, were seeded at low density and treated with increased concentration of Torin-1 and left to grow ~ 7-10 days. Cells then fixed and stained with Crystal violet and counted using automated colony counter. (a) Line graph represents the % survival factor of cells using colony formation assay. (b) Representative images of the colonies counted after treatment. Error bars represent standard error of the mean (S.E.M) from at least 3 independent experiments; ***$p \leq 0.001$.

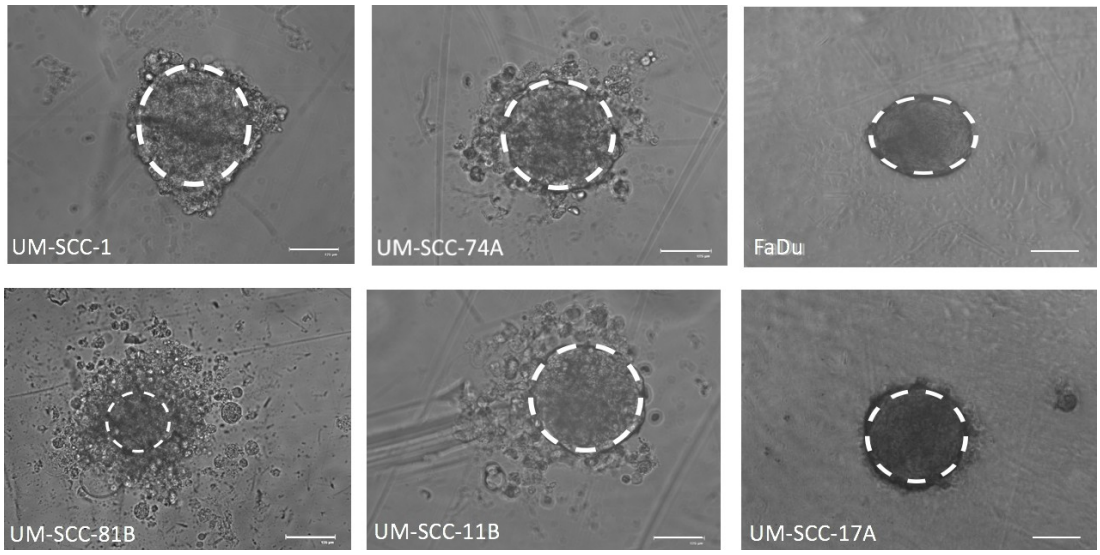

Figure 3.2.10: Most HNSCC cell lines failed to form well defined spheroids. Representative images of some of the HNSCC cell lines tested for their ability to form spheroids. Cells were seeded at either 300 or 500 cells /well in ultralow attachment 96 well plate and left to grow for three days. Scale bar 125 μm.

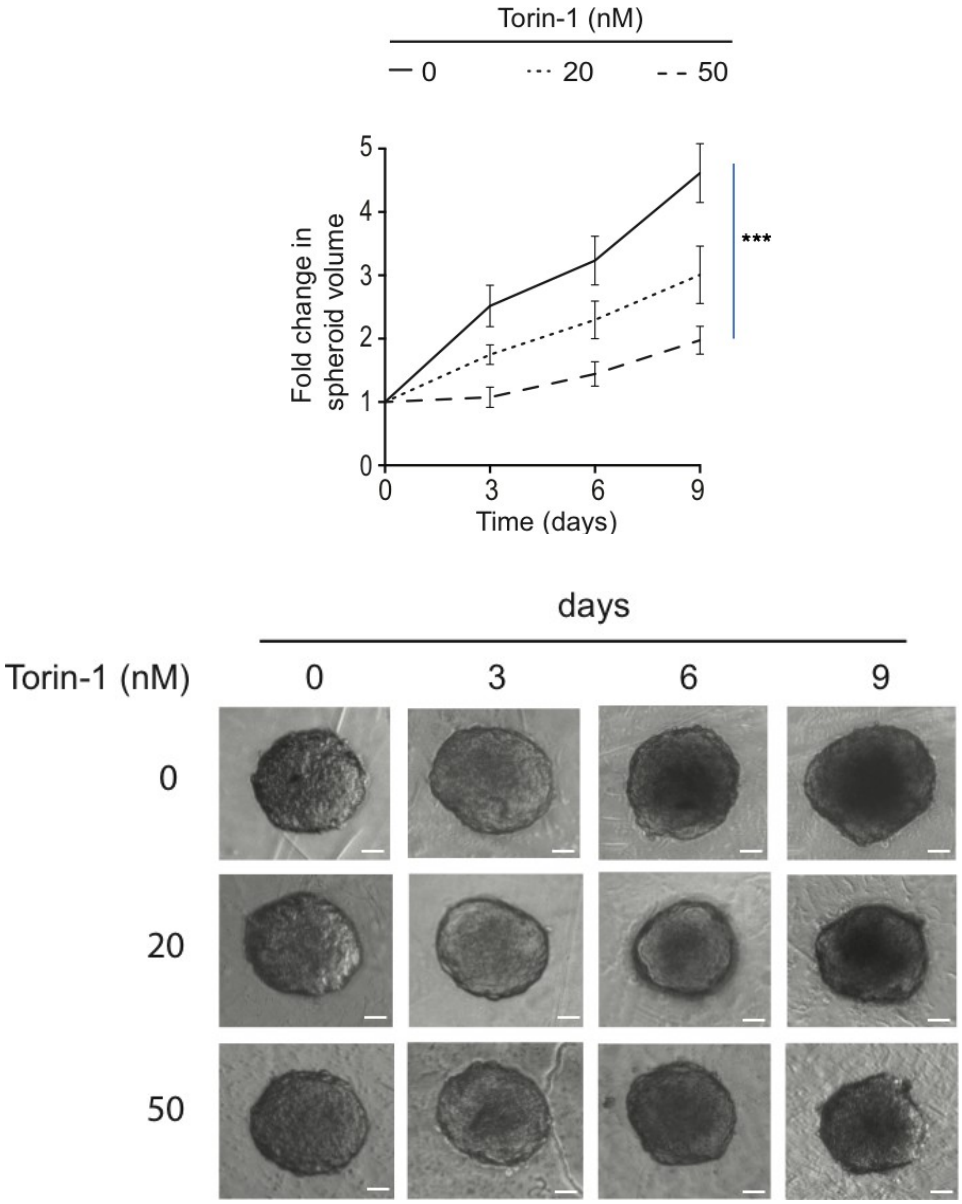

Figure 3.2.11: Torin-1 decreases tumour volume/growth in a 3D spheroid culture. FaDu cells were seeded in ULA 96 well plate at 300 cells/ well, spheroid culture was established for 72 h. The spheroids, once established, were treated with Torin-1 at 0, 20 and 50 nM. Cells were left to grow for 9 days and images of the spheroids were taken every 3 days. (a) Line graph representing the change in fold of spheroid volume over time. (b) Representative images of the spheroids in the indicated time and concentrations. Scale bar (100 μm). Error bars represents standard error of the mean (S.E.M) from at least 3 independent experiments; ***$p \leq 0.001$.

3.2.5 Torin-1-mediated reduction in clonogenicity is not due to enhanced apoptosis.

Since Torin-1 reduced clonogenicity of HNSCC cell lines, this could be a result of a decrease in proliferation rate or an increase in cellular death. To test whether Torin-1 causes apoptosis in the 4 cell lines, the extent of phosphatidylserine (PS) externalisation was measured. In healthy cells, the PS is located in the inner leaflet of the membrane. Upon the presence of an apoptotic stimuli, PS translocates to the outer surface of the membrane and the externalised PS molecules can be recognised by the protein, Annexin-V. Therefore, the cells were stained with Annexin-V, conjugated to FITC and the extent of FITC fluorescence (indicative of increased Annexin-V binding/PS externalisation) was measured by flow cytometry as a measurement of apoptosis. Cells treated with increasing concentrations of Torin-1 showed no signs of apoptosis above the basal level (Figure 3.2.12). In contrast, Cisplatin (10 μM), a DNA alkylating agent, was used as positive control to induce apoptosis in these cell lines (Figure 3.2.12). Furthermore, processing of the caspase substrate, poly-ADP ribose polymerase (PARP), as well as activation of pro caspase-3 could not be observed with increasing concentrations of Torin-1 (Figure 3.2.13). Finally, cells exposed to increasing concentration of Torin-1 appeared to divide at a slower rate compared to cisplatin, which induced significant cell death (Figure 3.2.14).

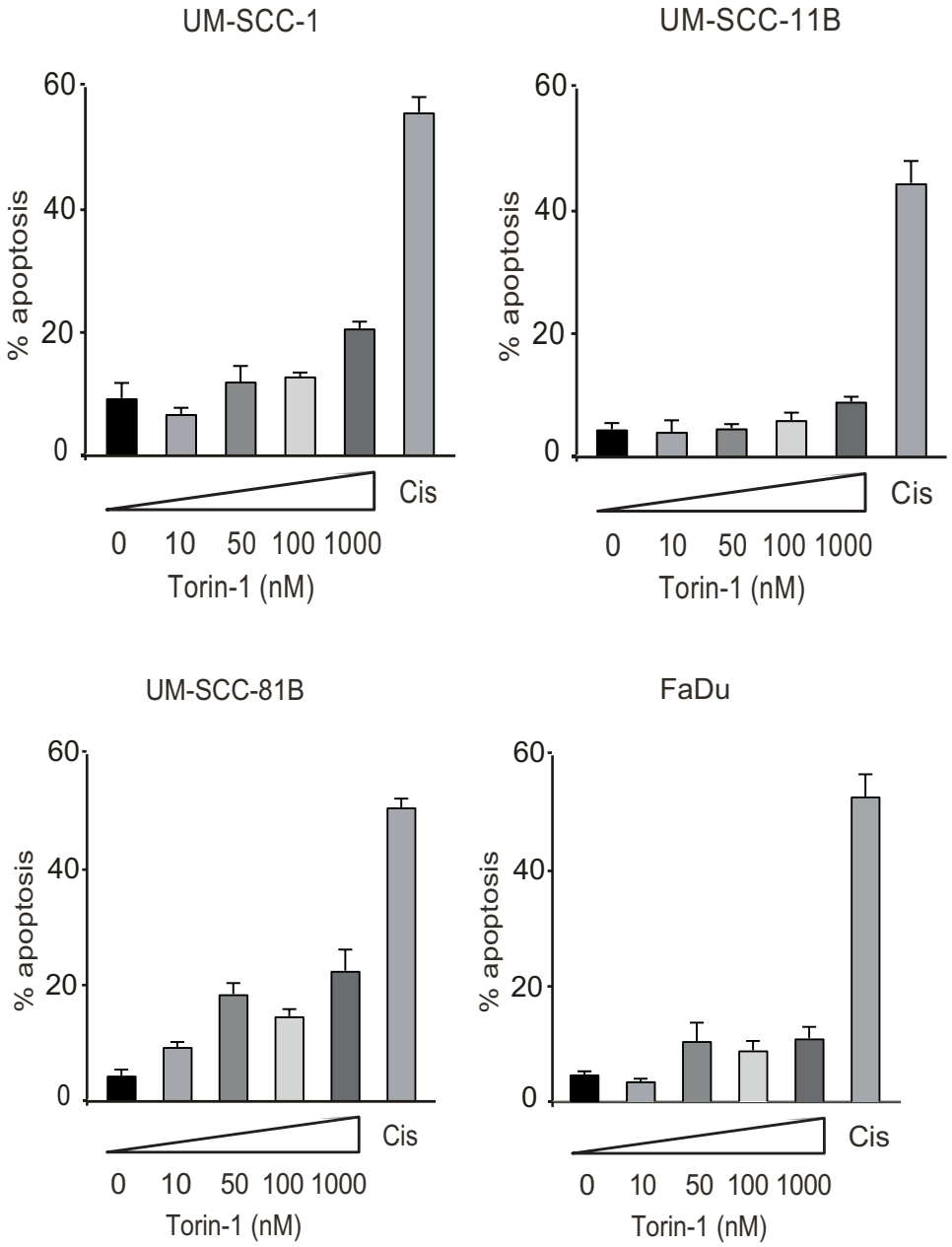

Figure 3.2.12: Torin-1 does not induce apoptosis in HNSCC cell lines. UM-SCC-1, UM-SCC-11B, UM-SCC-81B and FaDu cells were exposed to increasing concentrations of Torin-1 for 24 h and assessed for PS externalisation by flow cytometry. Cisplatin, a positive control, was used at (10 μM) for 24 h. This work was performed in collaboration with Mr. Basabrain in the Varadarajan lab. Error bars represent standarderror of the mean (S.E.M) from at least 3 independent experiments.

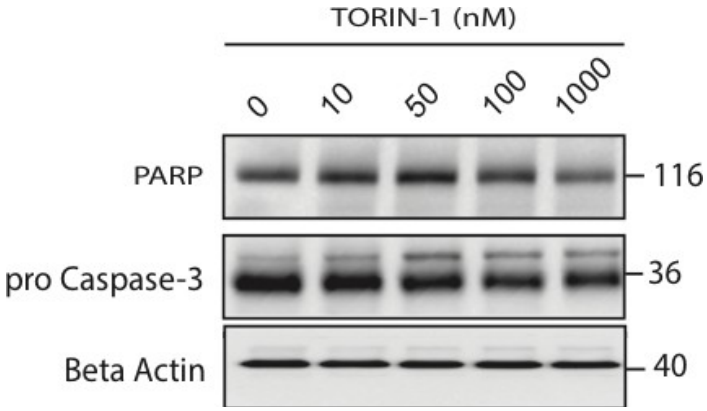

Figure 3.2.13: Torin-1 does not cause caspase activation. UM-SCC-11B were exposed to increasing concentrations of Torin-1 for 24 h and assessed for western blotting using indicated antibodies. Experiment was performed three times. This work was performed in collaboration with Mr.Basabrain in the Varadarajan lab.

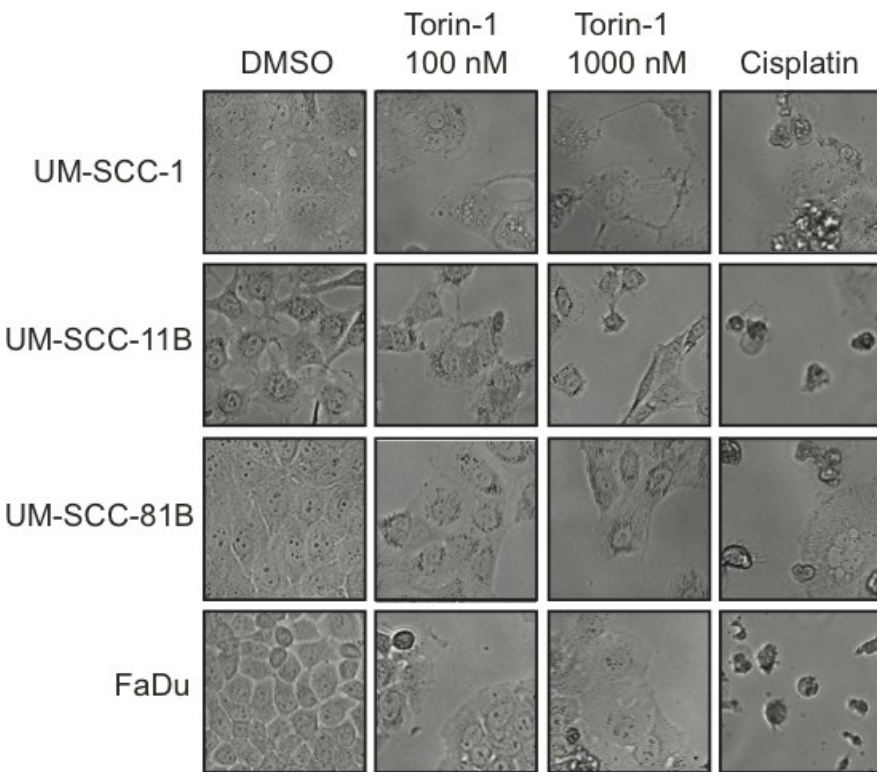

Figure 3.2.14: Torin-1 appears to cause proliferation defect but not apoptosis. Bright field images of HNSCC cell lines, UM-SCC-1, UM-SCC-11B, UM-SCC-81B and FaDu cells exposed to indicated concentrations of Torin-1 or Cisplatin (10 μM) for 24 h. Experiment was performed three times.

3.2.6 Torin-1 mediated reduction in clonogenicity of HNSCC cell lines is not due to an induction of autophagy.

To assess whether Torin-1-mediated reduction in clonogenicity is due to autophagy, UM-SCC-81B cells were exposed to Torin-1 for indicated time points and assessed for the induction of autophagy. In cells exposed to Torin-1, well-defined LC3 positive-autophagosomes were formed in a time-dependent manner, suggesting that Torin-1 was efficient in inducing autophagy (Figure 3.2.15). This could be inhibited with an autophagy inhibitor, 3-MA (Figure 3.2.16). Another inhibitor of autophagic flux, chloroquine prevented the lysosomal degradation of the autophagosomes, which resulted in the accumulation of large LC3 positive-autophagolysosomes (Figure 3.2.16). To test whether inhibiting autophagy has an effect on clonogenic survival, cells were exposed to Torin-1 in the presence of chloroquine or 3-MA. Both these inhibitors appeared to have varied responses in the cell lines tested. In 3 of the 4 cell lines tested, chloroquine appeared to overcome (albeit modestly) Torin-1-mediated reduction in clonogenicity (Figure 3.2.17). In contrast, chloroquine treatment in UM-SCC-11B was too toxic and hence, could not rescue the effects of Torin-1 (Figure 3.2.17). 3-MA rescued the effects of Torin-1 in UM-SCC-1 and UM-SCC-11B, had no effect in UM-SCC-81B, and enhanced Torin-1-mediated reduction in clonogenicity in FaDu (Figure 3.2.17). Since this experiment did not yield consistent results, RNA interference against two critical genes of autophagy, ATG5 and ATG7 were performed to inhibit autophagy. Although the siRNAs used efficiently knocked down these proteins, Torin-1-mediated reduction in clonogenicity could not be altered in cells lacking ATG5 and ATG7 (Figure 3.2.18). Taken together, it can be concluded that Torin-1-mediated reduction in clonogenicity could not be attributed to an induction of autophagy.

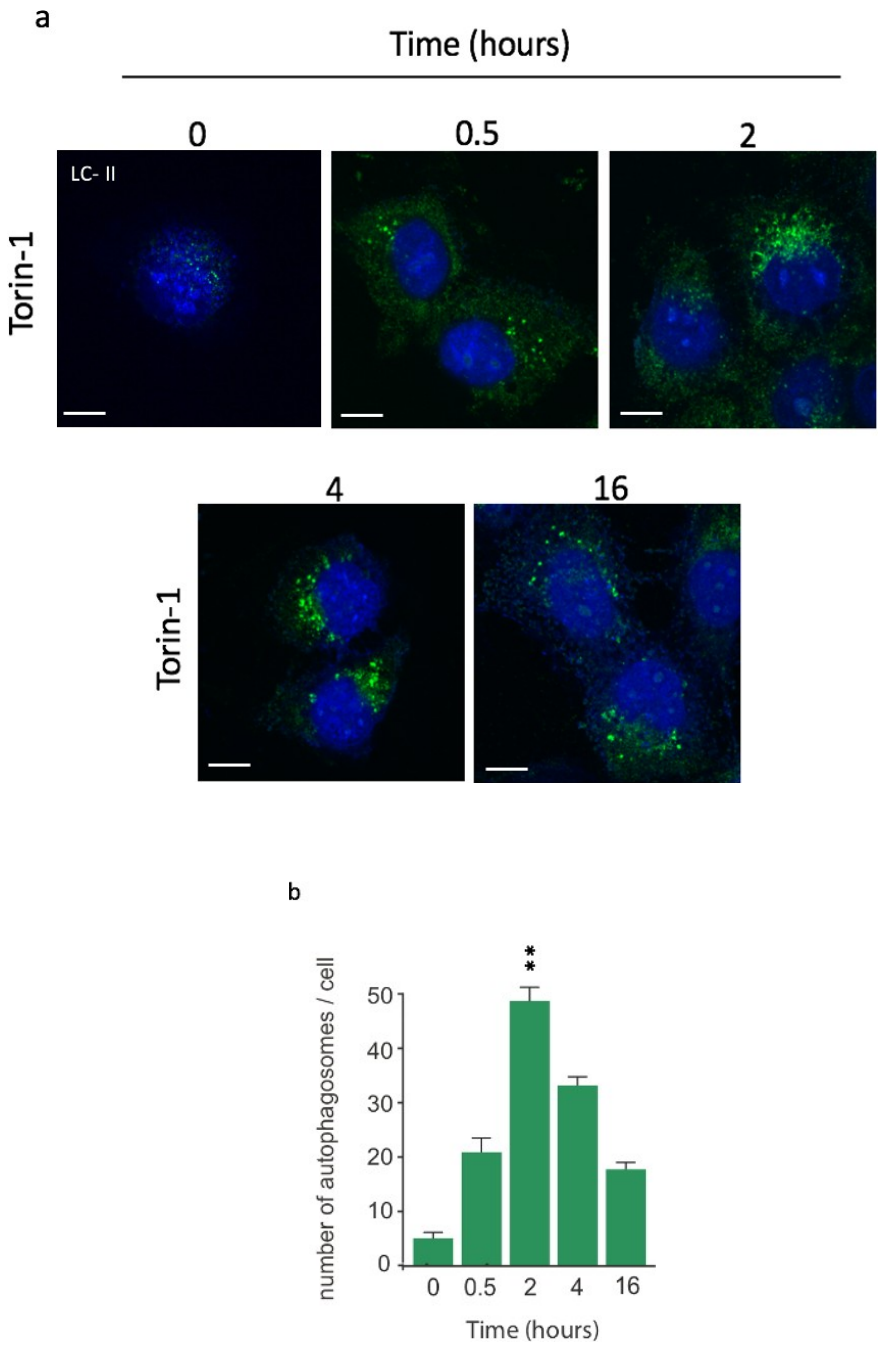

Figure 3.2.15: Torin-1 induces autophagy in a time dependent manner. UM-SCC-81B cells were grown on coverslips and exposed to 100 nM Torin-1 at multiple time points (0, 0.5, 2, 4, 16 h) and formation of autophagosomes was assessed by immunocytochemistry through the staining of endogenous LC3. Scale bar 10 µm. Quantification of autophagosomes was done by counting the number of autophagosomes per cell for 50 cells. Error bars represent standard error of the mean (S.E.M) from at least 3 independent experiments; **$p \leq 0.01$.

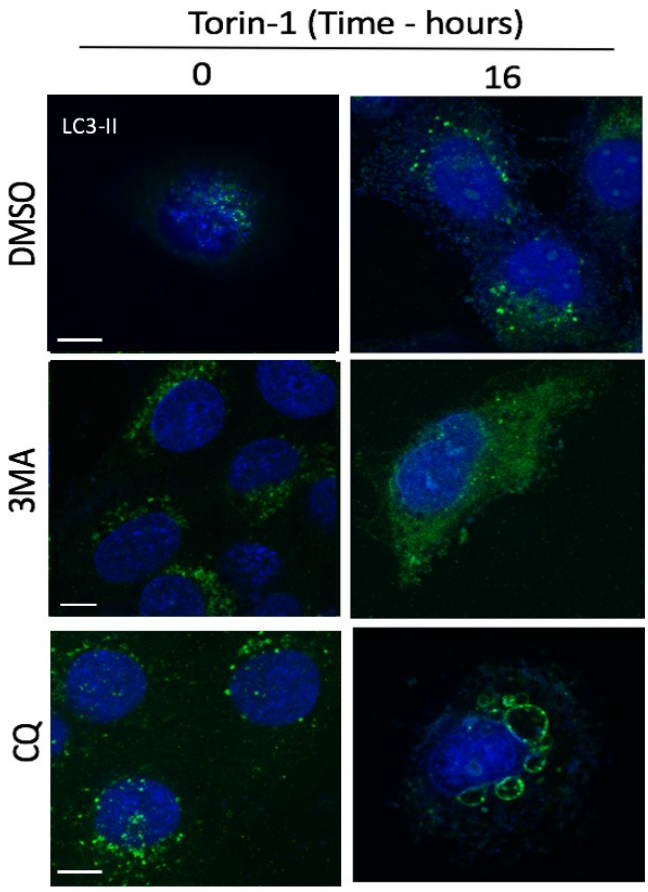

Figure 3.2.16: Torin-1 mediated autophagy can be inhibited by autophagy inhibitors, 3-MA and CQ. UM-SCC-81B were seeded and exposed to either Torin-1 (100 nM) alone or in combination with either 3-MA (10 mM) or CQ (100 μM) for 16 h. The formation of autophagosomes were assessed through the staining of endogenous LC3 from at least 3 independent experiments. Scale bar 10 μm.

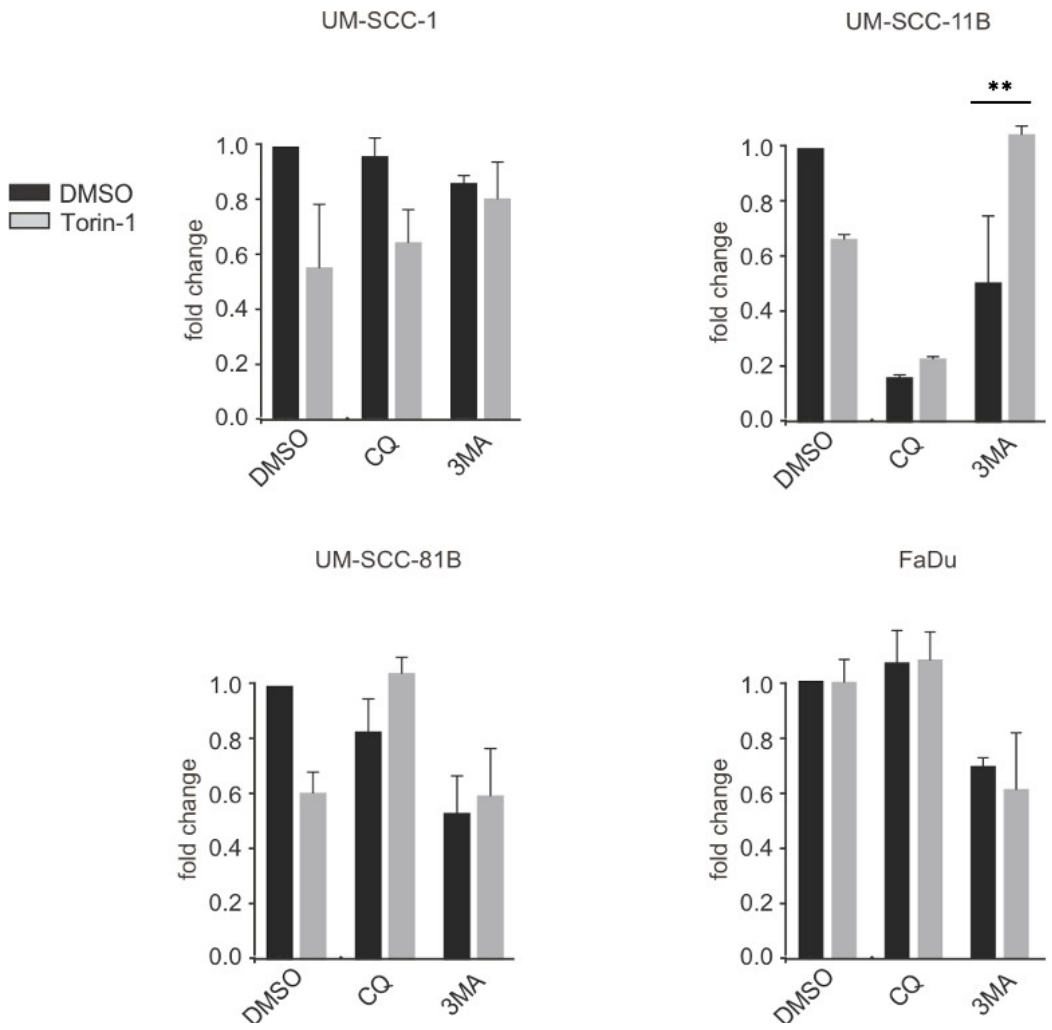

Figure 3.2.17: Torin-1-mediated reduction in clonogenic survival is not due autophagy. HNSCC cell lines, UM-SCC-1, UMSCC-11B, UM-SCC-81B and FaDu were seeded at low density and treated with Torin-1 (2 nM) alone, or in combination with either 3-MA (1 mM) or CQ (0.5 μM) and left to grow for ~ 7-10 days. Cells were then fixed and stained with crystal violet and colonies counted using automated colony counter. Error bars represents standard error of the mean (S.E.M) from at least 3 independent experiments, **$p \leq 0.01$.

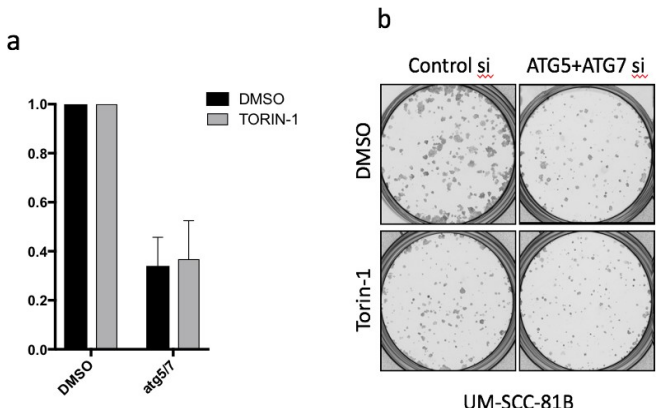

Figure 3.2.18: Genetic knockdown of proteins critical for autophagy induction does not overcome the effects of Torin-1 in decreasing clonogenicity. UM-SCC-81B cells were seeded and transfected with either control siRNA or siRNAs against ATG5 and ATG7. Cells were re-seeded 3 days post transfection at low density and treated with Torin-1 (2 nM) and left to grow for ~ 7-10 days. Cells were then fixed and stained with crystal violet and counted using automated colony counter. (a) Represents the fold change in clonogenic survival in UM-SCC-81B in cells with lowered expression of ATG5 and ATG7 in comparison to control si-transfected cells (the clonogenic potential is normalized to 1). (b) Representative images of the colonies observed after the indicated treatments. Error bars represent standard error of the mean (S.E.M) from at least 3 independent experiments.

3.3 Discussion

Dysregulation of the mTOR signalling pathway has been associated with several malignancies [141]. In HNSCC, inhibition of mTOR complexes 1 and 2 using Torin-1 was effective in reducing the clonogenic potential of different HNSCC cell lines in a 2D culture as well as reducing proliferation in a 3D spheroid model (Figures 3.2.6-3.2.9 and 3.2.11). The expression levels of mTOR and p-mTOR varied across the cell lines tested, which could be due to the different mutations that can occur in HNSCC [142, 143, 144, 145]. For instance, mutations in PI3K has been reported to make the cells more sensitive to mTOR/PI3K inhibitors [144] and loss of PTEN expression and/or function can modulate PI3K/mTOR sensitivity and resistance [146]. Out of 8 cell lines, A253 and UM-SCC-74A have missense mutation in PTEN gene while UM-SCC-1 and UM-SCC-11B carry a wild type gene. PI3KCA gene is amplified in UM-SCC-1, UM-SCC-11B and UM-SCC-74A while A253, FaDu and Detroit 562 have a wild type. Expression levels of p-mTOR correlated with its downstream signalling proteins, namely p-S6K and p-AMPK but not p-AKT (Figure 3.2.1). It must be noted that expression levels of p-AKT correlated well with the levels of total AKT, which suggested that there might be other kinases that are responsible for its phosphorylation. PI3K can activate AKT through the conversion of PIP2 to PIP3, in a reaction that can be inhibited by PTEN [136]. In 7 % of HNSCC, PTEN has a loss of function mutation [145], which could be attributed to the changes in the levels of p-AKT. Moreover, p-AKT is a downstream substrate of mTOR complex 2 and not complex 1, which again could impact its phosphorylation status (Figure 3.3.1) [147].

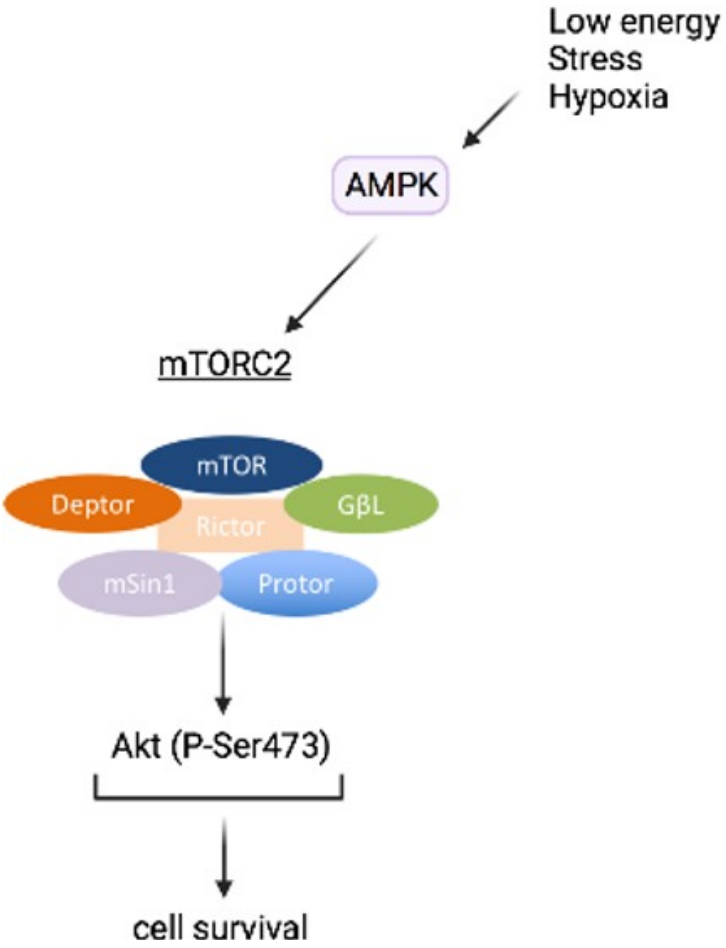

Figure 3.3.1: AMPK promotes mTORC2 signaling independently of mTORC1-mediated negative feedback. Akt can be phosphorylated at Ser473 indirectly by the phosphorylation of mTORC2 via AMPK during stress or low energy levels.

A comparison of the sensitivity of the different cell lines to Torin-1 (UM-SCC-1 > 81B > 17A > 11B = Detroit = 74A = FaDu > A253) to the expression levels of the major players in mTOR signalling, namely mTOR, p-mTOR, Raptor and Rictor revealed that the sensitivity of UM-SCC-1 could be due to the lowest expression levels of these proteins, which could enable Torin-1 to be most effective in this cell line (Figures 3.2.1 and 3.2.6). In contrast, A253 and FaDu express relatively high levels of these proteins and exhibit much resistance to Torin-1 (Figures 3.2.1,3.2.6 and 3.2.9). In the remaining cell lines, there was no direct correlation in respect to the level of expression and the sensitivity to Torin-1, suggesting that there may be other factors that may play a role in their resistance.

Out of 8 cell lines tested, only FaDu and UM-SCC-17A cells succeeded in forming spheroids without the need of other supplements, such as B27 and N2 (Figure 3.2.10). Although the other cell lines used in this study could be modulated to grow in spheroid culture with extra supplements (Dr. Parsons, University of Liverpool; personal communications), reports show that addition of such supplements could alter spheroid growth [148], which in turn could potentially alter mTOR signalling on its own. Furthermore, the concentration of Torin-1 used for treating spheroids was significantly higher than what was used in the clonogenic assay (Figure 3.2.11). This could be attributed to the differences in the access of the inhibitor to the cells, when grown as a 2D *versus* 3D culture.

Since mTOR is a major negative regulator of autophagy, inhibition of mTOR either by nutrient deprivation or pharmacological agents, such as Torin-1, should activate autophagy as a survival mechanism and to prevent apoptosis [149]. Indeed, exposure of cells to Torin-1 resulted in autophagy in a time dependant manner, with no indications of apoptosis (Figure 3.2.12 and 3.2.15). Exposure of cells to 3-MA

prevented the formation of autophagosomes by inhibiting phosphatidylinositol 3-kinases (PI3K) (Figure 3.2.16), whereas chloroquine accumulated in the lysosomes and neutralised its acidity, which in turn prevented the lysosomal degradation of the autophagosomes. This could be observed by the appearance of the swollen LC3-positive autophagolysosomes (Figure 3.2.16). Nevertheless, genetic knockdown of ATG5 and ATG7 convincingly demonstrated that the reduction in clonogenicity observed with Torin-1 is independent of an induction of autophagy (Figures 3.2.18). Therefore, it could be concluded that Torin-1 reduced the clonogenicity of HNSCC cell lines by some other mechanism.

Taken together, this chapter focused on the effect of Torin-1 on HNSCC cell proliferation and concluded that the effect of Torin-1 was independent of apoptosis and autophagy. Rather, Torin-1 appears to exert its effect through a protein translational defect. The next chapter will focus on exploring the potential of combining Torin-1 with other conventional therapies in HNSCC.

Chapter 4

Exploring potential therapies for combination with mTOR inhibition in HNSCC

1. Chapter contents

4.1 Introduction

Integrative approaches are needed for optimal management of head and neck cancers, as they comprise heterogenous tumours arising from different subsites [150]. Surgery and radiotherapy (RT) are among the most frequent modalities used in the treatment of head and neck patients [150]. The main goals of these regimes are to achieve a loco-regional control, better survival rate and minimal toxicity to the surrounding non-cancer tissues [151]. The extent of using RT as a treatment strategy for different cancers varies widely. In head and neck cancers, RT has been used as a primary treatment and in the early stages of HNSCC, RT as a single modality is an effective with its cure rate comparable to what is achieved by surgery [152, 153]. In more advanced HNSCC, a combination of surgery and RT is more effective in controlling metastasis and have a better survival rate in comparison to monotherapy [152]. Choosing the appropriate approach for a patient depends on different factors, such as functional impairment that can be caused by that method and patient performance status when choosing the method [154].

Combining RT with chemotherapeutic agents account for another promising approach for HNSCC patients. Radiosensitisers, such as PARP inhibitors, when used in conjunction with RT provides an increase in effectiveness of RT towards cancer cells. The rationale behind this combination is due the enzymatic functions of PARP (poly-ADP ribose polymerase) in repairing DNA damage [155]. Thus, upon inhibition, PARP prevents any repair from occurring and in turn enhances the efficacy of RT. Moreover, PARP is highly expressed in cancers like TNBC and breast cancer, which exhibit high sensitivity towards PARP inhibitors, as these cancer cells are dependent on PARP for survival [156]. In non-small cell lung carcinoma (NSCLC), Olaparib, a PARP inhibitor sensitizes the tumour to RT both *in vivo* and *in vitro)*[157]. Similarly,

EGFR monoclonal antibodies, such as Cetuximab and panitumumab have been used to sensitize the cytotoxic effect of RT, which results in complete or partial regression of tumour. In a randomized phase III trial, Cetuximab in conjunction with RT improved the overall survival in HNSCC patients and it was achieved without the toxic effects that normally occur with RT [158].

In spite of advances in RT (proton beam therapy), acute toxicity, mucositis and dysphagia are frequently observed as a consequence of RT in HNSCC patients. Mucositis and dysphagia are developed in approximately 50% of patients, as a result of which patients needed symptomatic care for 12 weeks from the 3rd week of initiation of RT [159]. Another rare but serious complication of RT is osteoradionecrosis (ORN), which can be defined as bone death that arises as a result of damage in blood vessels and normal tissues surrounding the bone following RT. This can result in significant deterioration of the patients' quality of life [160]. Surgery complemented with medical therapies such as topical or systemic antibiotics, pentoxifylline and tocopherol, or hyperbaric oxygen (HBO) can be used to treat ORN. The use of HBO was introduced in 1983 by Marx and later in 1985 was used as protentional therapy for ORN [161]. HBO is based on administrating 100% oxygen at high pressure to increase the level of oxygen dissolved in the plasma independently of haemoglobin which can help in healing tissues post RT [162].

Similarly, Cisplatin, first made in 1844 by M. Peyrone, has been of great interest over the years for treating solid tumours including cancers of head and neck [163, 164]. Cisplatin, a DNA alkylating agent that can interfere with DNA repair mechanism, considered as one of the first line treatment of HNSCC, either as a single agent or combined with irradiation. Combination of radiotherapy and Cisplatin in postoperative HNSCC patients resulted in controlled metastasis and low disease

progression [165]. Despite the benefits, this combination resulted in high toxicity and severe side effects, including vomiting and cytopenia [165].

In this chapter, mTOR kinases will be targeted using Torin-1 in conjunction with conventional therapies such as Cisplatin, RT and also other novel therapies including inhibitors of BCL-2 family members (BH3 mimetics), PARP kinase (Olaparib), Wee1 (AZD1775), the enzyme glutaminase (CB-839), protein kinase A (H-89) and PP2A activators (FTY720, DT-061). Following these combinations, the extent of clonogenic survival in different HNSCC cell lines will be assessed, in an attempt to identify promising leads that could be taken for further studies. When the effect seen after the administration of two or more agents exceeds what is expected from a single agent, it is known synergism or super additivity. On the other hand, additivity is when the effect of the combination is similar to what a single agent can cause. Throughout the experiments in this chapter, cells were treated with Torin-1 for 16 h followed by the designated treatment.

4.2 Results

4.2.1 Targeting mTOR kinases by Torin-1 does not exhibit a greater reduction in clonogenicity, when combined with cisplatin.

Since Torin-1 caused a decrease in clonogenic survival, it was hypothesized that Torin-1 when combined with other conventional therapies, such as cisplatin, could have a synergetic effect in HNSCC cell lines. Therefore, cisplatin at a concentration of 500 nM was chosen based on IC50 calculations (based on studies independent from this thesis) for these studies. The cell lines exhibited different sensitivity towards cisplatin, which can be ordered from the most sensitive to most resistant as follows:

UM-SCC-11B > UM-SCC-1 = UM-SCC-74A > FaDu

Although the concentration of cisplatin for different cell lines should have been modified to be better reflect the IC50 measurements, due to time constraints, the concentration of cisplatin was fixed at 500 nM, as it decreased but not abolished the clonogenicity of the chosen cell lines (Figures 4.2.1). Cisplatin did not enhance the effect of Torin-1 in UM-SCC-1 and FaDu. In UM-SCC-11B Cisplatin alone induced a significant reduction, which made the effect of Torin-1 difficult to notice. In contrast, a significant reduction effect was observed when cisplatin was treated in combination with Torin-1 in UM-SCC-74A cells (Figures 4.2.1). These results indicate that co- administration of Cisplatin with Torin-1 may not offer any benefit over Cisplatin monotherapy in HNSCC.

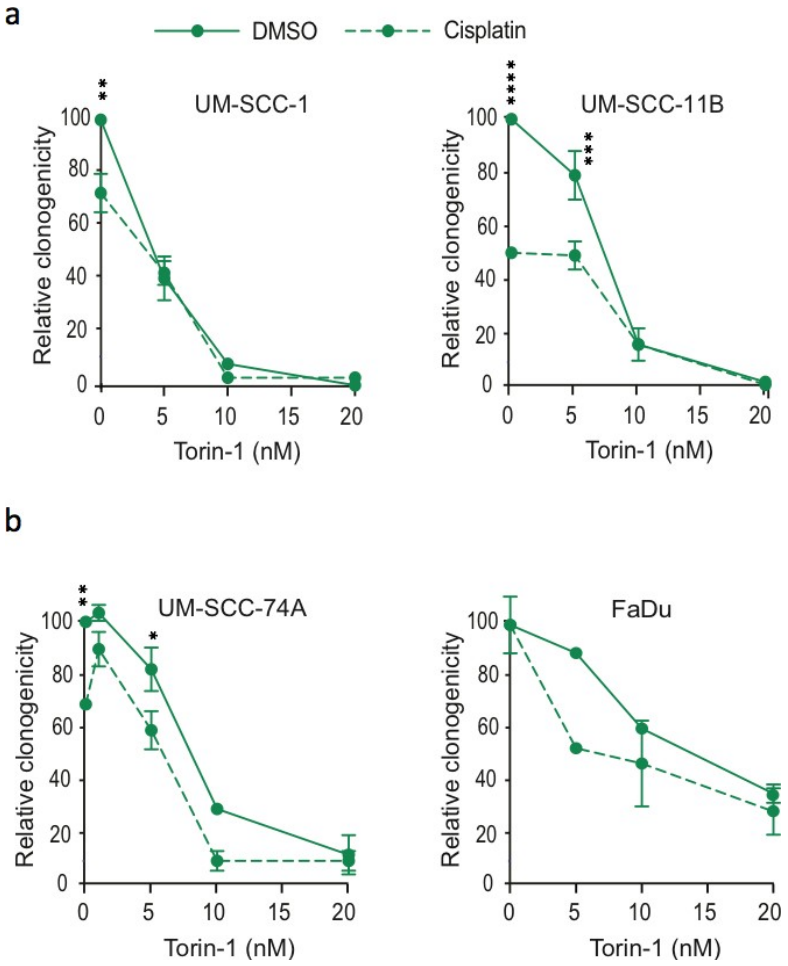

Figure 4.2.1: Torin-1 does not synergise with Cisplatin to reduce the clonogenic potential of HNSCC cell lines. Oral cavity cell line**,** UM-SCC-1, laryngeal cell line, UM-SCC-11B, oropharyngeal cell line, UM-SCC-74A, and hypopharyngeal cell line, FaDu, were seeded at low density and treated with increasing concentrations of Torin-1 first for 16 h, the following day they were combined with Cisplatin (500 nM). Cells were allowed to form colonies and counted for clonogenic assay using automated colony counter. Line graph represents the % relative clonogenicity of cells. Error bars represent standard error of the mean (S.E.M) from at least 3 independent experiments. ****$p \leq 0.0001$, ***$p \leq 0.001$, **$p \leq 0.01$, *$p \leq 0.05$.

4.2.2 Targeting mTOR kinases does not synergise with irradiation (IR) in HNSCC cell lines.

As cisplatin failed to have a synergetic effect with Torin-1 in most of the HNSCC cell lines; the next step was to assess the effect of Torin-1 in combination with another conventional therapy, such as IR. A range of doses of γ-radiation was chosen (0.25 Gy- 2 Gy), which appeared to decrease the clonogenicity of all cell lines tested. The cell lines exhibited differential sensitivity towards IR, which can be ordered from the most sensitive to most resistant as follows:

UM-SCC-1 > UM-SCC-74A > UM-SCC-11B > FaDu

In FaDu, exposure to increasing doses of IR did not enhance the effect of Torin-1 in reducing the clonogenicity at higher IR dose, it increased the clonogenic potential of this cell line. In UM-SCC-1, Torin-1 (2 nM) on its own had a significant effect in reducing the clonogenicity, whereas co-treatment with IR had only a modest reduction effect (Figure 4.2.2). This is most likely because the concentration of Torin-1 used in this experiment for UM-SCC-1 was already too high to induce a significant reduction in clonogenicity on its own. In contrast, a modest effect of the combination in reducing clonogenicity was observed in UM-SCC-11B and UM-SCC-74A (Figure 4.2.2). Taken together, these results suggested that combining Torin-1 with IR will most likely not have significant benefits over IR monotherapy in HNSCC patients.

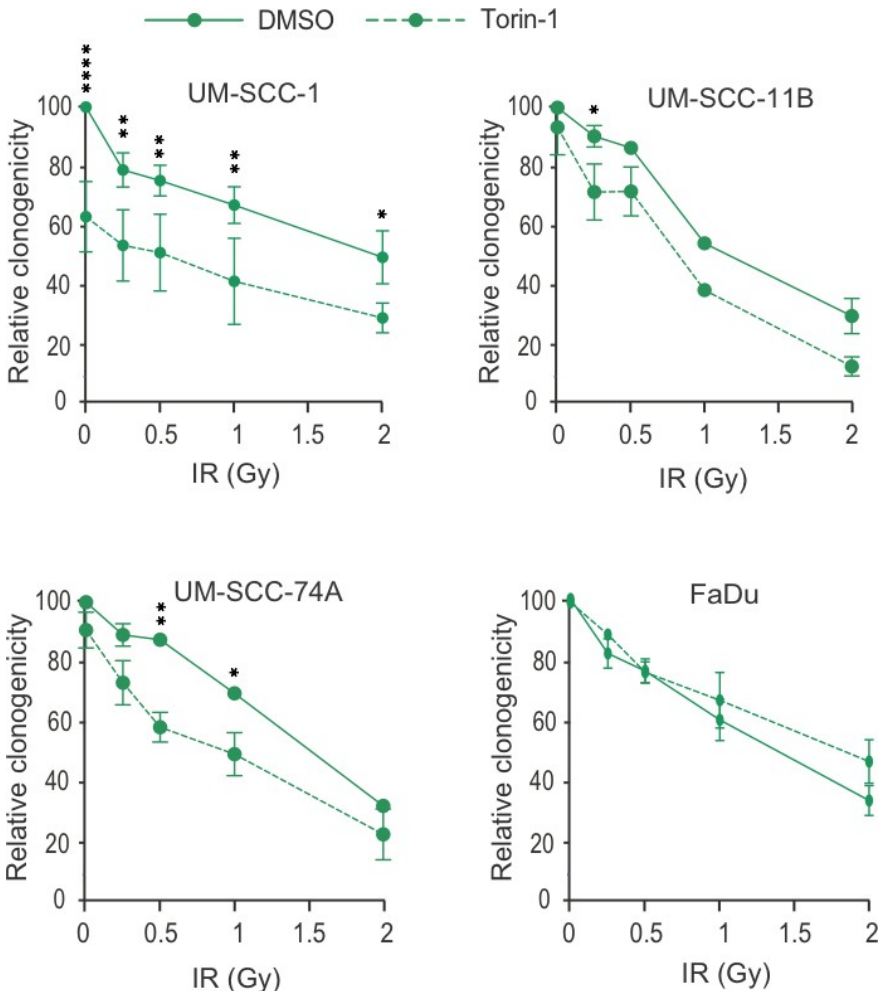

Figure 4.2.2: Combination of γ-radiation and Torin-1 failed to decrease clonogenicity of HNSCC cell lines. Oral cavity cell line**,** UM-SCC-1, laryngeal cell line, UM-SCC-11B, oropharyngeal cell line, UM-SCC-74A, and hypopharyngeal cell line, FaDu, were seeded in a 6-well plate at low density and treated with Torin-1 (2 nM) and exposed to 0, 0.5, 1, 1.5 and 2 Gy of γ-rays. Cells were allowed to form colonies and counted for clonogenic assay using automated colony counter. Colony counting showed additive effects of the combination in 3 out of the 4 cell lines tested but no synergy. Line graph represents the % relative clonogenicity of cells. Error bars represent standard error of the mean (S.E.M) from at least 3 independent experiments. ****$p \leq 0.0001$, **$p \leq 0.01$, *$p \leq 0.05$.

4.2.3 Targeting mTOR kinases does not synergise with Olaparib+IR combination in HNSCC

Olaparib, a potent PARP1 and PARP2 inhibitor, is an antitumor drug and a dose intensifier for radiotherapy. Therefore, Olaparib was combined with Torin-1 to assess its effect on clonogenicity of HNSCC cell lines. The concentration of Olaparib was fixed at 200 nM in all cell lines, as lower concentrations had minimal effects on decreasing clonogenicity (data not shown). Since Olaparib is a radiosensitiser, the speculation was that IR+Olaparib combination would greatly be enhanced with Torin-1. However, only a modest reduction in clonogenicity was observed in some of the cell lines when exposed to IR+Olaparib (Figure 4.2.3). Therefore, further optimisations were performed to determine appropriate concentrations of Olaparib, following which the effects of a triple combination of Torin-1, Olaparib and IR were assessed. UMSCC-1, UM-SCC-11B, UM-SCC-74A and FaDu exhibited a modest additive effect with the triple combination (Figure 4.2.3). These results indicated that Torin-1 does not enhance the effect mediated by the combination of RT and Olaparib in HNSCC cell lines, thus failing to offer therapeutic benefits over monotherapy.

4.2.4 Targeting mTOR kinases does not synergise with Wee1 kinase inhibitor + IR combination in HNSCC

The Olaparib study was further extended to include a WEE1 tyrosine kinase checkpoint inhibitor, AZD1775. Since AZD1775 causes DNA damage and forces the cells to enter M phase, HNSCC cells were exposed to AZD1775 (10 nM) with or without Torin-1 (2nM) in presence of IR. In UM-SCC-1, AZD1775 had an additive effect towards IR however, adding Torin-1 to this combination enhanced this effect and reduced the clonogenicity significantly (Figure 4.2.4).

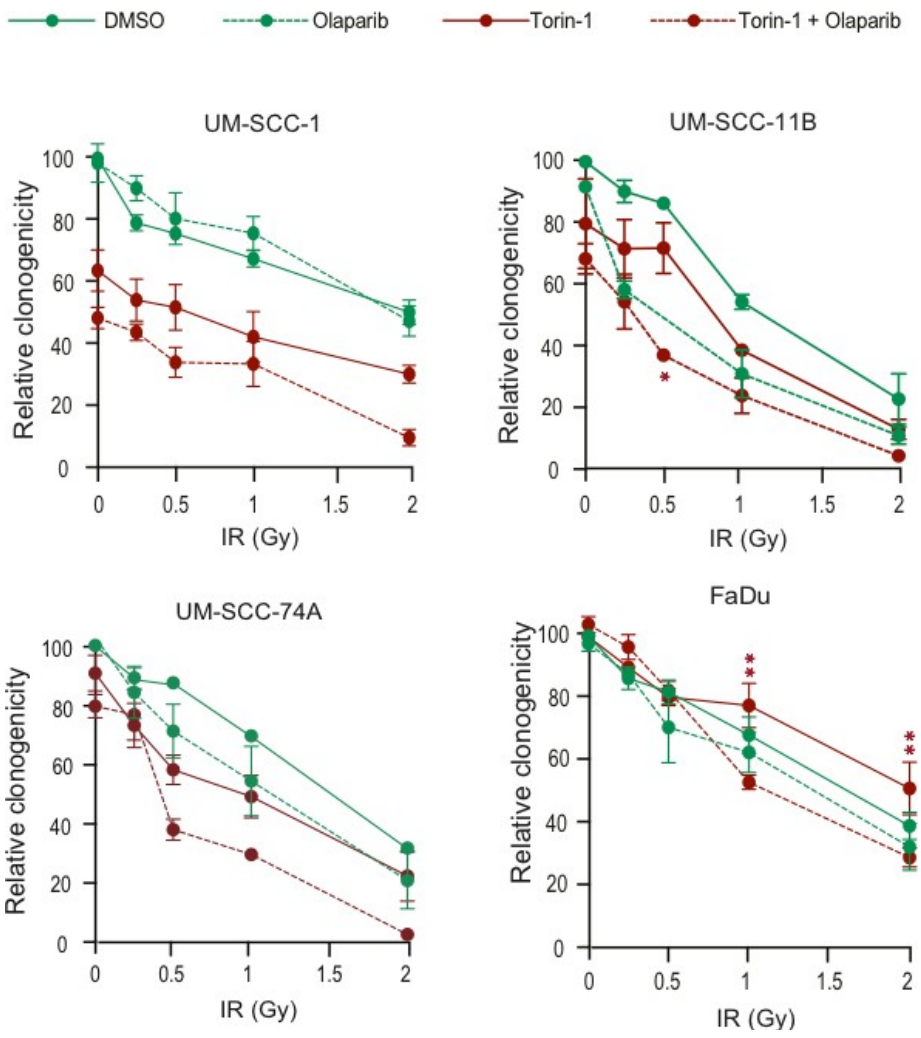

Figure 4.2.3: Torin-1 does not synergise with combination of Olaparib and IR to reduce the clonogenic potential of HNSCC cell lines. Oral cavity cell line**,** UM-SCC-1, laryngeal cell line, UM-SCC-11B, oropharyngeal cell line, UM-SCC-74A, and hypopharyngeal cell line, FaDu, were seeded at low density and treated with Torin-1 (2 nM) or Olaparib (200 nM) alone or in combination of both with increasing concentration of γ-rays (Gy). Cells were allowed to form colonies and colonies were counted for clonogenic assay using automated colony counter. Colony counting showed an additive effect of the combination and no synergy. Line graph represents the % relative clonogenicity of cells. Error bars represent standard error of the mean (S.E.M) from at least 3 independent experiments. **$p \leq 0.01$, *$p \leq 0.05$.

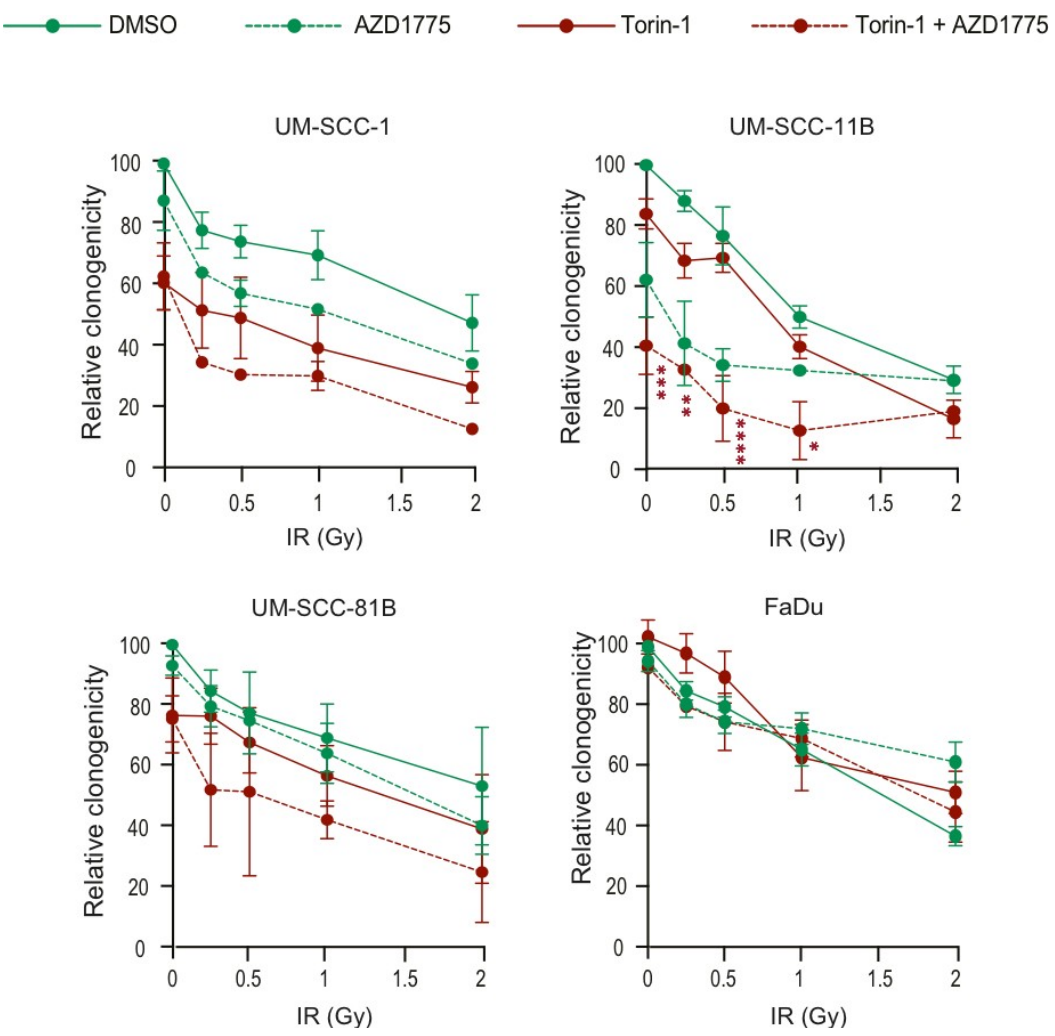

Figure 4.2.4: Torin-1 does not synergise with combination of Wee1 kinase inhibitor and IR to reduce the clonogenic potential of HNSCC cell lines. Oral cavity cell line**,** UM-SCC-1, laryngeal cell line, UM-SCC-11B, oropharyngeal cell line, UM-SCC-74A, and hypopharyngeal cell line, FaDu, were seeded at low density and treated with Torin-1 (2 nM) alone or AZD1775 (10 nM) or in combination of both with increasing concentration of γ-rays (Gy). Cells were allowed to form colonies and colonies were counted for clonogenic assay using automated colony counter. Error bars represent standard error of the mean (S.E.M) from at least 3 independent experiments. ****$p \leq 0.0001$, ***$p \leq 0.001$, **$p \leq 0.01$, *$p \leq 0.05$.

In UM-SCC-11B, there was a significant reduction in clonogenicity when the cells were exposed to AZD1775 and that effect was further enhanced with the addition of Torin-1 (Figure 4.2.4). In UM-SCC-81B there was a modest reduction in clonogenicity with either Torin-1 or AZD1775 and the triple combination had a modest effect in reducing the clonogenicity (Figure 4.2.4). These results indicated that Torin-1 does not enhance the effect mediated by the combination of RT and AZD1775 in HNSCC cell lines, thus failing to offer therapeutic benefits over monotherapy.

4.2.5 Targeting mTOR kinases does not synergise with inhibition of protein kinase A in most HNSCC cell lines

As conventional therapies failed in attenuating the effect of Torin-1 in reducing clonogenicity, the next step was to try novel therapies, such as the inhibitor of protein kinase A (PKA), H-89 and assess the effects on clonogenicity of HNSCC cell lines. H-89 is a cell permeable inhibitor of PKA, which has been shown to inhibit cell growth and induce apoptosis in pancreatic cancer cells [166]. Based on IC50 calculations, a concentration of 1 and 5 μM of H-89 was chosen for these studies. In three out of four cell lines tested, H-89 failed in decreasing the clonogenicity when combined with Torin-1. In UM-SCC-1, H-89 had an effect as a single agent and the effect was not enhanced by the addition of Torin-1 (Figure 4.2.5), whereas H89 significantly enhanced the effect of Torin-1 in UM-SCC-11B (Figure 4.2.5). In UM-SCC-81B, H-89 did not have any effect on clonogenicity but when combined with Torin-1, it had an adverse effect and increased the clonogenicity to a level that exceeded that of the control (Figure 4.2.6). FaDu exhibited a modest reduction when exposed to the combination (Figure 4.2.6). These results suggested that H-89 may not have therapeutic benefits for HNSCC patients when combined with Torin-1.

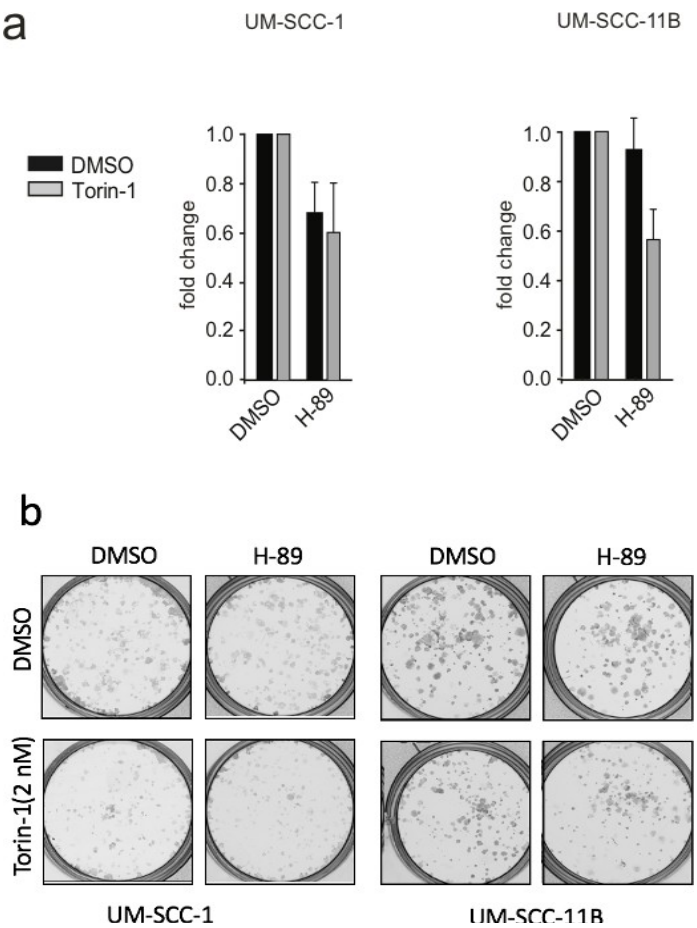

Figure 4.2.5: Torin-1 does not synergise with H-89 to reduce the clonogenic potential of UM-SCC-1 but did synergise with UM-SCC-11B cell lines. UM-SCC-1 and UM-SCC-11B were seeded at low density and treated with Torin-1 (2 nM) alone or in combination with H-89 (1 μM). Cells were allowed to form colonies and colonies were counted for clonogenic assay using automated colony counter. (a) Graph shows data in which DMSO and Torin-1 was normalised to 1.0, and the other treatments were depicted as fold changes in relation to DMSO. (b) Representative images of the colonies counted after treatment. Error bars represent standard error of the mean (S.E.M) from at least 3 independent experiments.

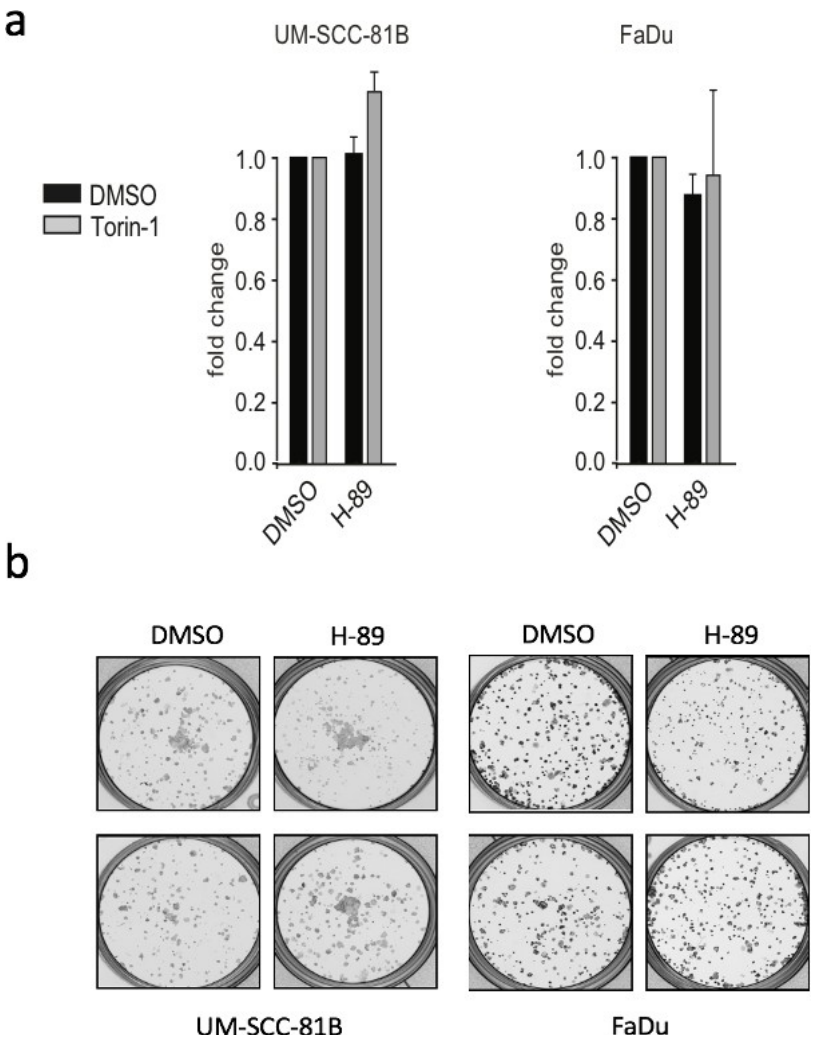

Figure 4.2.6: Torin-1 does not synergise with H-89 to reduce the clonogenic potential of UM-SCC-81B and FaDu cell lines. UM-SCC-81B and FaDu were seeded at low density and treated with Torin-1 (2 nM) alone or in combination with H-89 (1 μM and 5 μM respectively). Cells were allowed to form colonies and colonies were counted for clonogenic assay using automated colony counter. (a) Graph shows data in which DMSO and Torin-1 was normalised to 1.0, and the other treatments were depicted as fold changes in relation to DMSO. (b) Representative images of the colonies counted after treatment. Error bars represent standard error of the mean (S.E.M) from at least 3 independent experiments.

4.2.6 Targeting mTOR kinases does not synergise with activators of PP2A or glutamine inhibitor CB-839 in HNSCC cell lines.

Activators of the enzyme protein phosphatase 2 A (PP2A) have shown promise in conjunction with mTOR inhibitors in other malignancies [167]. To recapitulate these findings in HNSCC, PP2A activators, DT-061 and FTY720 (1 mM and 0.5 μM, respectively, based on IC50 calculations, as detailed previously) were chosen. For FTY720, UM-SCC-1 had a modest reduction in clonogenicity and combining it with Torin-1 did not enhance the effect further (Figure 4.2.7). In UM-SCC-11B and FaDu, FTY720 had a significant reduction in clonogenicity and when combined with Torin-1 it showed an adverse effect (Figure 4.2.7). In UM-SCC-81B the combination of FTY720 and Torin-1 showed a modest reduction in clonogenicity. DT-061 on the other hand, had a significant reduction in clonogenicity in UM-SCC-1 when combined with Torin-1 (Figure 4.2.7). However, this promising effect observed in UM-SCC-1 could not be reproduced in the other cell lines, especially in FaDu and UM-SCC-11B; as the results with DT-061 were similar to the findings with FTY720 (Figure 4.2.7).

Finally, a novel therapeutic combination of a glutaminase (GLS-1) inhibitor, CB-839 with Torin-1 was assessed. The rationale behind this is the activation of mTOR by GLS-1 [168]. Three out of the 4 cell lines tested, UM-SCC-1, UM-SCC-11B and FaDu had an additive effect when exposed to the combination of Torin-1 and CB-839, at a chosen concentration of 500 nM (Figure 4.2.8). In contrast, this combination did not exhibit any enhanced effect than single treatments in UM-SCC-81B (Figure 4.2.8). Taken together, these findings revealed that targeting mTOR kinases in HNSCC does not seem to offer a significant benefit in combination with treatments that have otherwise been deemed promising for other cancers.

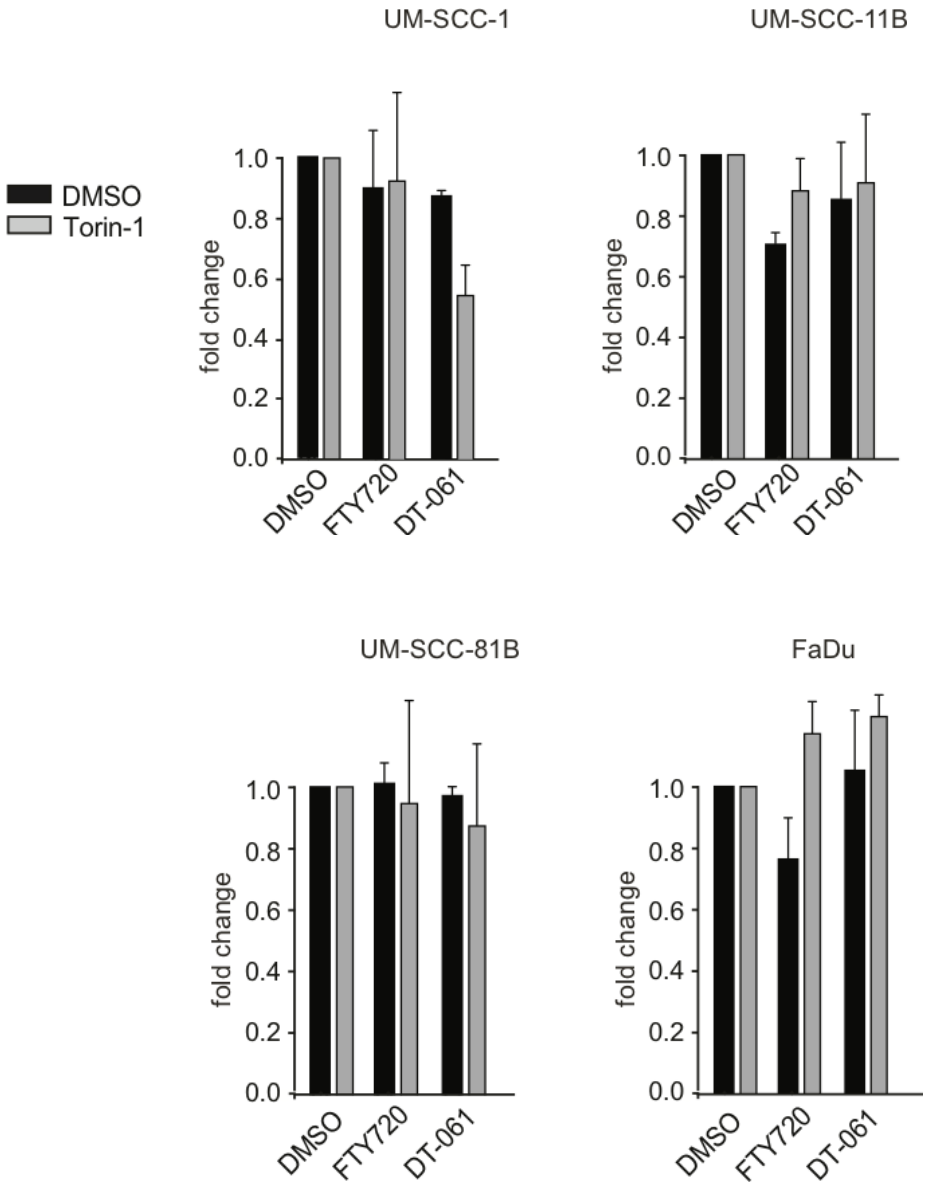

Figure 4.2.7: PP2A activators failed to synergise with Torin-1 in reducing clonogenicity in HNSCC cell lines. HNSCC cell lines were seeded at low density and treated with Torin-1 (2 nM) alone or in combination with FTY720 (500 nM) or DT-061 (1 mM). Cells were allowed to form colonies and colonies counted for clonogenic assay using automated colony counter. Colony counting showed an no significant effect of the combinations. Torin-1 was normalised to 1.0, and the other treatments were depicted as fold changes in relation to DMSO. Error bars represent standard error of the mean (S.E.M) from at least 3 independent experiments.

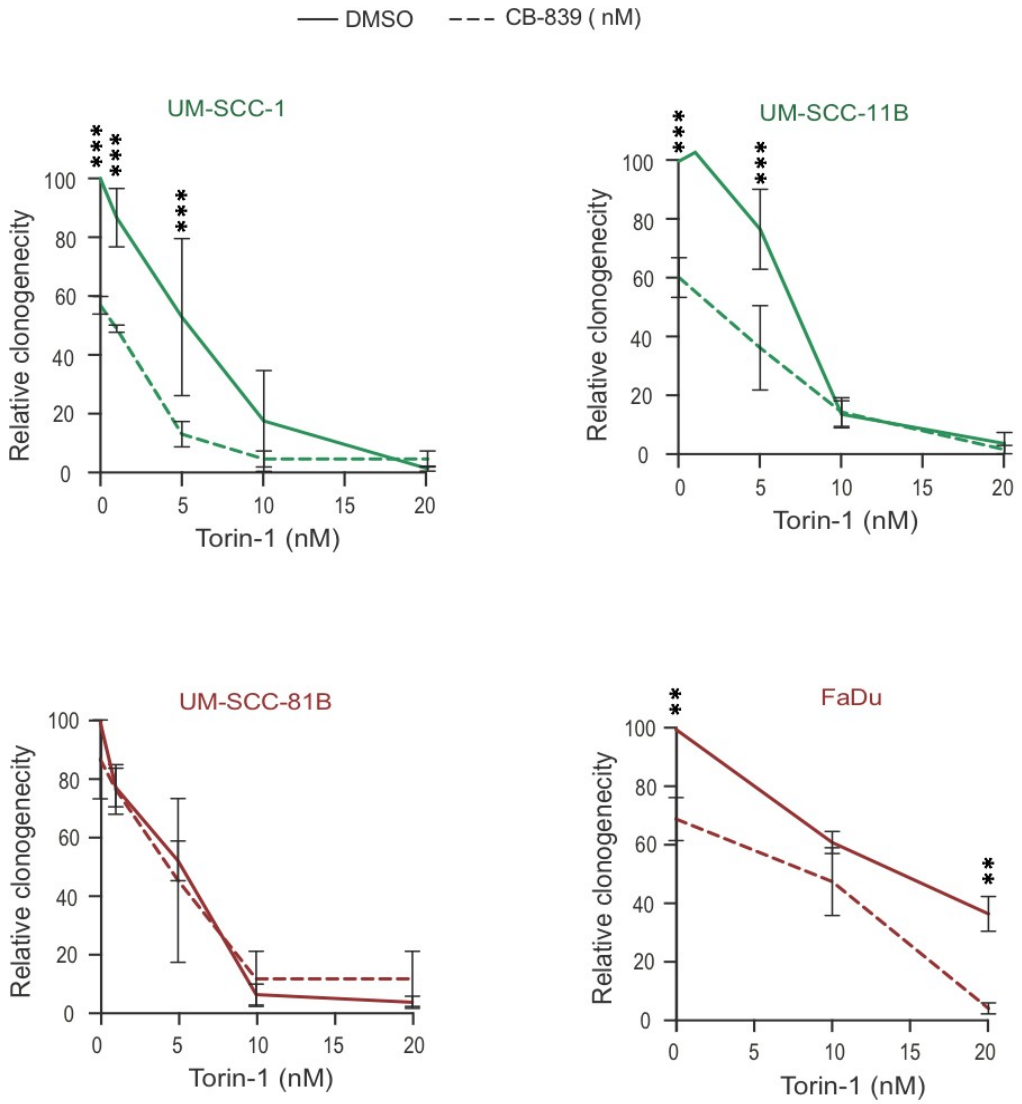

Figure 4.2.8: Torin-1 does not synergise with CB-839 to reduce the clonogenic potential of HNSCC cell lines. HNSCC cell lines were seeded at low density and treated with increasing concentration of Torin-1 in combination with CB-839 (500 nM). Cells were allowed to form colonies and colonies counted for clonogenic assay using automated colony counter. Colony counting showed no significant effect of the combinations. Error bars represent standard error of the mean (S.E.M) from at least 3 independent experiments. ***$p \leq 0.001$, ** $p \leq 0.01$.

4.2.7 Torin-1 does not synergise with inhibitors of either BCL-X_L or MCL-1 in most HNSCC cell lines

As BCL-X_L and MCL-1 are highly expressed in HNSCC cell lines, the next step was to test the effect of BCL-X_L or MCL-1 inhibitors in synergising with Torin-1 to reduce the clonogenic potential of HNSCC cell lines. The oral cavity cell lines, UM-SCC-1 exhibited a very modest additive effect with a combination of Torin-1 with either BCL-X_L inhibitor (A-1331852) or MCL-1 inhibitor (S63845) (Figure 4.2.9). In laryngeal cell lines, UM-SCC-11B, A-1331852 appeared to have pronounced effects and the effect was not enhanced by the addition of Torin-1 (Figure 4.2.9), whereas in the oropharynx cell lines, the additive effects, if any, were extremely modest (Figure 4.2.9). In hypopharyngeal cell lines, FaDu, exhibited an additive effect which was largely undetectable (Figure 4.2.9).

HNSCC depends on both BCL-X_L and MCL-1 for survival [169]. This was further confirmed by checking the effect of BCL-X_L inhibitor (A-1331852) and MCL-1 inhibitor (S63845) on tumour growth in a 3D spheroid culture. As evident in (Figure 4.2.10), single administration of S63845, but not A-1331852 slightly reduced the spheroid volume of UM-SCC-17A cells, in comparison to the control, DMSO-treated cells. In contrast, a combination of both A-1331852 and S63845 diminished the spheroid structure within the first three days of the 12-day long experiment (Figure 4.2.10).

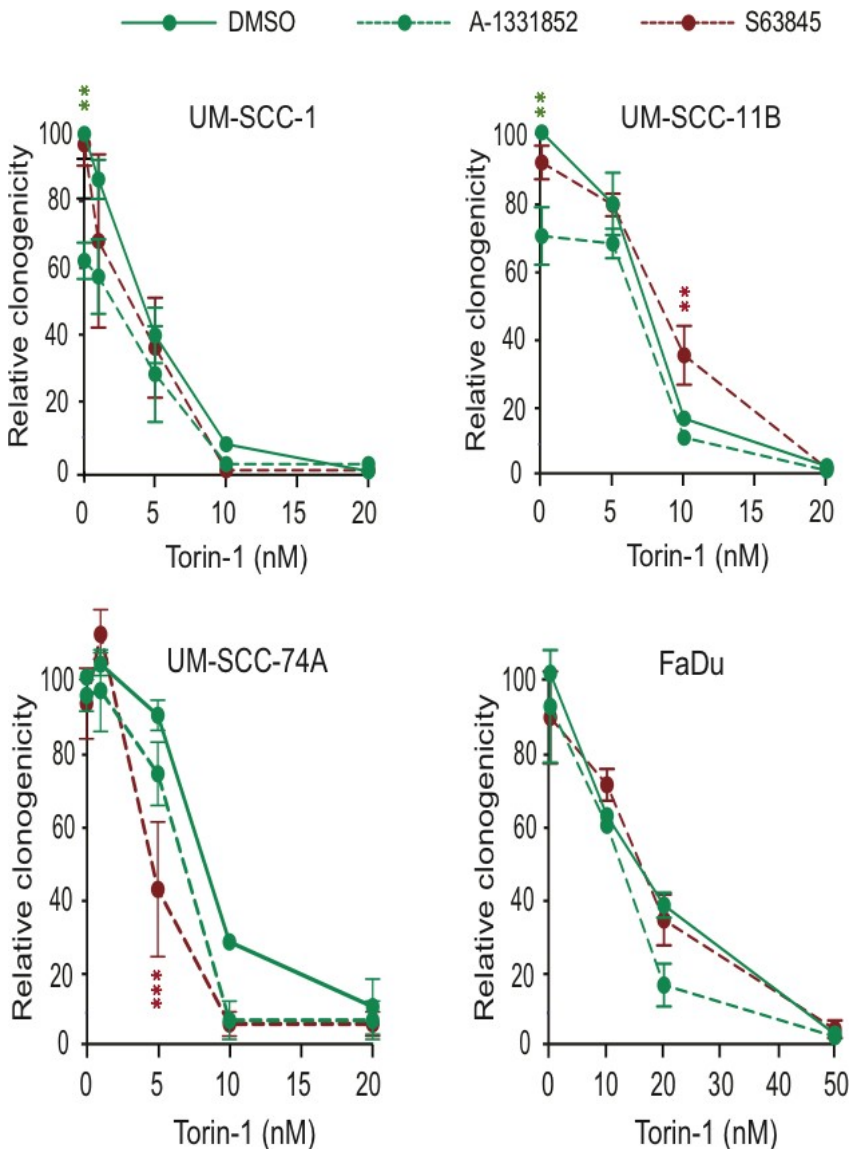

Figure 4.2.9: Torin-1 does not synergise with either A-1331852 or S63845 in decreasing clonogenic potential of HNSCC cell lines. HNSCC cell lines were seeded at low density and treated with increasing concentrations of Torin-1, either alone or in combination with S63845 (100 nM). Cells were allowed to form colonies for 7-10 days. Upon detection of individual colonies, cells were fixed, stained with crystal violet and colonies counted for clonogenic assay using automated colony counter. In the graphs, the solid lines represent treatment with Torin-1 alone, whereas the dotted lines represent the combination of Torin-1 and S63845. Error bars represent standard error of the mean (S.E.M) from at least 3 independent experiments. ***$p \leq 0.001$, **$p \leq 0.01$.

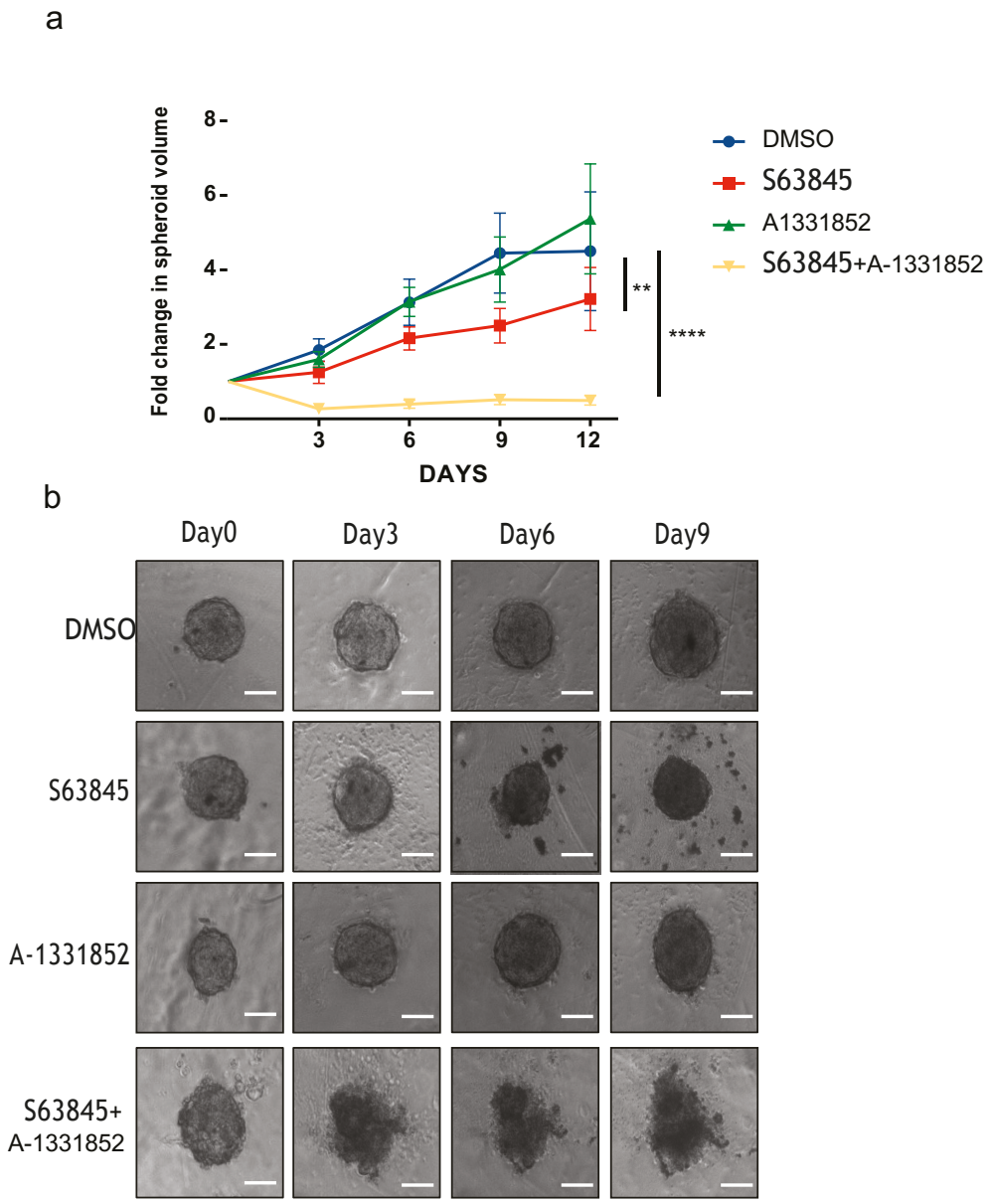

Figure 4.2.10: Spheroid volume was reduced following exposure to BH3 memtics in UM-SCC-17A. UM-SCC-17A cells were seeded at 500 cells/ well in ULA 96 well plate to form 3D spheroid structure. Once established, the spheroids were treated with either S63845 or A1331852 (100 nM each) or a combination of both agents for 12 days. (a) Line graph represents the change in fold of spheroid volume over time. (b) Phase contrast images were taken every 3 days and spheroid volume was measured (scale bars 100 μm). Three replicates were performed. Error bars = Mean ± SEM (standard error of the mean); ***$p \leq 0.0001$.

4.2.8 Torin-1 exhibits a very modest effect on the clonogenic survival in combination with BH3 mimetics

As a single agent, BH3 mimetics did not have an inhibitory effect on colony formation and spheroid growth (Figure 4.2.9-4.2.10). On the other hand, a combination of BH3 mimetics had a significant effect on spheroid growth; suggesting that HNSCC cells depend on both BCL-xl and MCL-1 for survival [169]. To assess whether Torin-1 would synergise with the combination of BH3 mimetics targeting BCL-xl and MCL-1, UM-SCC-81B cell line was treated with Torin-1 (2 nM) along with increasing concentration of both A-1331852 and S63845. Torin-1 (2 nM) alone reduced the clonogenicity by 40% when compared to the control (DMSO). The addition of both A-1331852 and S63845 (20 nM each) appeared to have a slight additive effect when combined with Torin-1 (Figure 4.2.11). At a higher concentration (50 nM) of the BH3 mimetics, UM-SCC-81B exhibited a significant decrease in clonogenicity, which was further elevated with the addition of Torin-1 (Figure 4.2.11). Taken together, these results suggested that Torin-1 could synergise with BH3 mimetics at a narrow therapeutic window. Furthermore, these results implicated that Torin-1 could potentially enhance BH3 mimetic-mediated apoptosis, which will be studied further in the next results chapter.

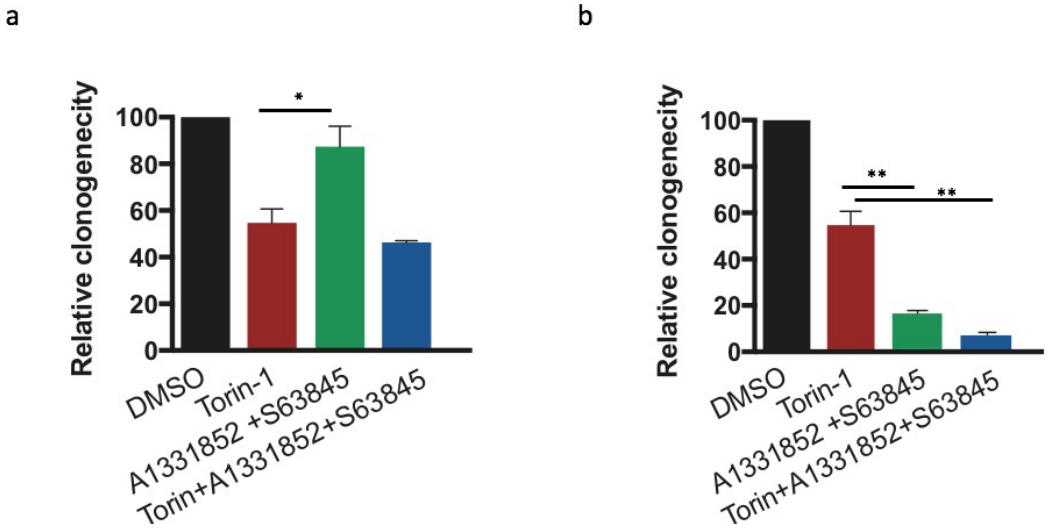

4.2.11: Torin-1 modestly synergises with the combination of A-1331852 and S63845 in decreasing clonogenic potential of UM-SCC-81B. UM-SCC-81B cell line was seeded at a low density and treated with Torin-1 (2 nM), either alone or in **a)** combination of S63845 (20 nM) and A1331852 (20 nM), and **b)** combination of S63845 (50 nM) and A1331852 (50 nM). Cells were allowed to form colonies for 7-10 days. Upon detection of individual colonies, cells were fixed, stained with crystal violet and colonies counted for clonogenic assay using automated colony counter. Error bars represent standard error of the mean (S.E.M) from at least 3 independent experiments. $^{**}p \leq 0.01$, $^{*}p \leq 0.05$.

4.3 Discussion

This chapter primarily focused on identifying potent therapeutic combinations with Torin-1 for treatments in HNSCC. Although other mTOR inhibitors, such as everolimus synergised with cisplatin in decreasing the growth of cancer cell lines, derived from nasopharyngeal carcinoma and urothelial bladder cancer [170, 171], Cisplatin failed to synergise with Torin-1 to decrease the clonogenicity of HNSCC cell lines (Figures 4.2.1) in this study. Whether this is due to the differences in the specificity of Torin-1 versus everolimus to target the different mTOR complexes remains to be studied.

In head and neck cancers, surgery and radiotherapy are the most frequent therapeutic options to treat patients. Despite the differences in side effects, both methods have a similar cure rate for early-stage tumours [172]. In advanced HNSCC, a single therapy is associated with poor outcome, thus necessitating effective combination therapies [172]. However, high doses of irradiation usually accompany severe side effects, ranging from dry mouth, loss of the ability to speak, mucositis and dysphagia and acute toxicity. For that reason, a combination of Torin-1 and low doses of radiation was examined. Unfortunately, this combination did not have a synergistic effect; thus arguing against the benefits this combination can offer over radiation as monotherapy (Figures 4.2.2). This was also the case for Olaparib and AZD1775 combinations either with Torin-1 or when used in combination with IR and Torin-1 (Figures 4.2.3-4.2.4).

Protein Phosphatase 2 A (PP2A) is a serine/threonine phosphatase that consists of a catalytic subunit C and a scaffolding subunit A which both contribute to the structure of the enzyme. It has a role in many cellular functions such as cellular growth, metabolism, cell cycle and apoptosis. PP2A is a negative regulator of PI3K and MAPK pathways and it is a tumour suppressor protein. Small molecules activators of PP2A (SMAPs) directly binds to PP2A and inhibit growth and induce apoptosis through dephosphorylation of ERK and AKT [167, 173]. Hence, the hypothesis was that the combination of PP2A activators (DT-061 and FTY720) and Torin-1 would inhibit P13K pathway and be a promising therapeutic target for HNSCC. Unfortunately, the combination did not offer the desired outcome and therefore, failed in being a potential therapeutic option for HNSCC (Figure 4.2.7). That could be due to a loss of function of PTEN or hyperactivation of PI3K, which is upstream of mTOR; thus obviating the need for Torin-1.

Glutaminolysis is an essential pathway where glutamine is converted to glutamate through a hydrolysis reaction catalysed by the enzyme glutaminase (GLS). It is the first and rate limited step in glutaminolysis pathway [174, 175]. Glutamine is the most abundant amino acid circulated in the blood and it is crucial for the survival of cancer cells as it is counted as a source of energy that promotes essential cellular processes, such as the synthesis of purines, pyrmidines, fatty acids, non-essential amino acids [174] and is responsible of the activation of mTOR (Figure 4.3.1). GLS has a high expression level in variety of cancer including non-small lung carcinoma [176], prostate cancer [177] breast, oesophagus and head and neck cancers and it is linked to a poor survival rate [178], which makes it a prognostic marker and therapeutic target for multiple cancers. CB-839, a glutaminase inhibitor, has shown efficacy in renal

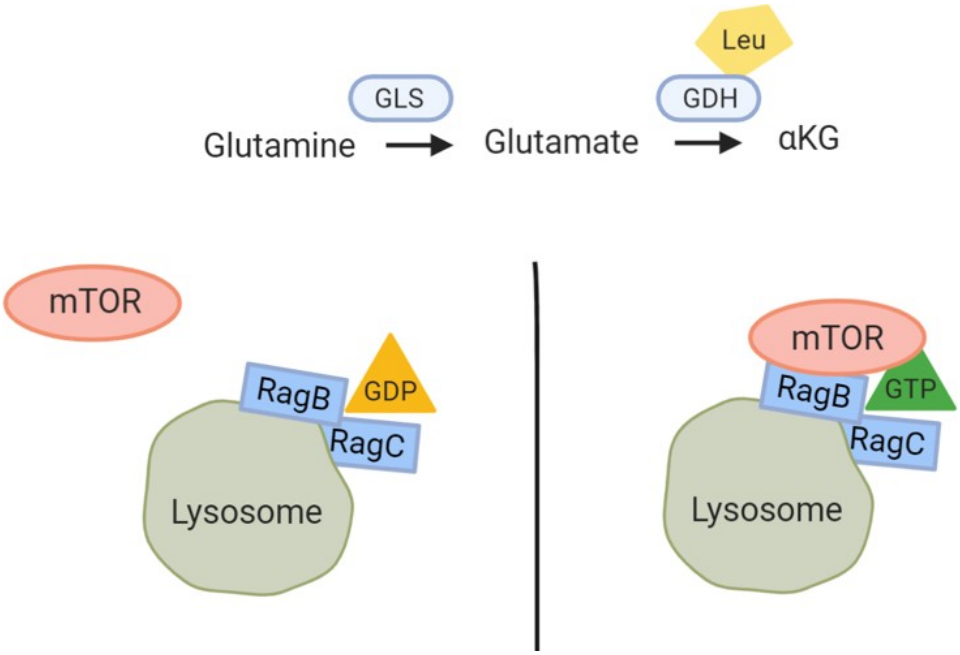

Figure 4.3.1: Illustration of α KG activation of mTOR. In the presence of Leucine, αKG converts GDP-bound Rag B/C complex to GTP-bound Rag B/C, which in turn activates mTOR.

carcinoma, non-small lung carcinoma and triple negative breast cancer [179, 180, 181]. Although CB-839, in combination with everolimus, is both well tolerated and efficacious against renal cell cancer [181], it failed to synergise with Torin-1 in HNSCC (Figure 4.2.8) in this study.

Apoptosis is one of the most widely studied subject in cell biology and understanding this pathway can provide insight not only into the progression of a disease, but also into how it can be treated. In cancer, there is an imbalance between the proliferation rate and cell death of abnormal cells, which leads to the accumulation of abnormal cells and formation of tumours, thus emphasising the need for new therapeutic options to target the apoptotic pathways [182]. Most cancer therapies are designed to induce cell death by targeting the intrinsic pathway of apoptosis. At mitochondrial level, this pathway is regulated by the BCL-2 family of proteins [84]. Cancer cells keep apoptosis in check by overexpressing the anti-apoptotic proteins (BCL-2, BCL-X_L and MCL-1), which bind to the pro-apoptotic BH3-only proteins, thus preventing mitochondrial outer membrane permeabilization, cytochrome c release and eventually apoptosis [84]. The high expression levels of BCL-2 family of proteins in multiple cancers have led to the development of a novel category of small molecule inhibitors called BH3 mimetics that target the anti-apoptotic BCL-2 family of proteins to induce apoptosis [183]. The first inhibitor identified was ABT-737 and its orally bio-available form, ABT-263 (Navitoclax), which inhibit BCL-2, BCL-w and BCL-X_L [128, 184]. These discoveries were followed by the development of more selective inhibitors, such as ABT-199 (Venetoclax), which selectively inhibits BCL-2 and was recently approved by FDA for the treatment of chemorefractory chronic lymphocytic leukaemia [129], S63845, which selectively inhibits MCL-1 and A-1331852, a selective

inhibitor of BCL-X_L [133, 183]. Chronic myeloid leukaemia cell line, K562, for instance, depends on BCL-X_L for survival, and using A-1331852 is the most appropriate approach to target that protein and induce apoptosis [96]. Unlike haematological malignancies, which depend on a single anti-apoptotic BCL-2 family of proteins for survival [185, 186], most solid tumours, including HNSCC depend on two anti-apoptotic proteins, BCL-X_L and MCL-1 [169]. In HNSCC cell lines, targeting either BCL-X_L or MCL-1 using A-1331852 or S63845, respectively was not enough to reduce clonogenicity when used as a single agent or when combined with Torin-1. However, a combination of Torin-1 and A-1331852 + S63845 resulted in significant reduction of spheroid growth in 3D culture. Similarly, a modest effect was detected in the clonogenic assay when this combination was used.

Collectively, these findings suggest that Torin-1 does not provide a promising therapeutic combination with either conventional or novel agents over monotherapies in head and neck cancer cell lines. This could be attributed to the mechanism by which Torin-1 inhibits mTOR in comparison to other inhibitors. Torin-1 is a highly selective ATP competitive inhibitor, whereas rapamycin, for instance, is an allosteric inhibitor. Moreover, it must be noted that clonogenic assays, whilst commonly used as a predictor of *in vitro* drug sensitivity, they have a number of limitations, such as plating efficiency, tumour heterogeneity, the difference between *in vivo* and *in vitro* sensitivities to drugs, as well as responsiveness to drugs when cells from different passage numbers are seeded at low densities. Therefore, it would be premature to dismiss the potential of these combinations solely based on negative results from clonogenic assays.

Chapter 5

Characterizing the mitochondrial role of mTOR inhibition in the context of apoptosis in HNSCC

Chapter contents

5.1 Introduction

BH3 mimetics induce apoptosis by disrupting the integrity of mitochondria. As mentioned earlier, mitochondrial membrane permeabilization is a major step in apoptosis and this process is highly regulated by a dynamic network within the mitochondrial structure, which allows it to constantly divide (fission) and fuse (fusion). Fission is a process by which mitochondria divide into two or more structures and it is regulated by Drp-1, a GTPase that belongs to dynamin family of proteins [187, 188]. During fission, Drp-1 translocates from the cytosol onto the mitochondrial fission sites, where it binds to its receptors, namely MFF, MiD49, MiD51 and Fis1. Subsequently, Drp-1 forms a tight ring-like structure around the mitochondria, providing a force which eventually leads to division. Drp-1 activity is dependent on its phosphorylation status. Phosphorylation of Drp-1 at Ser616 by cyclin-dependent kinases, for instance, induces its activity and results in enhanced fission. On the other hand, phosphorylation at Ser637 has the opposite effect [189].

Fusion, a process by which two individual mitochondria fuse together is regulated by GTPase proteins that belong to dynamin family of proteins, namely optic atrophy 1 (OPA-1), mitofusins 1 and 2 (MFN1 and MFN2). While MFN1 and MFN2 are responsible for fusion of the outer mitochondrial membranes, OPA-1 regulates the fusion of the inner mitochondrial membranes. Furthermore, OPA-1 is also responsible for maintaining cristae structure and cytochrome c redistribution within the mitochondria. OPA-1 exists as three short (S OPA-1) and two long (L OPA-1) isoforms. During cell death, mitochondrial membrane dynamics play an integral role as it marks the commencement of the intrinsic pathway. OPA-1 proteolysis results in reshaping of cristae and cytochrome c release into intermembrane space, following which cytochrome c can be released into the cytosol through BAK/BAX pores on the

outer mitochondrial membrane[190]. Previous work in Varadarajan lab showed that BH3 mimetics can induce mitochondrial structural changes, such as loss of cristae, matrix swelling and breakage in the outer-membrane, in a Drp-1 dependant manner [191].

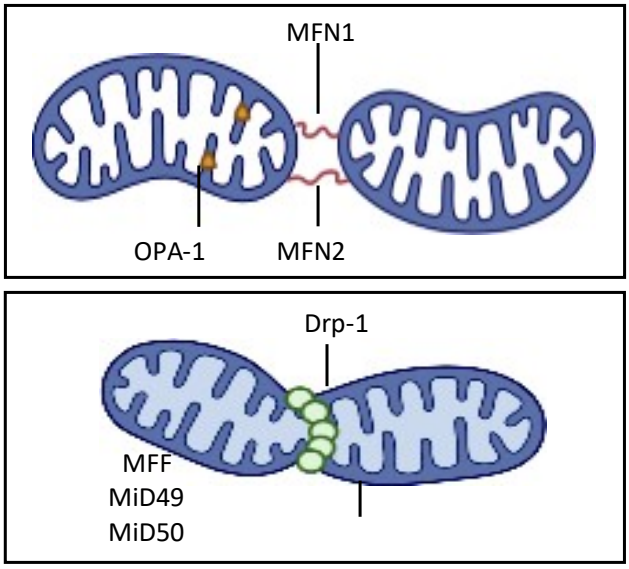

Figure 5.1.1: Mitochondrial fission and fusion processes. Fusion is mediated by MFN1 and MFN2 on the mitochondrial outer membrane and OPA-1 on the inner membrane where they promote the merging of two mitochondria. On the other hand, fission is controlled by DRP-1. Upon binding to its receptor, it aligns in a ring shape structure around the mitochondria which eventually segment the mitochondria into two parts.

mTORC1 promotes several mitochondrial processes such as respiration, tricarbolic acid (TCA) cycle and protein translation through the recruitment of specific mRNA to ribosomes for increased translation that result in energy production, cellular growth and proliferation. One of these proteins is mitochondrial fission process protein1 (MTFP1), also called MTP18. MTFP1 is an inner mitochondrial protein that inhibit mitochondrial hyperfusion and its overexpression results in mitochondrial fragmentation [192]. MTFP1 activity is coupled with the phosphorylation status of Drp-1. In nutrient rich situation, mTORC1 promotes the translation of MTFP1, which accompanies a normal balance between Drp-1 phosphorylation at Ser616 and Ser637 [192]. As a result, mitochondria in a nutrient rich environment are able to maintain a dynamic balance between fission and fusion. On the other hand, mTORC1 inhibition will result in a decreased expression of MTFP1 and increased phosphorylation of Drp-1 at Ser637, which results in hyperfused mitochondria. This could explain why mTORC1 inhibition does not result in enhanced apoptosis, as mitochondrial fragmentation (structural perturbation) is an integral feature of apoptosis induction.

Although targeting mTOR kinases, either alone or in combination with several chemo/radiotherapies, reduced the clonogenic survival of HNSCC cell lines, none of these combinations resulted in enhanced cell death. This chapter will be aimed at assessing the crosstalk between mTOR inhibition, apoptosis and mitochondrial dynamics in the context of HNSCC. In order to address this, this chapter is aimed at answering the following questions:

1. Does Torin-1 regulate mitochondrial membrane dynamics?
2. Does Torin-1 alter phosphorylation and mitochondrial translocation of Drp-1?
3. Could Torin-1-mediated mitochondrial effects impinge upon MOMP and apoptosis?

5.2 Results

5.2.1 Torin-1 results in mitochondrial hyperfusion.

Since Torin-1 failed in synergising with most therapeutic combinations to reduce the clonogenicity and increase the extent of apoptosis of HNSCC cell lines, it was speculated that this could be attributed to the effect of Torin-1 in regulating mitochondrial structure. To assess that, experiments were performed using UM-SCC-81B in which cells were exposed to an increasing concentration of Torin-1 (0-100 nM) for 16 h. Cells were fixed and assessed for mitochondrial integrity by immunofluorescence using antibodies against a mitochondrial marker (HSP70). Even at concentrations as low as 1 nM, mitochondria appeared elongated or hyperfused and HSP70 staining showed a filamentous network of mitochondria (Figure 5.2.1). These results suggested that Torin-1 indeed has an effect on mitochondrial structure integrity and might play a role in fission or fusion processes.

5.2.2 Torin-1- mediated mitochondrial hyperfusion accompanies changes in the phosphorylation status of Drp-1

To examine whether Torin-1-mediated mitochondrial hyperfusion is due to enhanced fusion or a loss of fission, the expression levels of mitochondrial fission and fusion proteins were analysed by western blotting. Although Torin-1 did not alter the expression levels of OPA-1 or total Drp-1, there was an increase in the phosphorylation levels of Drp-1 637 and a reduction in Drp-1 616 phosphorylation levels, which indicate that the fission process is supressed (Figure 5.2.2). These changes were accompanied with a loss in MTFP1 expression levels (Figure 5.2.2).

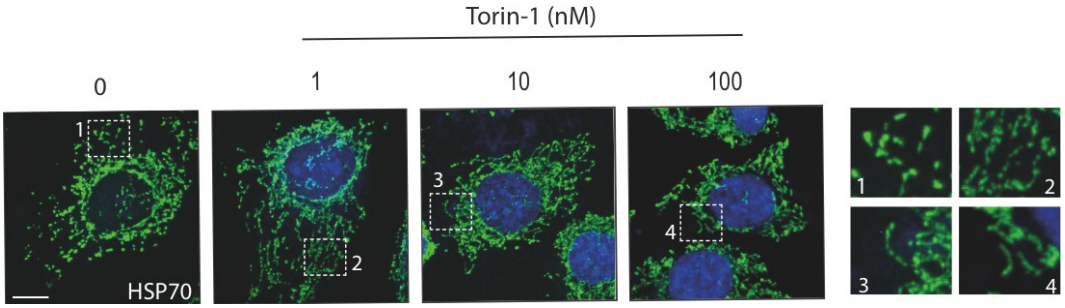

Figure 5.2.1: Exposure to Torin-1 causes mitochondrial hyperfusion. UM-SCC-81B cell lines were treated with increasing concentration of Torin-1 (1,10,100 nM) for 16 h. Cells were then fixed and immunostained against a mitochondrial marker HSP70. The dotted boxes in the images are enlarged in the right panel for better visualisation of the changes in mitochondrial structure. Scale bar 100 μm. Experiment was performed three times.

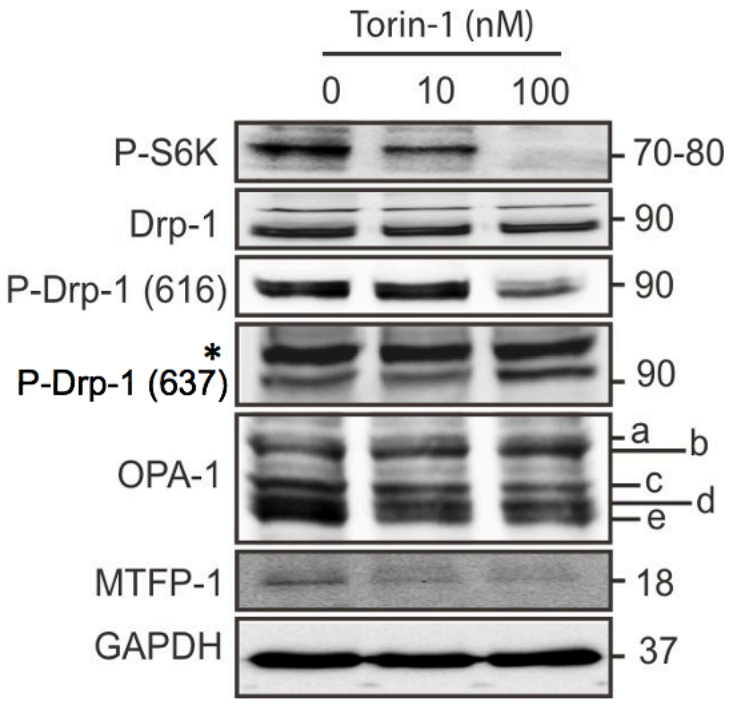

Figure 5.2.2: Torin-1 causes changes in mitochondrial dynamics and promotes a loss in MTFP1 expression. UM-SCC-81B were exposed to increasing concentration of Torin-1 (0,10,100 nM) for 16 h. The cells were assessed for western blotting using indicated antibodies (* denotes a non-specific band). (a,b,c,d,e) represents different isoforms of OPA-1.

5.2.3 Torin-1 does not appear to affect Drp-1 translocation

Since Torin-1 altered Drp-1 phosphorylation to favour hyperfusion, it was speculated that Torin-1 could affect the translocation of Drp-1 from cytosol to the mitochondrial membranes. To test this, UM-SCC-81B cell line was exposed to increasing concentration of Torin-1 (1,10,100 nM) for 16 h, following which the cells were processed for immunostaining with antibodies against Drp-1 and HSP70. In control cells, Drp-1 appeared to be scattered between the mitochondria and cytosol and the mitochondria appeared to be normal with no evidence of hyperfusion or fragmentation. Upon Torin-1 treatment, mitochondrial hyperfusion was evident as shown previously (Figure 5.2.1). However, Torin-1 did not appear to affect Drp-1 translocation to the mitochondria, as Drp-1 punctate distribution was observed both in the cytosol as well as the mitochondria (Figure 5.2.3). Since Torin-1-mediated hyperfusion accompanied changes in Drp-1 phosphorylation but not Drp-1 translocation, it could be concluded that the translocation experiment will have to be refined further to include extensive quantitation and other biochemical analyses, including subcellular fractionation.

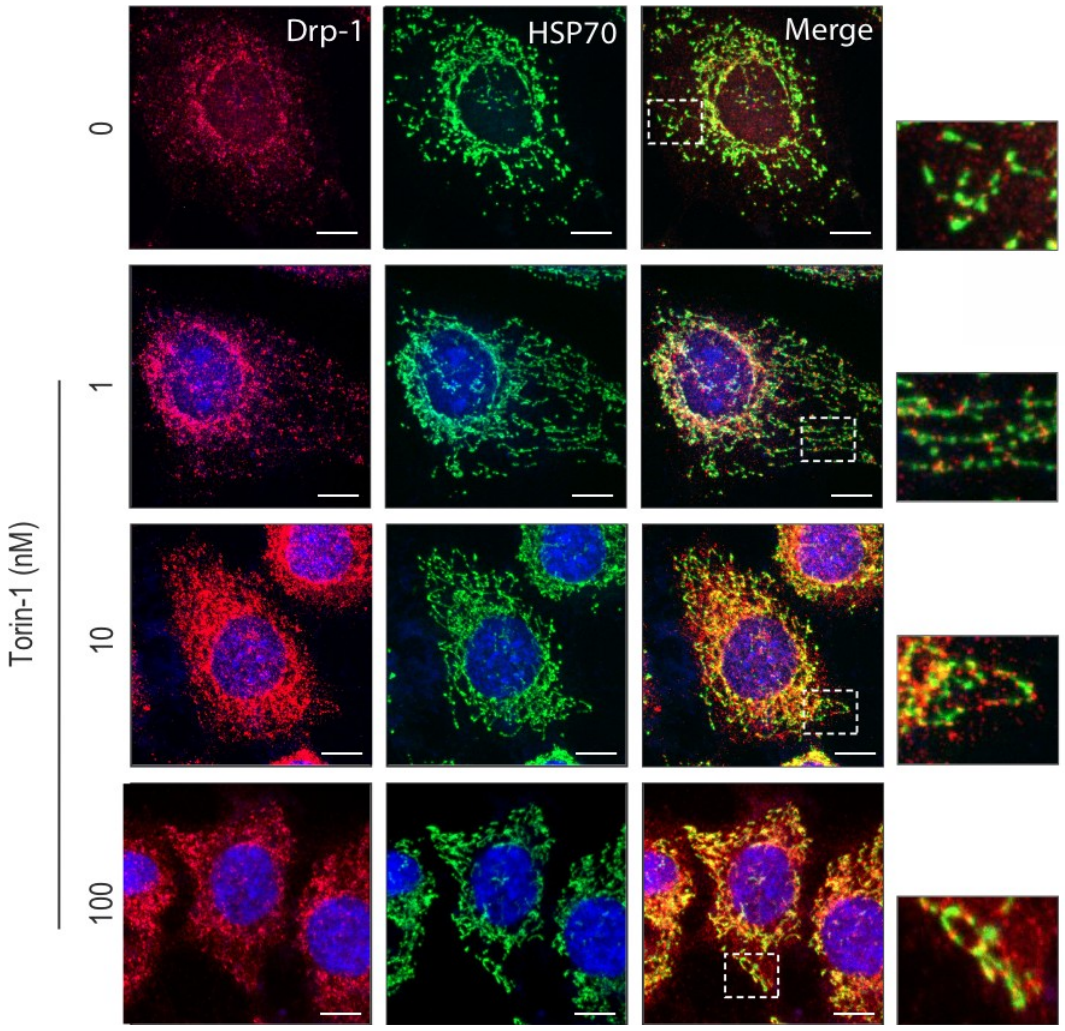

Figure 5.2.3: Torin-1 does not appear to prevent mitochondrial translocation of Drp-1 in UM-SCC-81B. UM-SCC-81B were treated with increasing concentration of Torin-1 (0,1,10,100 nM) for 16 h. After that, cells were fixed and immunostained for Drp-1 localisation (red) and mitochondrial marker HSP70 (green). The dotted boxes in the images are enlarged in the right panel for better visualisation of the changes in mitochondrial structure. Scale bar 10 μm.

5.2.4 Torin-1 -mediated mitochondrial hyperfusion does not confer resistance to apoptosis

Since HNSCC cell lines depend on both BCL-X_L and MCL-1 for survival, inhibitors that target both these proteins will induce apoptosis in these cells [169]. Previous reports showed that BH3 mediated apoptosis occur in a Drp-1-dependant manner [193]. Since Torin-1 resulted in mitochondrial hyperfusion, most likely via the phosphorylation of Drp-1, it was speculated that Torin-1 could antagonise BH3 mimetic-mediated apoptosis. For this, UM-SCC-81B were treated with Torin-1 for 16 h followed by 4 h exposure to A1331852+S63845. BH3 mimetics induced an extensive apoptotic death, which was not overcome by Torin-1 at any of the concentrations used (Figure 5.2.4). This indicated that Torin-1 does not prevent cell death mediated by BH3 mimetics.

These results were hardly surprising as Torin-1 enhanced BH3 mimetics-mediated apoptosis in chemoresistant cancer cell lines, derived from haematological malignancies. This was performed in an independent study in which chemoresistant haematological cell lines were re-sensitised to BH3 mimetic-mediated apoptosis by concurrent administration of Torin-1 (Figure 5.2.5). Since this study is not directly related to the main focus of this thesis, this is not addressed extensively beyond Figure 5.2.5.

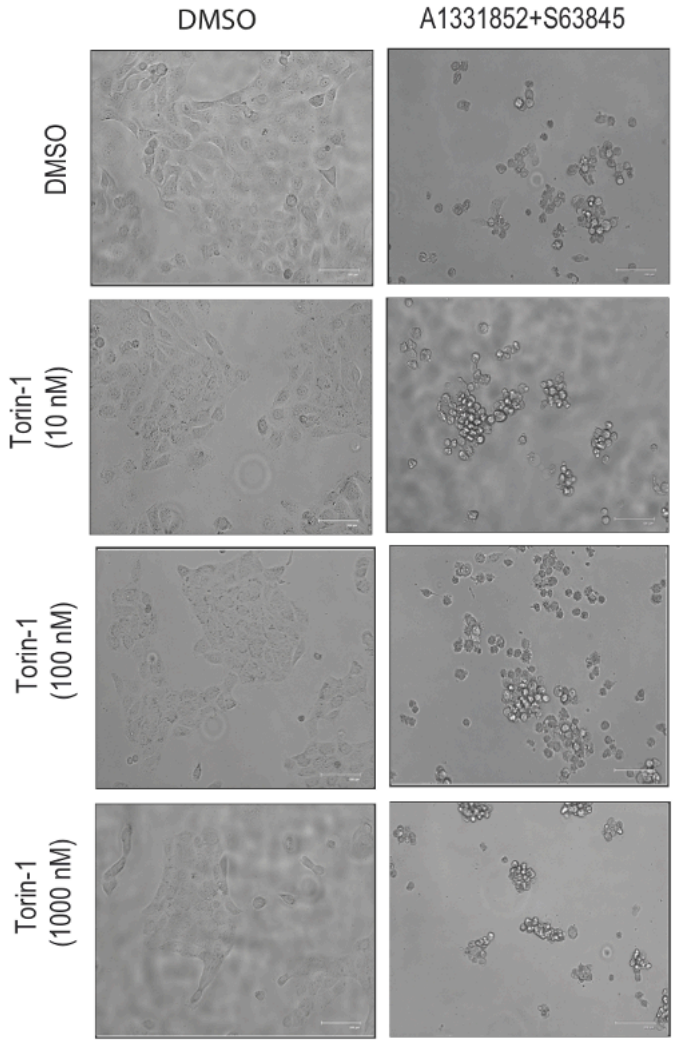

Figure 5.2.4: Torin-1 does not prevent apoptosis caused by BH3 mimetics. Bright field images of UM-SCC-81B exposed to indicated Torin-1 concentration for 16 h followed by a combination of S63845 and A13311852 at 100 nM each. Scale bars at 100 µm.

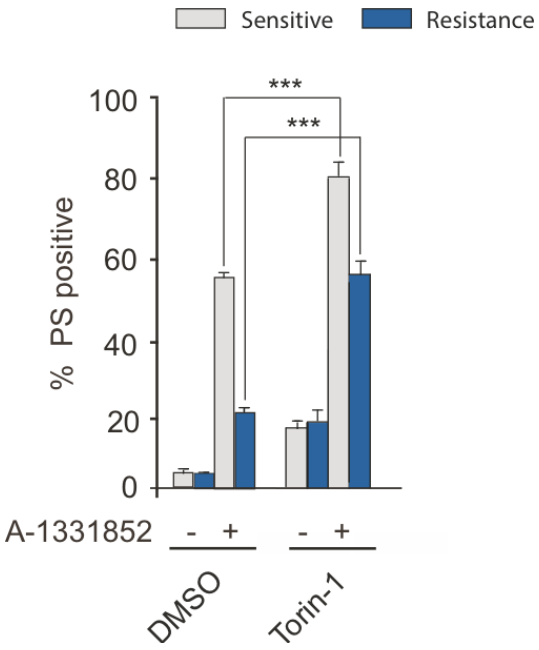

Figure 5.2.5: Torin-1 increases apoptosis in resistant K562 cell line. The bar graph shows the effect of Torin-1 on K562 cells, which are made resistant to the BH3 mimetic A-1331852. Cells were exposed to Torin-1 (10 nM) for 16 h followed by 4 h exposure to A-1331852 (50 nM) and PS externalisation was assessed by FACS. Error bars represent standard error of the mean (S.E.M) from at least 3 independent experiments. ***$p \leq 0.001$.

5.2.5 Torin-1-mediated mitochondrial hyperfusion does not prevent BH3 mimetic- mediated cytochrome c release

Drp-1 has previously been shown to be critical for BH3 mimetics-mediated cytochrome c release from the mitochondria. Since Torin-1 altered Drp-1 phosphorylation status without affecting Drp-1 translocation, it was important to confirm whether Torin-1 altered BH3 mimetic-mediated cytochrome c release upstream of apoptosis (Figure 5.2.6). To assess whether Torin-1 mediated mitochondrial hyperfusion could prevent BH3 mimetic-mediated cytochrome c release in HNSCC cell lines, UM-SCC-81B cells were exposed to a combination of A1331852 and S63845 (at 100 nM each) with increasing concentration of Torin-1 and assessed for cytochrome c release. As expected, cells exposed to a combination of A-1331852 and S63845 induced profound cytochrome c release in the cell line tested (Figure 5.2.7). Surprisingly, co-administration of Torin-1 did not antagonise BH3 mimetic-mediated cytochrome c release, suggesting that targeting mTOR kinases does not negatively regulate apoptosis. Therefore, it is important to determine the functional role of Torin-1-mediated phosphorylation of Drp-1 at Ser637.

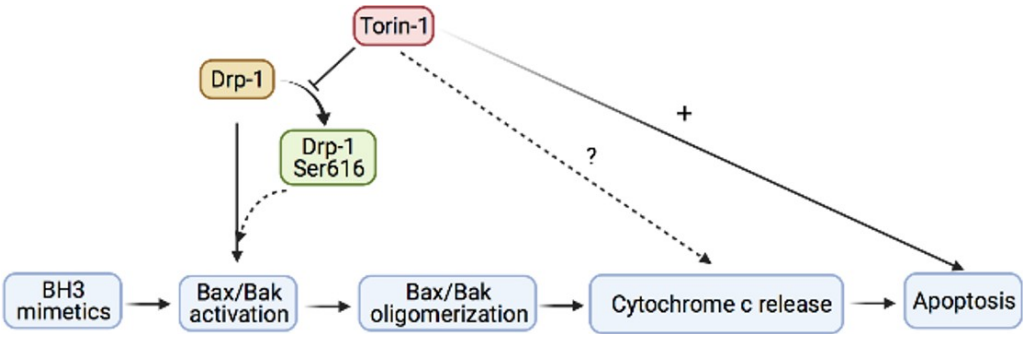

Figure 5.2.6: A schematic diagram of the effect of Torin-1 on the distinct steps leading to apoptosis. BH3 mimetics induce apoptosis by activating and oligomerizing pro-apoptotic proteins, BAX and BAK. Drp-1 has been shown to act upstream of BAX and BAK activation persumably by phosphorylation at Drp-1 Ser616. Since Torin-1 prevented Drp-1 phosphorylation at Ser616, it is possible that Torin-1 could negatively regulate the downstream pathways. However, Torin-1 has been shown to enhance BH3 mimetic- mediated apoptosis (denoted by + in the scheme). Whether Torin-1 will influence BH3 mimetic-mediated cytochrome c release (hence denoted by a dashed line) remains to be seen.

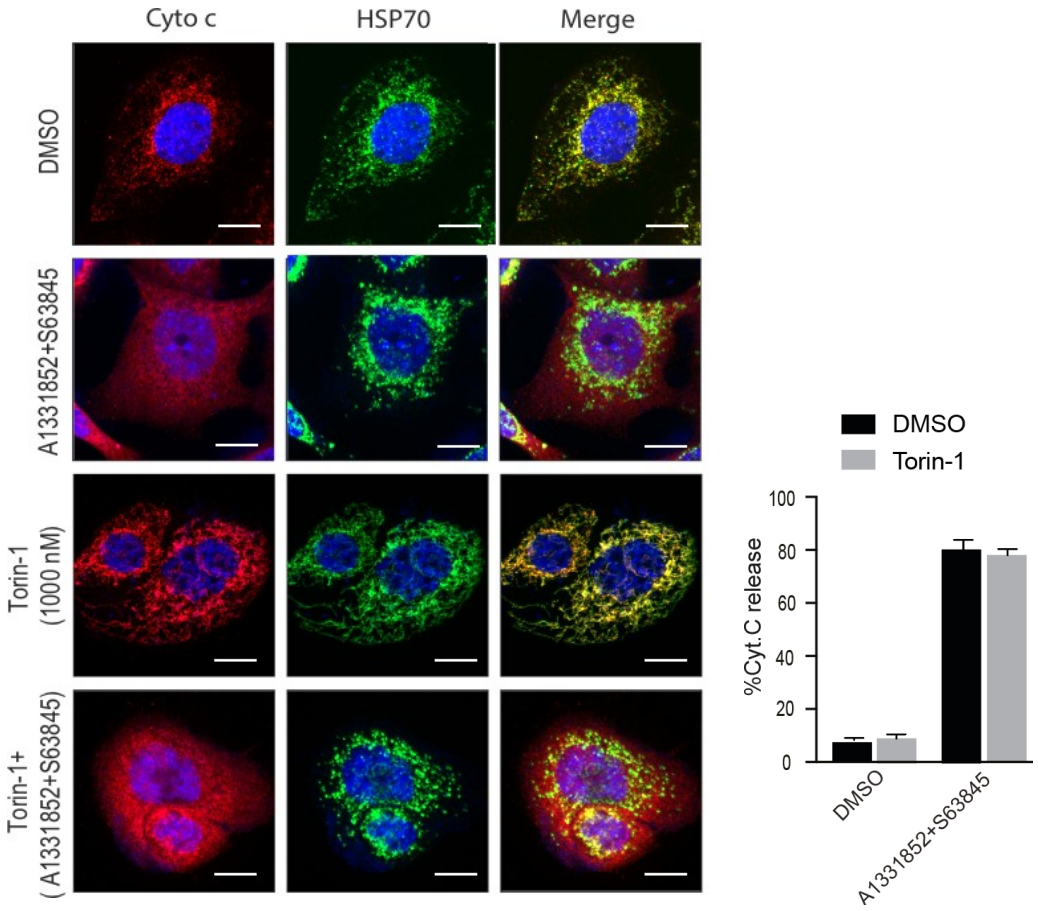

Figure 5.2.7: Torin-1 does not prevent BH3 mimetics mediated cytochrome c release. UM-SCC-81B were treated with increasing concentration of Torin-1 (0,10,100,1000 nM) for 16 h followed by Z-VAD (30 μM) for 30 mins. Cells were then exposed to a combination of A1331852 and S63845 (100 nM each) for 4 h. Cells were fixed and immunostained for mitochondrial marker HSP70 (green) and cytochrome c release (red). Scale bar 10 μm. Cytochrome c release was quantified by counting ~100 cells from 3 independent experiments.

5.2.6 Torin-1 alters the extent of mitochondrial fragmentation mediated by BAY-2402234

Dihydroorotate dehydrogenase (DHODH), a key enzyme in pyrimidine biosynthesis, is located in the mitochondria and it converts Dihydroorotate to orotate in the *De novo* pyrimidine biosynthesis pathway. BAY-2402234 is a DHODH inhibitor that binds to the catalytic site of the enzyme and suppress its action [194]. Targeting DHODH activity has been used to treat variety of diseases, including cancer [195]. In UM-SCC-81B, BAY- 2402234 (100 nM) resulted in extensive mitochondrial fragmentation, as evident by HSP70 staining (Figure 5.2.8). Exposure to Torin-1 (100 nM) resulted in the reversal of BAY-2402234-mediated mitochondrial fragmentation (Figure 5.2.8).

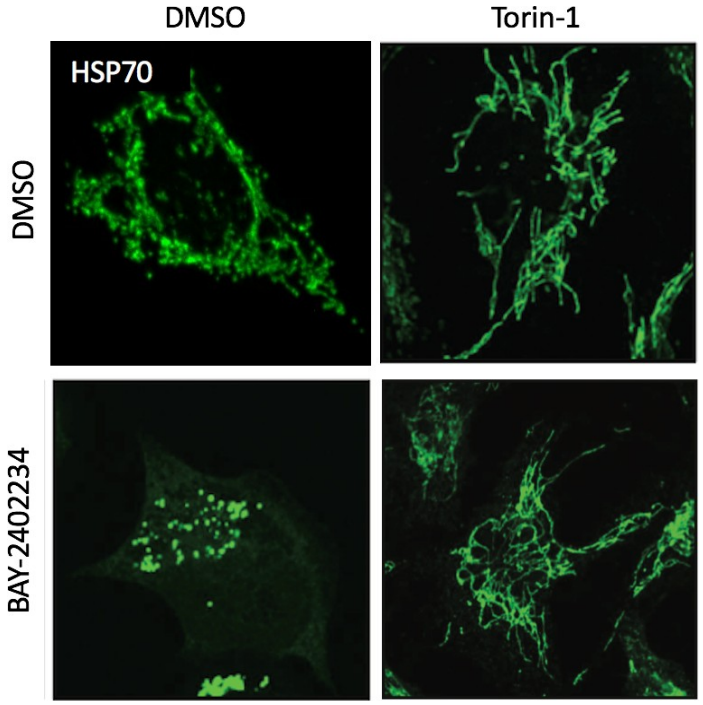

Figure 5.2.8: BAY-2402234-mediated mitochondrial fragmentation is reversed by co-administration of Torin-1. UM-SCC-81B cell lines were treated with Torin-1 16 h followed by BAY-2402234 (100 nM) for 36 h. Cells were then fixed and immunostained against a mitochondrial marker HSP70. Scale bar 100 µm.

5.2.7 Torin-1 rescues BAY-2402234 -mediated cell death

Further studies were performed to assess whether Torin-1 could rescue BAY-2402234-mediated cell death and other mitochondrial effects. Firstly, to assess the effect of Torin-1 on BAY-2402234-mediated cell death, UM-SCC-81B was treated with BAY-2402234 (100 nM) for 36 h. Exposure to BAY-2402234 resulted in extensive cell death, which was effectively rescued by Torin-1, as evidenced by bright field microscopy (Figure 5.2.9), as well as a reversal in PARP cleavage (Figure 5.2.10).

5.2.8 Torin-1 rescues other mitochondrial effects mediated by BAY-2402234

Since the extensive cell death mediated by BAY-2402234 was reversed by Torin-1, the next step was to determine if Torin-1 alters the expression levels of proteins that regulate mitochondrial dynamics. For this, the phosphorylation levels of Drp-1 at Ser637 and Ser616 were assessed. BAY-2402234 -mediated mitochondrial fragmentation accompanied a decrease of Drp-1 Ser637 and increase of Drp-1 Ser616 (both events are associated with enhanced mitochondrial fragmentation), both of which were completely reversed by Torin-1 (Figure 5.2.10). Taken together, these experiments convincingly demonstrated that Torin-1 prevented both mitochondrial effect and cell death triggered by BAY-2402234.

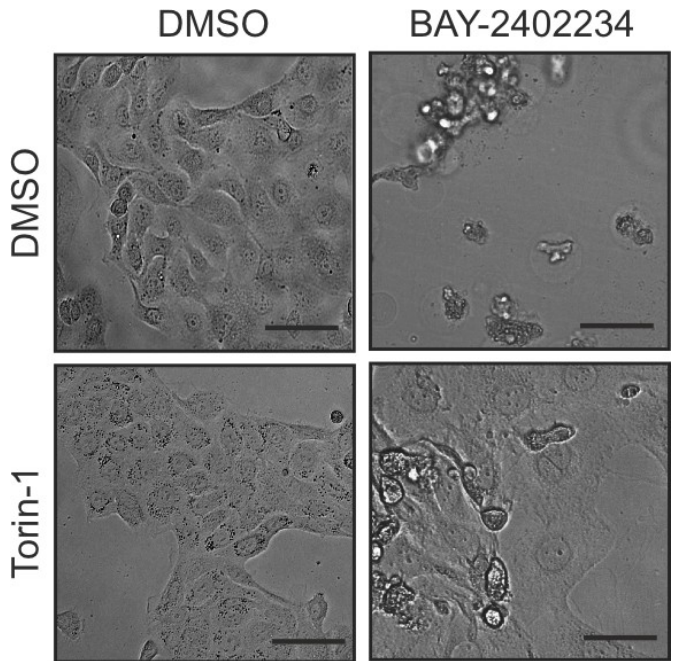

Figure 5.2.9: BAY-2402234 mediated cell death is rescued by exposure to Torin-1. Bright field images of UM-SCC-81B cell lines in which they were treated with BAY-2402234 (100 nM) followed by treatment of Torin-1 (100 nM) for 16 h. Scale bar 100 μ. Experiment was repeated three times.

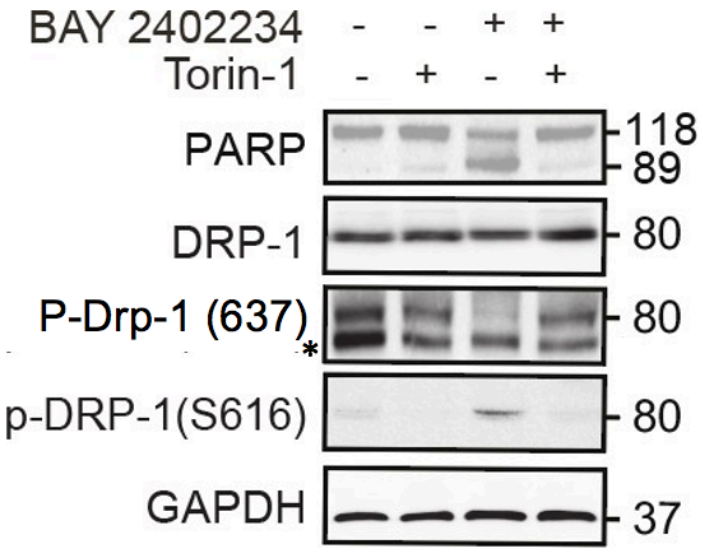

Figure 5.2.10: Torin-1 reverses mitochondrial changes mediated by BAY-2402234. UM-SCC-81B cell line was treated with Torin-1 (100 nM) for 16 h followed by BAY-2402234 (100 nM) for 36 h. Cells were lysed and processed for western blot analysis (* denotes a non-specific band).

5.2.9 The anti-apoptotic effect of Torin-1 does not extend to mTORC1 inhibitors

Although Torin-1 exhibited an antiapoptotic effect following BAY-2402234, as assessed by the extent of PS externilisation, other inhibitors of mTORC1 rapamycin (100 nM) and everolimus (100 nM) had little effect on BAY -2402234- mediated cell death (Figure 5.2.11). These findings suggested that simultaneous inhibition of mTORC1 and mTORC2 may be required to antagonize cell death mediated by BAY-2402234.

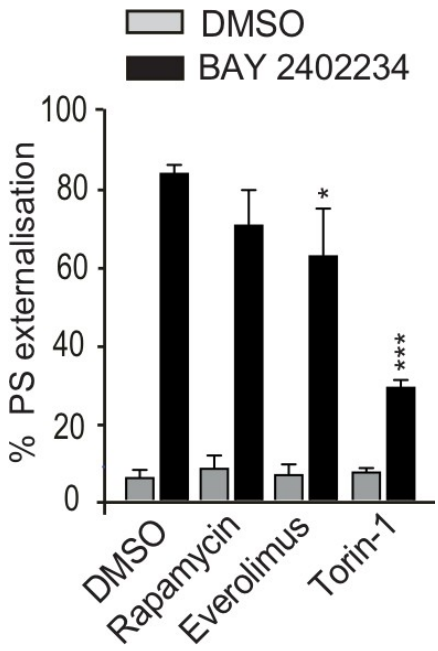

Figure 5.2.11: Torin-1 significantly recuses BAY-2402234- mediated cell death in comparison to rapamycin and everolimus. UM-SCC-81B cell line was treated with BAY-2402234 (100 nM) for 36 h, alone or in combination with either Torin-1 (100 nM), rapamycin (100 nM) or everolimus (100 nM). Error bars represents standard error of the mean (S.E.M) from at least 3 independent experiments. ***$p \leq 0.001$, *$p \leq 0.05$.

5.3 Discussion

This chapter is focused on understanding the connection between mTOR inhibition and mitochondrial dynamics in the context of apoptosis. Torin-1 resulted in significant mitochondrial hyperfusion, which accompanied changes in Drp-1 phosphorylation (Figure 5.2.1-5.2.2). Moreover, Torin-1 also decreased the translation of MTFP1 (Figure 5.2.2). These changes in MTFP1 expression and Drp-1 phosphorylation could explain why the mitochondria are hyperfused. This is in agreement with a previous report that shows a reduction in MTFP1 expression mediated by mTOR inhibition resulted in elongated branched mitochondria and this mitochondrial morphology was accompanied with changes in Drp-1 phosphorylation status [192]. Furthermore, this could also explain the cytostatic effect observed following Torin-1 treatment (Figure 3.2.12).

Since Torin-1 causes mitochondrial hyperfusion, proliferative defect and no apoptosis, it was speculated to antagonise BH3 mimetic-mediated mitochondrial fragmentation and apoptosis. However, Torin-1 treatment failed to reverse BH3 cytochrome c release (Figure 5.2.7). Although Torin-1-mediated changes in Drp-1 phosphorylation has been attributed to mitochondrial hyperfusion (Figure 5.2.2), whether Torin-1 would retain this function in the presence of BH3 mimetics has yet to be confirmed. In contrast, when another apoptotic agent, such as BAY-2402234 was used, Torin-1 not only prevented mitochondrial fragmentation, but it also reversed BAY-2402234 mediated changes in Drp-1 phosphorylation (Figures 5.2.8 and 5.2.10). To explain further, BAY-2402234 causes an increase in Drp-1 Ser616, which results in mitochondrial fragmentation and this in turn can be reversed by Torin-1, as Torin-

1 decreases Drp-1 Ser616 phosphorylation and consequently prevent fragmentation (Figures 5.2.8 and 5.2.10). It is interesting to note that Torin-1-mediated changes in Drp-1 phosphorylation does not influence the mitochondrial translocation of Drp-1 (Figure 5.2.3). There is some evidence that BH3 mimetic-mediated apoptosis does not involve any alteration in Drp-1 phosphorylation [196]. This could explain why Torin-1 when combined with BH3 mimetics does not prevent mitochondrial fragmentation, unlike the rescue observed when combined with BAY-2402234. Therefore, the effect observed with Torin-1 could be a stimulus-dependant effect and could occur independently of Drp-1 phosphorylation status. Further studies are required to couple /uncouple Drp-1 phosphorylation and mitochondrial translocation in the context of Torin-1 and BH3 mimetics.

Since Torin-1 does not affect BH3 mimetic-mediated mitochondrial translocation of Drp-1 or mitochondrial fragmentation, it is hardly surprising to note that Torin-1 does not prevent BH3 mimetics-mediated cytochrome c release and apoptosis (Figures 5.2.4 and 5.2.7). In contrast, Torin-1 antagonises BAY-2402234-mediated Drp-1 phosphorylation, mitochondrial fragmentation as well as apoptosis (Figures 5.2.8-5.2.10). Therefore, it is reasonable to assume that Torin-1 probably also prevented BAY-2402234-mediated mitochondrial translocation of Drp-1, BAX/BAK activation and oligomerisation as well as cytochrome c release. These experiments, however, could not be performed in this thesis due to time constraints. Nevertheless, this hypothesis could couple Drp-1 phosphorylation and mitochondrial translocation in the context of apoptosis.

Chapter 6
General discussion

6.1 mTOR inhibitors in cancer therapy

Given the wide range of cellular events that mTOR complexes control, it is no surprise that mTOR signalling activation is linked to cancer incidence and progression. The activation of mTOR complexes offers tumours a significant growth advantage, with increased protein synthesis and decreased autophagy. Enabled mTOR signalling has been linked to an increase in tumour progression and, in some cases, a decrease in patient survival [197]. mTOR expression levels, as well as its downstream targets eIF4E, 4EBP1, S6K1, and S6, have been shown in some studies to be a potential diagnostic and prognostic biomarkers for cancers, such as head and neck. In a study that involved 25 laryngeal squamous cell carcinoma (LSCC) patients, treated with surgery followed by RT, mTOR expression levels were high, which correlated with higher risk of recurrence and reduced rate of disease-free survival [198]. As a result, targeting mTOR pathway and the use of mTOR inhibitors offers a promising option for cancer therapies. To achieve this, scientists have developed first- and second-generation mTOR inhibitors for cancer therapy.

Despite the high efficacy of these inhibitors in blocking mTOR activity, their therapeutic potential in cancer treatments is limited. A study using everolimus on 656 advanced gastric cancer patients concluded that everolimus did not have a significant effect on overall survival [199]. Similarly, in another clinical study for non-small cell lung carcinoma (NSCLC), everolimus did not have desirable clinical benefits for patients, despite reaching tolerable doses in patients [200]. Clinical trials using other mTOR inhibitors, such as Temsilrolimus in advanced prostate cancer also failed to exhibit sufficient clinical benefits on the patients [201]. This can be due to different reasons. Firstly, the majority of alterations and mutations resulting in mTOR activation in cancer are observed in the signalling proteins that are located upstream

of mTOR. One of the most common alteration occurs within the catalytic domain of PI3K, which results in the activation of mTOR through Akt/TSC complex [202]. This alteration has been shown in a variety of cancers. For instance, PI3K gene is often amplified in ovarian cancer, and mutation within PI3K kinase domain is common in breast, colorectal, endometrial and gastric cancers [203]. Moreover PTEN, a tumour suppressor and negative regulator of PI3K, is a commonly mutated gene and its loss of function can lead to hyperactivation of mTOR. PTEN mutation has been observed in a variety of cancers, including hepatic cell carcinoma [204] breast and prostate cancers [205]. Genetic heterogeneity in the mTOR signalling pathway could also be a contributing factor to ineffective therapies. An immunohistochemical staining of phosph-4E-BP1and phosph-S6K1, as a marker for mTOR activity in human cancer cells, exhibited varying degree of staining within the same sample [206]. In addition, genome sequencing of human renal carcinoma cells displayed mutation within mTOR kinase domain that was not present in every single renal carcinoma cell [207]. Secondly, negative feedback loops are commonly found to disrupt overactive mTOR signalling. For instance, PI3K/AKT/mTROC1 when active leads to activation of its downstream effector, S6K. S6K in turn results in the phosphorylation and degradation of insulin receptor substrate (IRS-1). This prevents IRS-1 from binding to its receptor, thereby inhibiting mTOR activation through insulin/IGF-1 signalling [208] [209]. Pharmacological inhibition of mTOR could relieve this negative feedback pathway and as a result, constitutively activate PI3K/AKT [208, 209]. This will be counterintuitive as uncontrolled PI3K/AKT activation could result in cancer cell proliferation. Furthermore, a short-term inhibition of mTORC1 using rapalogs can result in the compensatory activation of mTORC2 [210], which also promotes cell survival via Akt activation and phosphorylation at Ser473 [210]. Thirdly, mutations in the kinase and FRB domains of

mTOR as well as in TSC1/TSC2 have been associated with chemoresistance to rapalogs in treatment of renal [211] and bladder cancers [212].

Due to the unsatisfactory response to the first generation mTOR inhibitors (most likely for the reasons mentioned above), mTOR inhibitors have been used in combination with other conventional therapies to maximise their effect. In a phase II trial of RCC patients, everolimus was combined with Lenvatinib, a VEGF (vascular growth factor) inhibitor, and it resulted in extended progression free survival in comparison to monotherapy [213]. In phase II trials of patients with metastatic large-cell neuroendocrine carcinoma (LCNEC), everolimus was combined with carboplatin and paclitaxel in which the drug combination showed high efficacy and maximum tolerance [214]. In a phase II trial of patients with non-Hodgkin's lymphoma, a combination of Rituximab and everolimus showed an improved response rate and it was well tolerated by patients [215]. Although these studies are encouraging, numerous other studies report no therapeutic advantage. For instance, a combination of everolimus with EGFR inhibitor, Gefinitib in patients with metastatic prostate cancer exhibited no anti-tumour activity [216]. Similarly, everolimus had no effect when combined with Sunitinib in advanced RCC [217]. However, studies exploring therapeutic combinations with mTOR inhibitors continue to be conducted. In patients with locally advanced/metastatic ER+ (Estrogen Receptor Positive) breast cancer, AZD2014, a dual mTOR inhibitor, is administered in combination with Palbociclib (a cyclin dependent kinase inhibitor) in an ongoing phase II trial to assess the effect on tumour size (ClinicalTrials.gov Identifier: NCT02599714).

The recently developed dual mTOR inhibitors as well as PI3K/mTOR inhibitors demonstrate excellent efficacy in cell lines as well as xenograft models but are yet to

be examined in the context of clinical trials [218, 219, 220, 221]. INK128, for instance, can enhance the radiosensitivity of pancreatic carcinoma cell lines [219]. Similarly, Paclitaxel- resistant gastric cancer cell lines demonstrate enhanced anti-tumour response when treated with BEZ235, a dual PI3K/mTOR inhibitor, in comparison with everolimus [222]. It would be interesting to assess whether the *in vitro* potency and efficacy of these new inhibitors could extend to cancer therapy in patients.

It must however be noted that treatment with mTOR inhibitors could result in undesirable adverse effects. These include hyperglycaemia, hypertriglyceridemia, and hypercholesterolemia, as well as thrombocytopenia, anaemia, nausea, and stomatitis [223, 224]. This is unsurprising as mTOR inhibition has been reported to impair glucose homeostasis and increase insulin resistance and gluconeogenesis in the liver [225], as well reduce fatty acid β-oxidation and ketogenesis [226]. In a phase II study of patients with metastatic prostate cancer, MLN0128, a dual mTOR inhibitor, has been associated with adverse side effects including fatigue, anorexia, and rash [227]. On a more worrying note, a study involving the mTORC1 inhibitor, everolimus on HNSCC patients reported that 30% of the cohort were withdrawn as a result of intolerable toxicity, whereas the rest experienced grade 3 toxicity [228].

In the context of head and neck cancer, mTOR inhibitors have generally been promising as monotherapy. Reduced cell proliferation has been observed following rapamycin in SCC-15 cells [229] and temsirolimusin FaDu and FaDu 9000 cells [230]. Similar reduction in tumour growth of xenografts, derived from HNSCC cell lines, HN21, CAL27, and UM-SCC-11B, have been observed following rapamycin [229] and temsirolimus[230]. everolimus, repressed tumour growth and decreased the number of lymph nodes in mice upon treatment and resulted in overall survival [231]. In the clinic, mTOR inhibitors, rapamycin, everolimus, Temsirolimus, have been used as

monotherapy in advanced or metastatic head and neck cancer. In a phase II clinical trial, 16 patients received rapamycin for 21 days. Despite the short treatment time, rapamycin resulted in significant clinical response, marked by reduction in tumour growth measured clinically by CT (computerized tomography) and FDG-PET (fluorodeoxyglucose (FDG)-positron emission tomography) scans, as well as immunohistochemistry staining for p-S6K1 and p-Akt levels, as a marker for mTOR signalling inhibition [232]. In contrast, the efficacy of everolimus in 9 patients with recurrent/metastatic HNSCC was rather discouraging in that 7 out of the 9 patients had no response to treatment and 2 patients experienced high toxicity and discontinued the treatment. This indicated that everolimus as monotherapy may not be effective in HNSCC [228]. In another study involving a larger cohort of cetuximab-refractory, recurrent and/or metastatic squamous cell carcinoma, temsirolimusreduced tumour size and enhanced progression free survival rate of patients [233]. However, the lack of predictive parameter for treatment success with these inhibitors highlight the need for precise molecular analyses for future studies. The reasons for such disparate response to the different rapalogs are not clear. Moreover, rapalogs cause cancer stabilization but not tumour regression, demonstrating that they are cytostatic. As a result, rapalogs are unlikely to cure cancer, despite the fact that some clinical trials are still studying their anticancer efficacy [234].

Combining mTOR inhibitors with radiation, chemotherapeutic agents, or other targeted therapeutic agents has been shown in some studies to result in synergistic suppression of head and neck cancer. In mice with FaDu- and SCC40-derived xenografts, a combination of temsirolimusand radiation resulted in augmented inhibiton in tumour size in comparison to radiation alone [235]. A combination of temsirolimuswith paclitaxel, and carboplatin in patients with recurrent/metastatic

HNSCC revealed a partial response from the 18 patients enrolled in the study, as several patients experienced high toxicity (anaemia, leukopenia, thrombocytopenia, and hyperglycaemia). As a result, a second phase of this study is ongoing using a lower dose of temsirolimus[236].

In clinical trials for HNSCC, the use of mTOR inhibitors has emerged as a novel treatment choice. However, there is not enough clinical trials to validate the direct function of these agents in HNSCC tumour response or survival, since no prospective, randomized Phase III trials have been reported to date (Table 6.1). Furthermore, most of these trials revealed that mTOR inhibition often accompanies moderate to severe skin, kidney and haematological side effects. This usually requires dose reduction, which in turn affects the treatment efficacy. Finally, the expression levels of mTOR varies greatly in cancers and blocking its activity is rather challenging. All these reasons, taken together, could explain why mTOR inhibitors are not effective as monotherapy in treatment of cancer [234].

Treatment	Phase	Condition	Trial ID	Status
everolimus + Cisplatin +RT	I	IHNSCC	NCT01057277	Terminated
everolimus + Carboplatin + Paclitaxel	I/II	IHNSCC	NCT01333085	Completed
everolimus + previous RT	I	HNSCC	NCT03578432	Recruiting
everolimus + Erlotinib	II	RHNSCC	NCT00942734	Completed
everolimus + Docetaxel + Cisplatin	I	LAHNSCC	NCT00935961	Completed
Temsirolimus + Cetuximab	II	RMHNSC	NCT01256385	Completed
Temsirolimus + Cisplatin + Cetuximab	I/II	RMHNSC	NCT01015664	Terminated

Table 6.1: mTOR inhibitors in HNSCC trials as monotherapy or in combination with other conventional therapies. INHNSCC stands for inoperable HNSCC; RHNSCC - recurrent HNSCC; LAHNSCC - locally advanced HNSCC; RMHNSCC - recurrent or metastatic HNSCC.

6.2 Factors contributing to inconsistent success rates of mTOR inhibitors in combination therapy

Solid tumours arise as a result of genetic aberration that causes alteration in their metabolic signalling pathways. Targeting theses pathways utilising a single therapeutic agent does not provide a sustainable effect towards tumours. Therefore, the use of two or more selective agents in combination, to block or substantially delay signal traffic down these pathways, will result in optimal and long-term clinical gain. In breast cancer, PARP inhibitor Olaparib, when combined with everolimus in BRCA2-mutated patient-derived xenografts showed tumour regression [237]. Another study revealed that inhibition of PI3K/mTOR pathway can sensitise endometrial cancer cells to Olaparib [238]. These studies suggest the possibility of combining mTOR inhibitors with PARP inhibitor for a targeted therapeutic strategy for cancer patients. However, a similar effect was not seen in this thesis as combination of Olaparib and Torin-1 did not sensitise the cells to IR (Figure 4.2.3). One possibility to explain the lack of efficacy could be due to the HPV negative status of the cells used in this thesis. It is known that HPV positive HNSCC tend to activate mTOR signalling pathway through increased mitochondrial respiration, whereas HPV negative HNSCC demonstrate high glucose metabolism, evident by high oxygen consumption and lactate production [239]. HPV negative HNSCC exhibit radio resistance and increased growth and survival in comparison to HPV positive cells, as HPV positive have high expression levels of pyruvate dehydrogenase, which inhibits pyruvate entry into the mitochondria to elicit TCA cycle. This can lead to higher sensitivity towards IR [239]. Another mechanism that explains the high radio sensitivity of HPV positive cells is IR promote cell death by the accumulation of double strand break (DSBs) within DNA and HPV positive cells lack the ability for DNA repair due to an increase expression

level of p16 which impair the recruitment of RAD51, an enzyme that aid in DNA DSBs repair, to the site of DNA damage by downregulation of cyclin D1 expression [240]. Taken together, the combination of Olaparib and Torin-1 could be more promising in sensitising the HPV positive HNSCC cells to IR.

Tumour cells evade apoptosis in a highly orchestrated mechanism that involves changes in the expression levels of distinct BCL-2 family of proteins [84]. Targeting these proteins to enhance apoptosis in cancer cells is an attractive therapeutic approach. For this reason, BH3 mimetics that target the anti-apoptotic BCL-2 family of proteins were developed as anti-tumour drugs. One of the challenges associated with BH3 mimetic therapy is the acquired chemoresistance that is brought about by the upregulation of multiple members of the BCL-2 family, thereby altering the dependence of a cancer cell from one protein to another. For instance, in resistant acute lymphoblastic leukemia (ALL), combining mTOR inhibitor, CCI-779, with BCL-2/BCL-X_L inhibitor, ABT-737, enhanced apoptosis of the resistant cells [241]. This was attributed to CCI-779-mediated reduction of MCL-1 expression, which was deemed to be the contributing factor of chemoresistance [241]. Regardless of combination therapies, BH3 mimetics have generally been quite promising in haematological cancers, as these malignancies often depend on a single BCL-2 family member for survival. For instance, CLL depends on BCL-2 for survival, CML on BCL-X_L and AML on MCL-1 [96, 129, 133, 186]. However, unlike haematological malignancies, BH3 mimetics do not offer a promising therapeutic option in solid tumours. The reason for this is attributed to the dependence of solid tumours on multiple BCL-2 proteins. In the case of HNSCC, the cells depend on both BCL-X_L and MCL-1 for survival [169]As a result, in this thesis, a synergic effect could not be seen when individual BH3 mimetics were combined with Torin-1 in the cell lines tested (Figure 4.2.9). On the

other hand, a triple combination of Torin-1, BCL-X_L and MCL-1 inhibitors had a significant effect in comparison to the use of single BH3 mimetics (Figure 4.2.11). This finding is not in agreement with another study that reported that a combination of mTOR inhibitor, either BEZ235 or AZD8055 with ABT-263 (BCL-2 and BCL-X_L antagonist) resulted in significant apoptosis in triple negative breast cancer cells, as well as in a xenograft model, in comparison to utilising each inhibitor alone [242]. Since these cell lines depend on both MCL-1 and BCL-X_L for survival [243], the synergistic effect was attributed to the reduction of MCL-1 expression levels via mTOR inhibition, which in turn resulted in sensitising the cells to ABT-263-induced cell death [242]. Given that rationale, HNSCC cell lines would have been expected to be sensitised to A-1331852-mediated apoptosis, particularly when MCL-1 expression is downregulated via mTOR inhibition. However, a similar effect was not seen in this study. It is likely that the concentration of Torin-1 used in this study was not sufficient to induce a reduction in MCL-1 expression levels. alternatively, Torin-1 could induce a compensatory mechanism enabling the overexpression of other antiapoptotic proteins for survival. It must be noted that mutations in EGFR genes are more common in HNSCC compared to TNBC[244], which correlates with poor overall survival [245]. Whether this contributes to the difference in sensitivity to BEZ235 or AZD8055 with ABT-263 remains to be characterised.

Protein Phosphatase 2A (PP2A) is a serine/threonine phosphatase that is responsible for regulating different signalling pathway such as, KRAS [246], cell cycle progression, p53 stability, as well as DNA damage response [247, 248]. PP2A is a tumour suppressor but can act as an oncogene when downregulated, thus indicating its important role in regulating kinase activity. In pancreatic cancer, PP2A activity generally downregulated, owing to high expression levels of its endogenous inhibitor,

Cancerous inhibitor of protein phosphatase 2A (CIP2A), and correlates with reduced survival rate [249]. In pancreatic cancer, mTOR inhibition as monotherapy has had little success in inducing cell death, and could be attributed to KRAS-mediated enhanced MYC activity, which occurs upstream of PI3K/mTOR pathway [250]. This could be overcome by combining PP2A activators, such as DT1154 and OP449, along with an mTOR inhibitor, INK128, to reduce MYC expression and inhibit PI3K/mTOR pathway [250]. Since HNSCC has been reported to exhibit high expression levels of CIP2A, which also correlated with disease progression [251], it was speculated that a similar combination of PP2A activator and mTOR inhibition could enhance cell death in HNSCC cell lines. However, in this thesis, no such synergy was observed when Torin-1 was combined with PP2A activators, FTY720 and DT-061. Whether such lack of efficacy is due to CIP2A expression levels remains to be seen, as some pancreatic cancer cells that had high CIP2A levels also failed to respond to this proposed combination [252].

As PI3K/Akt/mTOR pathway is altered in cancers, Ras/Raf/MEK/ERK (MAPK) is often activated by changes in upstream signalling molecules, such as tyrosine kinase receptors [253]. Mutations in Ras, observed in 30% of human cancers, can result in constitutively active Ras kinase that leads to the activation of its downstream effectors, thus promoting cancer cell survival and proliferation [254]. An interconnection between PI3K/Akt/mTOR and MAPK have been identified through multiple studies. Ras has been shown to directly bind and activate PI3K, which in turn can activate mTOR [255]. Alternatively, Ras-mediated activation of ERK can phosphorylate TSC1/TSC2 and regulate mTOR activity [256]. This crosstalk pathway is inundated with multiple feedback loops, as mTORC1-mediated S6K1 activation can negatively regulate PI3K (negative feedback), which in turn could prevent Ras

activation [257]. Thus, mTORC1 inhibition can lead to Ras activation and that is dependent on the negative feedback of S6K on PI3K [257] (Figure 6.1).

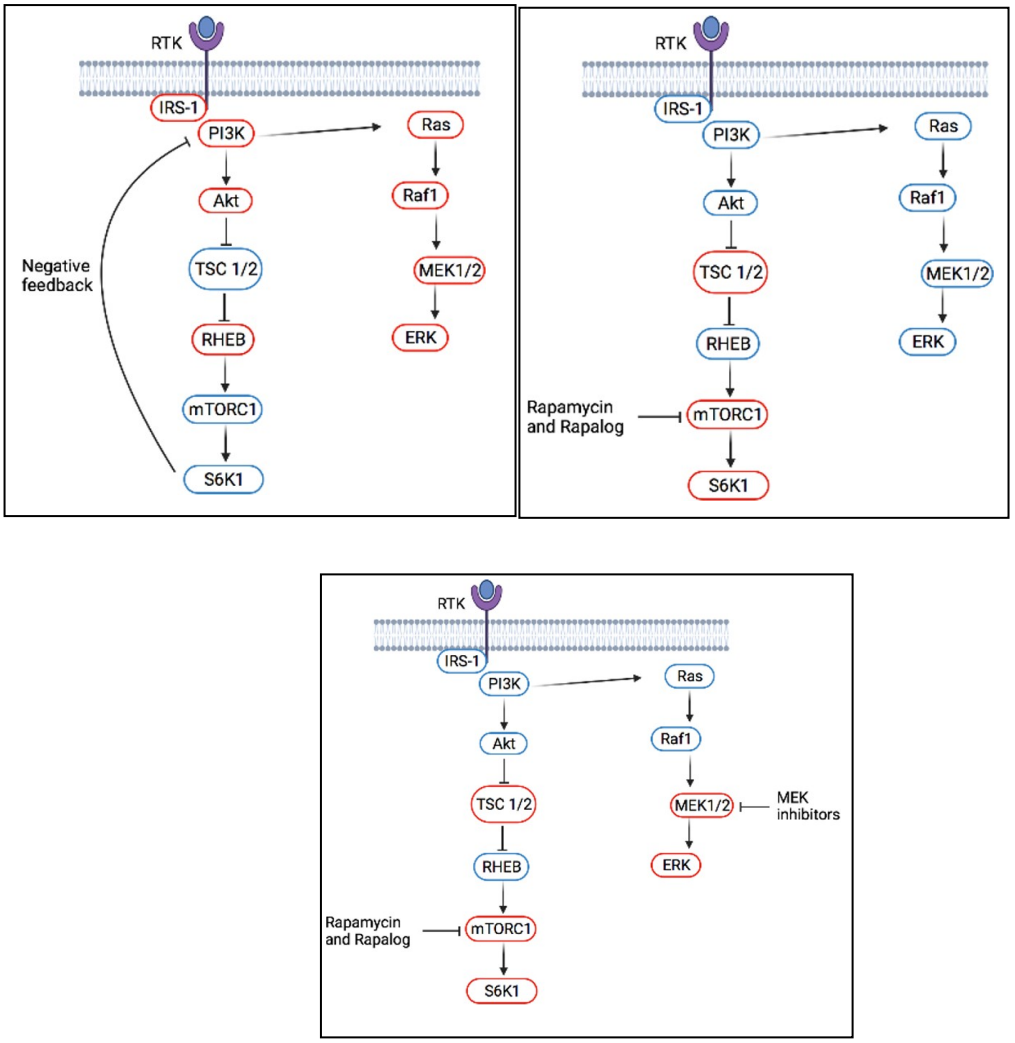

Fig 6.1: Schematic diagram of the mechanisms of action of mTOR and MEK inhibitors. mTOR activation leads to S6K1 activation, which results in inhibiting PI3K, as well as Ras pathway via a negative feedback loop (top left). Upon using mTOR inhibitors, this negative feedback signal is lost and result in activation of PI3K and Ras pathway (top right). Combining both mTOR and MEK inhibitors inhibit cell survival (bottom). Activated proteins are represented by blue outline, whereas inhibited proteins are represented by red outlines.

In cancer cell biology, MEK kinase is one of the most known kinase of Ras/Raf/MEK/ERK cascade. MEK dysregulation is observed in variety of cancers including melanoma, pancreatic, lung, colorectal, ovarian and breast cancers and it plays an important role in cancer cell survival which makes it a potential therapeutic target for cancer therapy [258, 259, 260]. In hepatocellular carcinoma (HCC), both MAPK and mTOR pathway is hyperactivated and an administration of MEK inhibitor, PD901, and mTOR inhibitor, MLN0128, resulted in profound reduction in cellular growth of HCC both *in vivo* and *in vitro* [261]. A similar effect was seen in ovarian cancer cell line when dual PI3K/mTOR inhibitor, PF-04691502, and MEK inhibitor, PD-0325901. The combination resulted in synergistic growth suppression *in vivo* and *in vitro* [262]. Since this combination was effective in cell lines it is reasonable to test if the same effect is feasible in patients. Several clinical trials are underway using a combination of PI3K/mTOR and MEK inhibitors [263]. This combination has not been tried in the context of HNSCC in this thesis, due to time constraints. It would be interesting to assess the relative expression levels of the distinct members of the MAPK pathway, their crosstalk mechanisms in HNSCC and whether targeting MEK and mTOR together would result in synergy.

One of the most essential amino acids in cancer cells metabolism is glutamine. As cancer cells undergo rapid growth and proliferation, they require a source of energy, so they adapt their nutrient metabolism to utilise glutamine. Since the establishment of the importance of glutamine for cancer cell survival, several studies have been conducted to exploit glutamine availability for anti-cancer therapies [264]. Benzylserine and L-γ-glutamyl-p-nitroanilide (GPNA) is an inhibitor of glutamine transporter SLC1A5 that in non-small cell lung carcinoma (NSCLC) showed a decrease in glutamine uptake, cellular growth and induced apoptosis [265]. However, this

effect was not specific to cancer cells and resulted in toxicity to normal cells. Inhibitors of the enzyme GLS, CB-839 and bis-2-(5-phenylacetamido-1,2,4-thiadiazol-2-yl)ethyl sulfide (BPTES) (69-70)[266, 267], supressed tumour growth in a variety of cancers *in vivo* and *in vitro* [179, 268]. In hepatocellular carcinoma, a recent study elucidated that glutamine deficiency when combined with mTOR inhibition results in an adaptive mechanism for survival through autophagy. Increased autophagy flux aids in restoring Akt levels, post-glutamine deficiency and abrogates its proteasomal degradation, which in turn results in cell survival [269]. Although this adaptive mechanism was seen in hepatocellular carcinoma, the specificity of this phenomena is unknown. However, this highlighted an important link between mTOR pathway and glutamine metabolism, which could explain our findings upon using Torin-1 and CB-839.

The interpretations of efficacy or lack of it based on cell line-based assays do not provide an accurate estimation of the therapeutic combinations mentioned in this study. It limits the evaluation of the effect as it lacks the *in vivo* microenvironment present in patient tumour. This could be alleviated only by performing suitable *in vivo* studies. Moreover, clonogenic assay, that forms the major read-out to determine the therapeutic efficacy of drug combinations in this thesis, is an *in vitro* assay that measures the ability of a single cell to divide and form a colony of ~50 cells. Although it is widely used method to assess the effect of a drug/gene on cellular proliferation rate, the measurement is based on the assumption of a linear relationship between the number of cells seeded versus the number of colonies counted. Errors in plating efficiency could vastly compromise the accuracy of this method [270, 271]. Proliferation and viability assays in cell cultures are two distinct techniques used to monitor health and response of cells post treatments. Viability assays are used to measure the number of healthy living cells based on their metabolic activity, for instance MTT

assay, it measures the ability of living cells to metabolise and reduce yellow tetrazole is to purple formazan which can then be measure by spectrophotometer. Another simple inexpensive technique of measuring viable cells is Trypan blue, a dye exclusion test, viable cells will not take up the dye which makes it easy to differentiate between live and dead cells under the microscope. Proliferation assays are used to monitor cellular division and cell number over a period of time. Clonogenic assay can measure the ability of cells to proliferate as it is based on the ability of a single cell to grow and form a colony. A possibility of a better option to study the effectiveness of this drug combination is by using explant culture. Explant culture has more advantages in comparison to 2D culture, as it simulates the environment of tumour within an organ. They can retain the biological signals required for the morphology and homeostasis of the tumour. This would be ideal to assess cell death by monitoring the cleavage of PARP or caspase-3 (apoptotic markers). However, since the combinations used in this study were mainly cytostatic and only caused a proliferation defect with no induction of apoptosis, the proliferation defect could be potentially studied by utilising proliferation markers, such as Ki67 [272]. Another method would be to use 3D organoid models, which can be developed within months. Organoids that resemble tissue including liver, pancreas, thyroid, kidney, lung and retina have been successfully established in vitro [273, 274, 275]. However, despite the advances in making organoids models and the resemblance towards real tumour tissues, they lack vasculature that is essential for nutrient and waste transportation, as well as tissue complexity seen in vivo [275]. A more sophisticated approach to study cancer biology and metabolism is the use of animal model. Animal models are important for pre-clinical research as they give an insight of tumour growth, metastasis, drug response as well as providing the accurate resemblance of tumour microenvironment.

6.3 Avenues to enhance the therapeutic efficacy of mTOR inhibition

In some cancer cell lines, such as neuroblastoma, glioblastoma, and colorectal cancer, a novel form of cell death known as micropinocytosis has been identified [276]. Micropinocytosis is characterized by the formation of macropinosomes vesicles through the fusion of a plasma membrane ruffles or lamellipodia with the plasma membrane and enclosing extracellular fluid [277]. These vesicles are formed by projecting from the plasma membrane and contain no organelle and thus, are distinctive from autophagosomes by containing only a single membrane [277]. These vacuoles can fuse together and rupture causing cell death. Dual inhibition of mTORC1 and mTORC2 using MLN0128, Torin-1, PP242 and OSI-027 causes extensive macropinosomes formation in rhabdomyosarcoma (RMS) cells [277]. rapamycin or mTORC2 knockdown alone have a minimum or reduced effect of micropinocytosis, in comparison to the combination of rapamycin and mTORC2 downregulation [277]. This indicates that mTORC2 is important for macropinosomes formation, and has been shown in both cell line and xenograft models of RMS. This has also been observed in HeLa, MCF7 and CW9019 cells [277], which indicates that this phenomenon occurs in a variety of cancer cell lines. The cell death that occurs as a result of micropinocytosis is distinct from apoptosis (absence of cleaved caspase 3) or autophagy (no induction of LC3B) [277]. Therefore, further exploration of how Torin-1 influences micropinocytosis, and the precise molecular events involved in micropinocytosis could enhance our understanding of how this can be exploited in a therapeutic context.

Mitochondria elongation is mediated through mTOR/4EBP1/MTFP1 axis. mTOR promotes the mRNA translation of MTFP1, the levels of which regulates mitochondrial fission-fusion dynamics. Downregulation of MTFP1 results in

mitochondrial hyperfusion whereas overexpression of MTFP1 results in mitochondrial fragmentation [192]. Hyperfusion is an adaptive mechanism acquired by the cell to evade cell death mediated by mTOR inhibition. MTFP1 regulates fusion/fission processes by modulating DRP-1 phosphorylation downstream of mTOR by mechanisms that are yet to be understood. In theory, MTFP1 levels can be modulated to alter the effects (hyperfusion/ fission or survival/death) of Torin-1 (Figure 6.2).

Doxorubicin is a chemotherapeutic agent that has been used in treatment of variety of cancers [278]. Doxorubicin increases the formation of free radical and oxidative stress within the cell which leads to mitochondrial changes and activation of apoptotic pathway [279]. In cardiomyocytes, exposure to Doxorubicin induced apoptosis and caused mitochondrial fission in a time dependant manner and this effect was accompanied with an increase in MTFP1 expression levels [280]. In theory, MTFP1 levels can be modulated by using Doxorubicin and in combination of Torin-1 and in can have a potential therapeutic outcome for patients.

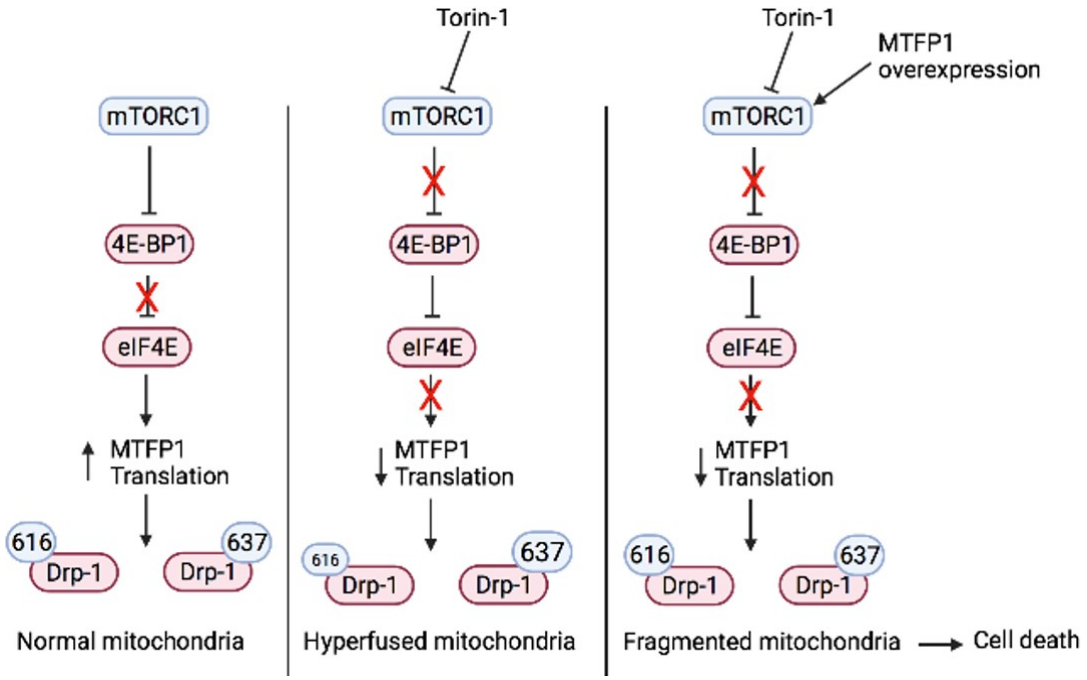

Figure 6.2: Illustration of mTOR inhibition on mitochondrial dynamics. mTOR controls cell fate by regulating the expression level of MTFP1. mTOR regulates mitochondrial fission by promoting the translation of MTFP1. When mTOR is inhibited, MTFP1 expression levels decrease, which leads to mitochondrial hyperfusion coupled with DRP-1 phosphorylation. When mTOR inhibition is combined with overexpression of MTFP1 it will lead to cell death via mitochondrial fragmentation (Adapted from Morita, M., et al 2017).

6.4 Conclusion

The main conclusions from this study are as follows:

- Inhibition of mTORC1 and mTORC2 impaired cellular growth and reduced proliferation in 2D and 3D spheroid culture of HNSCC cell lines.
- Co administration of Torin-1 does not seem to provide a therapeutic advantage over monotherapies in the clonogenic assay of HNSCC cell lines. Further *in vivo* studies will have to be performed to confirm these observations.
- Unlike its cytostatic effect and autophagy induction, Torin-1 differentially regulated apoptosis in a stimulus dependant manner.
- The antiapoptotic property of Torin-1 could be attributed to its role in mitochondrial hyperfusion, changes in phosphorylation levels of Drp-1 as well as MTFP1 expression.

References

1. Sehgal, S., Baker, H. & Vezina, C. rapamycin (AY-22, 989), a new antifungal antibiotic II. Fermentation, isolation and characterization. *The Journal of antibiotics* **28**, 727-732 (1975).

2. Garber, K. rapamycin's resurrection: a new way to target the cancer cell cycle. *Journal of the National Cancer Institute* **93**, 1517-1519 (2001).

3. Jiang, B.-H. & Liu, L.-Z. Role of mTOR in anticancer drug resistance: perspectives for improved drug treatment. *Drug resistance updates* **11**, 63-76 (2008).

4. Sabatini, D.M., Erdjument-Bromage, H., Lui, M., Tempst, P. & Snyder, S.H. RAFT1: a mammalian protein that binds to FKBP12 in a rapamycin-dependent fashion and is homologous to yeast TORs. *Cell* **78**, 35-43 (1994).

5. Brown, E.J. *et al.* A mammalian protein targeted by G1-arresting rapamycin–receptor complex. *Nature* **369**, 756-758 (1994).

6. Sabers, C.J. *et al.* Isolation of a protein target of the FKBP12-rapamycin complex in mammalian cells. *Journal of Biological Chemistry* **270**, 815-822 (1995).

7. Saxton, R.A. & Sabatini, D.M. mTOR signaling in growth, metabolism, and disease. *Cell* **168**, 960-976 (2017).

8. Wullschleger, S., Loewith, R. & Hall, M.N. TOR signaling in growth and metabolism. *Cell* **124**, 471-484 (2006).

9. Yang, H. *et al.* mTOR kinase structure, mechanism and regulation. *Nature* **497**, 217-223 (2013).

10. Yonezawa, K., Tokunaga, C., Oshiro, N. & Yoshino, K.-i. Raptor, a binding partner of target of rapamycin. *Biochemical and biophysical research communications* **313**, 437-441 (2004).

11. Wang, L., Harris, T.E., Roth, R.A. & Lawrence Jr, J.C. PRAS40 regulates mTORC1 kinase activity by functioning as a direct inhibitor of substrate binding. *Journal of Biological Chemistry* **282**, 20036-20044 (2007).

12. Sarbassov, D.D. *et al.* Rictor, a novel binding partner of mTOR, defines a rapamycin-insensitive and raptor-independent pathway that regulates the cytoskeleton. *Current biology* **14**, 1296-1302 (2004).

13. Pearce, L.R. *et al.* Identification of Protor as a novel Rictor-binding component of mTOR complex-2. *Biochemical Journal* **405**, 513-522 (2007).

14. Yang, Q., Inoki, K., Ikenoue, T. & Guan, K.-L. Identification of Sin1 as an essential TORC2 component required for complex formation and kinase activity. *Genes & development* **20**, 2820-2832 (2006).

15. Sabatini, D.M. Twenty-five years of mTOR: Uncovering the link from nutrients to growth. *Proceedings of the National Academy of Sciences* **114**, 11818-11825 (2017).

16. Chao, L.H. & Avruch, J. Cryo-EM insight into the structure of MTOR complex 1 and its interactions with Rheb and substrates. *F1000Research* **8** (2019).

17. Aylett, C.H. *et al.* Architecture of human mTOR complex 1. *Science* **351**, 48-52 (2016).

18. Yang, H. *et al.* Mechanisms of mTORC1 activation by RHEB and inhibition by PRAS40. *Nature* **552**, 368-373 (2017).

19. Peterson, T.R. *et al.* DEPTOR is an mTOR inhibitor frequently overexpressed in multiple myeloma cells and required for their survival. *Cell* **137**, 873-886 (2009).

20. Loewith, R. *et al.* Two TOR complexes, only one of which is rapamycin sensitive, have distinct roles in cell growth control. *Molecular cell* **10**, 457-468 (2002).

21. Sarbassov, D.D. *et al.* Prolonged rapamycin treatment inhibits mTORC2 assembly and Akt/PKB. *Molecular cell* **22**, 159-168 (2006).

22. Schreiber, K.H. *et al.* rapamycin-mediated mTORC 2 inhibition is determined by the relative expression of FK 506-binding proteins. *Aging cell* **14**, 265-273 (2015).

23. Kakumoto, K., Ikeda, J.-i., Okada, M., Morii, E. & Oneyama, C. mLST8 promotes mTOR-mediated tumor progression. *PloS one* **10**, e0119015 (2015).

24. Sarbassov, D.D., Guertin, D.A., Ali, S.M. & Sabatini, D.M. Phosphorylation and regulation of Akt/PKB by the rictor-mTOR complex. *Science* **307**, 1098-1101 (2005).

25. Pópulo, H., Lopes, J.M. & Soares, P. The mTOR signalling pathway in human cancer. *International journal of molecular sciences* **13**, 1886-1918 (2012).

26. Sekulić, A. *et al.* A direct linkage between the phosphoinositide 3-kinase-AKT signaling pathway and the mammalian target of rapamycin in mitogen-stimulated and transformed cells. *Cancer research* **60**, 3504-3513 (2000).

27. Inoki, K., Li, Y., Zhu, T., Wu, J. & Guan, K.-L. TSC2 is phosphorylated and inhibited by Akt and suppresses mTOR signalling. *Nature cell biology* **4**, 648-657 (2002).

28. Inoki, K., Li, Y., Xu, T. & Guan, K.-L. Rheb GTPase is a direct target of TSC2 GAP activity and regulates mTOR signaling. *Genes & development* **17**, 1829-1834 (2003).

29. Gwinn, D.M. *et al.* AMPK phosphorylation of raptor mediates a metabolic checkpoint. *Molecular cell* **30**, 214-226 (2008).

30. Brugarolas, J. *et al.* Regulation of mTOR function in response to hypoxia by REDD1 and the TSC1/TSC2 tumor suppressor complex. *Genes & development* **18**, 2893-2904 (2004).

31. Manning, B.D. Balancing Akt with S6K: implications for both metabolic diseases and tumorigenesis. *The Journal of cell biology* **167**, 399-403 (2004).

32. Kazyken, D. *et al.* AMPK directly activates mTORC2 to promote cell survival during acute energetic stress. *Science signaling* **12** (2019).

33. Mossmann, D., Park, S. & Hall, M.N. mTOR signalling and cellular metabolism are mutual determinants in cancer. *Nature Reviews Cancer* **18**, 744-757 (2018).

34. Magnuson, B., Ekim, B. & Fingar, D.C. Regulation and function of ribosomal protein S6 kinase (S6K) within mTOR signalling networks. *Biochemical Journal* **441**, 1-21 (2012).

35. Crino, P.B. The mTOR signalling cascade: paving new roads to cure neurological disease. *Nature Reviews Neurology* **12**, 379 (2016).

36. Düvel, K. *et al.* Activation of a metabolic gene regulatory network downstream of mTOR complex 1. *Molecular cell* **39**, 171-183 (2010).

37. Peterson, T.R. *et al.* mTOR complex 1 regulates lipin 1 localization to control the SREBP pathway. *Cell* **146**, 408-420 (2011).

38. Glick, D., Barth, S. & Macleod, K.F. Autophagy: cellular and molecular mechanisms. *The Journal of pathology* **221**, 3-12 (2010).

39. Jung CH, et al. ULK-Atg13-FIP200 complexes mediate mTOR signaling to the autophagy machinery. *Molecular biology of the cell **20 (7***): 2009.

40. Liu, M. *et al.* Co-ordinated activation of classical and novel PKC isoforms is required for PMA-induced mTORC1 activation. *PloS one* **12**, e0184818 (2017).

41. Jacinto, E. *et al.* Mammalian TOR complex 2 controls the actin cytoskeleton and is rapamycin insensitive. *Nature cell biology* **6**, 1122-1128 (2004).

42. Gan, X. *et al.* PRR5L degradation promotes mTORC2-mediated PKC-δ phosphorylation and cell migration downstream of Gα 12. *Nature cell biology* **14**, 686-696 (2012).

43. Thomanetz, V. *et al.* Ablation of the mTORC2 component rictor in brain or Purkinje cells affects size and neuron morphology. *Journal of Cell Biology* **201**, 293-308 (2013).

44. Lieberthal, W. & Levine, J.S. Mammalian target of rapamycin and the kidney. I. The signaling pathway. *American Journal of Physiology-Renal Physiology* **303**, F1-F10 (2012).

45. Guertin, D.A. *et al.* mTOR complex 2 is required for the development of prostate cancer induced by Pten loss in mice. *Cancer cell* **15**, 148-159 (2009).

46. García-Martínez, J.M. & Alessi, D.R. mTOR complex 2 (mTORC2) controls hydrophobic motif phosphorylation and activation of serum-and glucocorticoid-induced protein kinase 1 (SGK1). *Biochemical Journal* **416**, 375-385 (2008).

47. Sehgal, S. Sirolimus: its discovery, biological properties, and mechanism of action. Transplantation proceedings; 2003: Elsevier; 2003. p. S7-S14.

48. Xie, J., Wang, X. & Proud, C.G. mTOR inhibitors in cancer therapy. *F1000Research* **5** (2016).

49. Xu, T., Sun, D., Chen, Y. & Ouyang, L. Targeting mTOR for fighting diseases: A revisited review of mTOR inhibitors. *European journal of medicinal chemistry* **199**, 112391 (2020).

50. Zheng, Y. & Jiang, Y. mTOR inhibitors at a glance. *Molecular and cellular pharmacology* **7**, 15 (2015).

51. Kwitkowski, V.E. *et al.* FDA approval summary: temsirolimus as treatment for advanced renal cell carcinoma. *The oncologist* **15**, 428 (2010).

52. Faivre, S., Kroemer, G. & Raymond, E. Current development of mTOR inhibitors as anticancer agents. *Nature reviews Drug discovery* **5**, 671-688 (2006).

53. Witzig, T.E. *et al.* Phase II trial of single-agent temsirolimus (CCI-779) for relapsed mantle cell lymphoma. *Journal of Clinical Oncology* **23**, 5347-5356 (2005).

54. Chan, S. *et al.* Phase II study of temsirolimus (CCI-779), a novel inhibitor of mTOR, in heavily pretreated patients with locally advanced or metastatic breast cancer. *Journal of Clinical Oncology* **23**, 5314-5322 (2005).

55. Hua, H. *et al.* Targeting mTOR for cancer therapy. *Journal of hematology & oncology* **12**, 1-19 (2019).

56. Mita, M.M. *et al.* Phase I trial of the novel mammalian target of rapamycin inhibitor deforolimus (AP23573; MK-8669) administered intravenously daily for 5 days every 2 weeks to patients with advanced malignancies. *Journal of Clinical Oncology* **26**, 361-367 (2008).

57. Hartford, C.M. *et al.* A phase I trial to determine the safety, tolerability, and maximum tolerated dose of deforolimus in patients with advanced malignancies. *Clinical Cancer Research* **15**, 1428-1434 (2009).

58. Hess, G. *et al.* Phase III study to evaluate temsirolimus compared with investigator's choice therapy for the treatment of relapsed or refractory mantle cell lymphoma. *Journal of Clinical Oncology* **27**, 3822-3829 (2009).

59. Hung, C.-M., Garcia-Haro, L., Sparks, C.A. & Guertin, D.A. mTOR-dependent cell survival mechanisms. *Cold Spring Harbor perspectives in biology* **4**, a008771 (2012).

60. Schatz, J.H. Targeting the PI3K/AKT/mTOR pathway in non-Hodgkin's lymphoma: results, biology, and development strategies. *Current oncology reports* **13**, 398 (2011).

61. Neijt, J.P. *et al.* Exploratory phase III study of paclitaxel and cisplatin versus paclitaxel and carboplatin in advanced ovarian cancer. *Journal of Clinical Oncology* **18**, 3084-3092 (2000).

62. Brana, I. *et al.* Recent Developments in Anticancer Agents Targeting PI3K, AKT and mTORC1/2. *Top. Anti-Cancer Res.* **2**, 95-196 (2013).

63. Baumann, P., Mandl-Weber, S., Oduncu, F. & Schmidmaier, R. The novel orally bioavailable inhibitor of phosphoinositol-3-kinase and mammalian target of rapamycin, NVP-BEZ235, inhibits growth and proliferation in multiple myeloma. *Experimental cell research* **315**, 485-497 (2009).

64. Manara, M.C. *et al.* NVP-BEZ235 as a new therapeutic option for sarcomas. *Clinical Cancer Research* **16**, 530-540 (2010).

65. Pallet, N. & Legendre, C. Adverse events associated with mTOR inhibitors. *Expert opinion on drug safety* **12**, 177-186 (2013).

66. Apsel, B. *et al.* Targeted polypharmacology: discovery of dual inhibitors of tyrosine and phosphoinositide kinases. *Nature chemical biology* **4**, 691-699 (2008).

67. Pike, K.G. *et al.* Optimization of potent and selective dual mTORC1 and mTORC2 inhibitors: the discovery of AZD8055 and AZD2014. *Bioorganic & medicinal chemistry letters* **23**, 1212-1216 (2013).

68. Hsieh, A.C. *et al.* The translational landscape of mTOR signalling steers cancer initiation and metastasis. *Nature* **485**, 55-61 (2012).

69. Thoreen, C.C. *et al.* An ATP-competitive mammalian target of rapamycin inhibitor reveals rapamycin-resistant functions of mTORC1. *Journal of Biological Chemistry* **284**, 8023-8032 (2009).

70. Liu, Q. *et al.* Discovery of 1-(4-(4-propionylpiperazin-1-yl)-3-(trifluoromethyl) phenyl)-9-(quinolin-3-yl) benzo [h][1, 6] naphthyridin-2 (1 H)-one as a highly potent, selective mammalian target of rapamycin (mTOR) inhibitor for the treatment of cancer. *Journal of medicinal chemistry* **53**, 7146-7155 (2010).

71. Liu, Q. *et al.* Kinome-wide selectivity profiling of ATP-competitive mammalian target of rapamycin (mTOR) inhibitors and characterization of their binding kinetics. *Journal of Biological Chemistry* **287**, 9742-9752 (2012).

72. Francipane, M.G. & Lagasse, E. Selective targeting of human colon cancer stem-like cells by the mTOR inhibitor Torin-1. *Oncotarget* **4**, 1948 (2013).

73. Atkin, J. *et al.* Torin1-mediated TOR kinase inhibition reduces Wee1 levels and advances mitotic commitment in fission yeast and HeLa cells. *Journal of cell science* **127**, 1346-1356 (2014).

74. Liu, Q. *et al.* Characterization of Torin2, an ATP-competitive inhibitor of mTOR, ATM, and ATR. *Cancer research* **73**, 2574-2586 (2013).

75. Kerr, J.F., Wyllie, A.H. & Currie, A.R. Apoptosis: a basic biological phenomenon with wideranging implications in tissue kinetics. *British journal of cancer* **26**, 239-257 (1972).

76. Saraste, A. & Pulkki, K. Morphologic and biochemical hallmarks of apoptosis. *Cardiovascular research* **45**, 528-537 (2000).

77. Häcker, G. The morphology of apoptosis. *Cell and tissue research* **301**, 5-17 (2000).

78. Varanita, T. *et al.* The OPA1-dependent mitochondrial cristae remodeling pathway controls atrophic, apoptotic, and ischemic tissue damage. *Cell metabolism* **21**, 834-844 (2015).

79. Olichon, A. *et al.* Loss of OPA1 perturbates the mitochondrial inner membrane structure and integrity, leading to cytochrome c release and apoptosis. *Journal of Biological Chemistry* **278**, 7743-7746 (2003).

80. Bratton, S.B. *et al.* Recruitment, activation and retention of caspases-9 and-3 by Apaf-1 apoptosome and associated XIAP complexes. *The EMBO journal* **20**, 998-1009 (2001).

81. Jiang, X. & Wang, X. Cytochrome c promotes caspase-9 activation by inducing nucleotide binding to Apaf-1. *Journal of Biological Chemistry* **275**, 31199-31203 (2000).

82. Sato, T., Irie, S., Krajewski, S. & Reed, J.C. Cloning and sequencing of a cDNA encoding the rat Bcl-2 protein. *Gene* **140**, 291-292 (1994).

83. Letai, A. *et al.* Distinct BH3 domains either sensitize or activate mitochondrial apoptosis, serving as prototype cancer therapeutics. *Cancer cell* **2**, 183-192 (2002).

84. Kale, J., Osterlund, E.J. & Andrews, D.W. BCL-2 family proteins: changing partners in the dance towards death. *Cell Death & Differentiation* **25**, 65-80 (2018).

85. Yip, K. & Reed, J. Bcl-2 family proteins and cancer. *Oncogene* **27**, 6398-6406 (2008).

86. Wang, J.-L. *et al.* Structure-based discovery of an organic compound that binds Bcl-2 protein and induces apoptosis of tumor cells. *Proceedings of the National Academy of Sciences* **97**, 7124-7129 (2000).

87. Schenk, R.L., Strasser, A. & Dewson, G. BCL-2: Long and winding path from discovery to therapeutic target. *Biochemical and biophysical research communications* **482**, 459-469 (2017).

88. Lamers, F. *et al.* Targeted BCL2 inhibition effectively inhibits neuroblastoma tumour growth. *European Journal of Cancer* **48**, 3093-3103 (2012).

89. Zhao, D.-p., Ding, X.-w., Peng, J.-p., Zheng, Y.-x. & Zhang, S.-z. Prognostic significance of bcl-2 and p53 expression in colorectal carcinoma. *Journal of Zhejiang University Science B* **6**, 1163-1169 (2005).

90. Swellam, M., Abd-Elmaksoud, N., Halim, M.H., Khatab, H. & Khiry, H. Incidence of Bcl-2 expression in bladder cancer: relation to schistosomiasis. *Clinical biochemistry* **37**, 798-802 (2004).

91. Jiang, S.X., Sato, Y., Kuwao, S. & Kameya, T. Expression of bcl-2 oncogene protein is prevalent in small cell lung carcinomas. *The Journal of pathology* **177**, 135-138 (1995).

92. Hellemans, P. *et al.* Prognostic value of bcl-2 expression in invasive breast cancer. *British journal of cancer* **72**, 354-360 (1995).

93. l'Adulte, G.d.E.d.L.d. Prognostic significance of bcl-2 protein expression in aggressive non-Hodgkin's lymphoma. *Blood* **87**, 265-272 (1996).

94. Warren, C.F., Wong-Brown, M.W. & Bowden, N.A. BCL-2 family isoforms in apoptosis and cancer. *Cell death & disease* **10**, 1-12 (2019).

95. Levine, B., Sinha, S.C. & Kroemer, G. Bcl-2 family members: dual regulators of apoptosis and autophagy. *Autophagy* **4**, 600-606 (2008).

96. Lucas, C. *et al.* High CIP2A levels correlate with an antiapoptotic phenotype that can be overcome by targeting BCL-X L in chronic myeloid leukemia. *Leukemia* **30**, 1273-1281 (2016).

97. Zhang, K. *et al.* Bcl-xL overexpression and its association with the progress of tongue carcinoma. *International journal of clinical and experimental pathology* **7**, 7360 (2014).

98. Scherr, A.-L. *et al.* Bcl-x L is an oncogenic driver in colorectal cancer. *Cell death & disease* **7**, e2342-e2342 (2016).

99. Castilla, C. *et al.* Bcl-xL is overexpressed in hormone-resistant prostate cancer and promotes survival of LNCaP cells via interaction with proapoptotic Bak. *Endocrinology* **147**, 4960-4967 (2006).

100. Minn, A.J., Boise, L.H. & Thompson, C.B. Bcl-xS antagonizes the protective effects of Bcl-xL. *Journal of Biological Chemistry* **271**, 6306-6312 (1996).

101. Edlich, F. *et al.* Bcl-xL retrotranslocates Bax from the mitochondria into the cytosol. *Cell* **145**, 104-116 (2011).

102. Kozopas, K.M., Yang, T., Buchan, H.L., Zhou, P. & Craig, R.W. MCL1, a gene expressed in programmed myeloid cell differentiation, has sequence similarity to BCL2. *Proceedings of the National Academy of Sciences* **90**, 3516-3520 (1993).

103. Young, A.I. *et al.* MCL-1 inhibition provides a new way to suppress breast cancer metastasis and increase sensitivity to dasatinib. *Breast Cancer Research* **18**, 1-15 (2016).

104. Yin, J. *et al.* Copy-number variation of MCL1 predicts overall survival of non-small-cell lung cancer in a Southern Chinese population. *Cancer medicine* **5**, 2171-2179 (2016).

105. Campbell, K.J. *et al.* MCL-1 is a prognostic indicator and drug target in breast cancer. *Cell death & disease* **9**, 1-14 (2018).

106. Palve, V., Mallick, S., Ghaisas, G., Kannan, S. & Teni, T. Overexpression of Mcl-1L splice variant is associated with poor prognosis and chemoresistance in oral cancers. *PloS one* **9**, e111927 (2014).

107. Wei, D. *et al.* Targeting mcl-1 for radiosensitization of pancreatic cancers. *Translational oncology* **8**, 47-54 (2015).

108. Kaufmann, S.H. *et al.* Elevated expression of the apoptotic regulator Mcl-1 at the time of leukemic relapse. *Blood, The Journal of the American Society of Hematology* **91**, 991-1000 (1998).

109. Yu, X. *et al.* Targeting MCL-1 sensitizes human esophageal squamous cell carcinoma cells to cisplatin-induced apoptosis. *BMC cancer* **17**, 1-13 (2017).

110. Thomas, L.W., Lam, C. & Edwards, S.W. Mcl-1; the molecular regulation of protein function. *FEBS letters* **584**, 2981-2989 (2010).

111. Warr, M.R. *et al.* BH3-ligand regulates access of MCL-1 to its E3 ligase. *FEBS letters* **579**, 5603-5608 (2005).

112. Varadarajan, S. *et al.* Maritoclax and dinaciclib inhibit MCL-1 activity and induce apoptosis in both a MCL-1-dependent and-independent manner. *Oncotarget* **6**, 12668 (2015).

113. Shen, L. *et al.* miR-497 induces apoptosis of breast cancer cells by targeting Bcl-w. *Experimental and therapeutic medicine* **3**, 475-480 (2012).

114. Wilson, J.W. *et al.* Bcl-w expression in colorectal adenocarcinoma. *British journal of cancer* **82**, 178-185 (2000).

115. Adams, C.M., Mitra, R., Gong, J.Z. & Eischen, C.M. Non-Hodgkin and Hodgkin lymphomas select for overexpression of BCLW. *Clinical Cancer Research* **23**, 7119-7129 (2017).

116. Placzek, W. *et al.* A survey of the anti-apoptotic Bcl-2 subfamily expression in cancer types provides a platform to predict the efficacy of Bcl-2 antagonists in cancer therapy. *Cell death & disease* **1**, e40-e40 (2010).

117. Nagy, B. *et al.* Abnormal expression of apoptosis-related genes in haematological malignancies: overexpression of MYC is poor prognostic sign in mantle cell lymphoma. *British journal of haematology* **120**, 434-441 (2003).

118. Antignani, A. & Youle, R.J. How do Bax and Bak lead to permeabilization of the outer mitochondrial membrane? *Current opinion in cell biology* **18**, 685-689 (2006).

119. Ionov, Y., Yamamoto, H., Krajewski, S., Reed, J.C. & Perucho, M. Mutational inactivation of the proapoptotic gene BAX confers selective advantage during tumor clonal evolution. *Proceedings of the National Academy of Sciences* **97**, 10872-10877 (2000).

120. Gavathiotis, E., Reyna, D.E., Davis, M.L., Bird, G.H. & Walensky, L.D. BH3-triggered structural reorganization drives the activation of proapoptotic BAX. *Molecular cell* **40**, 481-492 (2010).

121. Todt, F. *et al.* Differential retrotranslocation of mitochondrial Bax and Bak. *The EMBO journal* **34**, 67-80 (2015).

122. Ferrer, P.E., Frederick, P., Gulbis, J.M., Dewson, G. & Kluck, R.M. Translocation of a Bak C-terminus mutant from cytosol to mitochondria to mediate cytochrome C release: implications for Bak and Bax apoptotic function. *PLoS One* **7**, e31510 (2012).

123. Echeverry, N. *et al.* Intracellular localization of the BCL-2 family member BOK and functional implications. *Cell Death & Differentiation* **20**, 785-799 (2013).

124. Oda, E. *et al.* Noxa, a BH3-only member of the Bcl-2 family and candidate mediator of p53-induced apoptosis. *Science* **288**, 1053-1058 (2000).

125. Certo, M. *et al.* Mitochondria primed by death signals determine cellular addiction to antiapoptotic BCL-2 family members. *Cancer cell* **9**, 351-365 (2006).

126. Kim, H. *et al.* Hierarchical regulation of mitochondrion-dependent apoptosis by BCL-2 subfamilies. *Nature cell biology* **8**, 1348-1358 (2006).

127. Kuwana, T. *et al.* BH3 domains of BH3-only proteins differentially regulate Bax-mediated mitochondrial membrane permeabilization both directly and indirectly. *Molecular cell* **17**, 525-535 (2005).

128. Tse, C. *et al.* ABT-263: a potent and orally bioavailable Bcl-2 family inhibitor. *Cancer research* **68**, 3421-3428 (2008).

129. Souers, A.J. *et al.* ABT-199, a potent and selective BCL-2 inhibitor, achieves antitumor activity while sparing platelets. *Nature medicine* **19**, 202-208 (2013).

130. Lessene, G. *et al.* Structure-guided design of a selective BCL-X L inhibitor. *Nature chemical biology* **9**, 390 (2013).

131. Tao, Z.-F. *et al.* Discovery of a potent and selective BCL-XL inhibitor with in vivo activity. *ACS medicinal chemistry letters* **5**, 1088-1093 (2014).

132. Leverson, J. *et al.* Potent and selective small-molecule MCL-1 inhibitors demonstrate on-target cancer cell killing activity as single agents and in combination with ABT-263 (navitoclax). *Cell death & disease* **6**, e1590-e1590 (2015).

133. Kotschy, A. *et al.* The MCL1 inhibitor S63845 is tolerable and effective in diverse cancer models. *Nature* **538**, 477-482 (2016).

134. Ferlay, J. *et al.* Estimating the global cancer incidence and mortality in 2018: GLOBOCAN sources and methods. *Int J Cancer* **144**, 1941-1953 (2019).

135. Galbiatti, A.L.S. *et al.* Head and neck cancer: causes, prevention and treatment. *Brazilian journal of otorhinolaryngology* **79**, 239-247 (2013).

136. Bose, P., Brockton, N.T. & Dort, J.C. Head and neck cancer: from anatomy to biology. *International journal of cancer* **133**, 2013-2023 (2013).

137. Kobayashi, K. *et al.* A Review of HPV-Related Head and Neck Cancer. *J Clin Med* **7** (2018).

138. Chuang, S.-C. *et al.* Diet and the risk of head and neck cancer: a pooled analysis in the INHANCE consortium. *Cancer Causes & Control* **23**, 69-88 (2012).

139. Gao, W., Li, J.Z., Chan, J.Y., Ho, W.K. & Wong, T.S. mTOR Pathway and mTOR Inhibitors in Head and Neck Cancer. *ISRN Otolaryngol* **2012**, 953089 (2012).

140. Tan, F.H., Bai, Y., Saintigny, P. & Darido, C. mTOR signalling in head and neck cancer: heads up. *Cells* **8**, 333 (2019).

141. Gao, W., Li, J.Z.H., Chan, J.Y.W., Ho, W.K. & Wong, T.-S. mTOR pathway and mTOR inhibitors in head and neck cancer. *International Scholarly Research Notices* **2012** (2012).

142. Pickering, C.R. *et al.* Integrative genomic characterization of oral squamous cell carcinoma identifies frequent somatic drivers. *Cancer discovery* **3**, 770-781 (2013).

143. Network, C.G.A. Comprehensive genomic characterization of head and neck squamous cell carcinomas. *Nature* **517**, 576 (2015).

144. Lui, V.W. *et al.* Frequent mutation of the PI3K pathway in head and neck cancer defines predictive biomarkers. *Cancer discovery* **3**, 761-769 (2013).

145. Stransky, N. *et al.* The mutational landscape of head and neck squamous cell carcinoma. *Science* **333**, 1157-1160 (2011).

146. M Dillon, L. & W Miller, T. Therapeutic targeting of cancers with loss of PTEN function. *Current drug targets* **15**, 65-79 (2014).

147. De Martino, M.C. *et al.* The role of mTOR pathway as target for treatment in adrenocortical cancer. *Endocrine connections* **8**, R144-R156 (2019).

148. Li, N., Li, X., Chen, K., Dong, H. & Kagami, H. Characterization of spontaneous spheroids from oral mucosa-derived cells and their direct comparison with spheroids from skin-derived cells. *Stem cell research & therapy* **10**, 1-15 (2019).

149. Lane, J.D., Yonekawa, T. & Thorburn, A. Autophagy and cell death. *Essays in biochemistry* **55**, 105-117 (2013).

150. Yeh, S.-A. Radiotherapy for head and neck cancer. Seminars in plastic surgery; 2010: Thieme Medical Publishers; 2010. p. 127.

151. Vokes, E.E. *et al.* Concomitant chemoradiotherapy as primary therapy for locoregionally advanced head and neck cancer. *Journal of Clinical Oncology* **18**, 1652-1661 (2000).

152. Cognetti, D.M., Weber, R.S. & Lai, S.Y. Head and neck cancer: an evolving treatment paradigm. *Cancer* **113**, 1911-1932 (2008).

153. Mendenhall, W.M. *et al.* Definitive radiotherapy for tonsillar squamous cell carcinoma. *American journal of clinical oncology* **29**, 290-297 (2006).

154. Seiwert, T.Y., Salama, J.K. & Vokes, E.E. The chemoradiation paradigm in head and neck cancer. *Nature clinical practice Oncology* **4**, 156-171 (2007).

155. Amé, J.C., Spenlehauer, C. & de Murcia, G. The PARP superfamily. *Bioessays* **26**, 882-893 (2004).

156. Morales, J. *et al.* Review of poly (ADP-ribose) polymerase (PARP) mechanisms of action and rationale for targeting in cancer and other diseases. *Critical Reviews™ in Eukaryotic Gene Expression* **24** (2014).

157. Senra, J.M. *et al.* Inhibition of PARP-1 by olaparib (AZD2281) increases the radiosensitivity of a lung tumor xenograft. *Molecular cancer therapeutics* **10**, 1949-1958 (2011).

158. Ang, K.K. *et al.* Randomized phase III trial of concurrent accelerated radiation plus cisplatin with or without cetuximab for stage III to IV head and neck carcinoma: RTOG 0522. *J Clin Oncol* **32**, 2940-2950 (2014).

159. Muzumder, S., Srikantia, N., Udayashankar, A.H., Kainthaje, P.B. & John Sebastian, M.G. Burden of acute toxicities in head-and-neck radiation therapy: A single-institutional experience. *South Asian J Cancer* **8**, 120-123 (2019).

160. Fan, H. *et al.* New approach for the treatment of osteoradionecrosis with pentoxifylline and tocopherol. *Biomater Res* **18**, 13 (2014).

161. Moen, I. & Stuhr, L.E. Hyperbaric oxygen therapy and cancer--a review. *Target Oncol* **7**, 233-242 (2012).

162. Peddi, P. *et al.* Cisplatin, cetuximab, and radiation in locally advanced head and neck squamous cell cancer: a retrospective review. *Clin Med Insights Oncol* **9**, 1-7 (2015).

163. Dasari, S. & Tchounwou, P.B. Cisplatin in cancer therapy: molecular mechanisms of action. *European journal of pharmacology* **740**, 364-378 (2014).

164. Le, X. & Hanna, E.Y. Optimal regimen of cisplatin in squamous cell carcinoma of head and neck yet to be determined. *Annals of translational medicine* **6** (2018).

165. Bernier, J. *et al.* Postoperative irradiation with or without concomitant chemotherapy for locally advanced head and neck cancer. *New England Journal of Medicine* **350**, 1945-1952 (2004).

166. Farrow, B. *et al.* Inhibition of pancreatic cancer cell growth and induction of apoptosis with novel therapies directed against protein kinase A. *Surgery* **134**, 197-205 (2003).

167. Tohmé, R. *et al.* Direct activation of PP2A for the treatment of tyrosine kinase inhibitor–resistant lung adenocarcinoma. *JCI insight* **4** (2019).

168. Durán, R.V. *et al.* Glutaminolysis activates Rag-mTORC1 signaling. *Molecular cell* **47**, 349-358 (2012).

169. Carter, R.J. *et al.* Exploring the potential of BH3 mimetic therapy in squamous cell carcinoma of the head and neck. *Cell death & disease* **10**, 1-10 (2019).

170. Ma, B.B. *et al.* The activity of mTOR inhibitor RAD001 (everolimus) in nasopharyngeal carcinoma and cisplatin-resistant cell lines. *Investigational new drugs* **28**, 413-420 (2010).

171. Pinto-Leite, R. *et al.* everolimus combined with cisplatin has a potential role in treatment of urothelial bladder cancer. *Biomedicine & Pharmacotherapy* **67**, 116-121 (2013).

172. Nutting, C. Radiotherapy in head and neck cancer management: United Kingdom National Multidisciplinary Guidelines. *The Journal of Laryngology & Otology* **130**, S66-S67 (2016).

173. Yang, Y., Huang, Q., Lu, Y., Li, X. & Huang, S. Reactivating PP2A by FTY720 as a novel therapy for AML with C-KIT tyrosine kinase domain mutation. *Journal of cellular biochemistry* **113**, 1314-1322 (2012).

174. Yang, L., Venneti, S. & Nagrath, D. Glutaminolysis: a hallmark of cancer metabolism. *Annual review of biomedical engineering* **19**, 163-194 (2017).

175. Gao, P. *et al.* c-Myc suppression of miR-23a/b enhances mitochondrial glutaminase expression and glutamine metabolism. *Nature* **458**, 762-765 (2009).

176. Van Den Heuvel, A.P.J., Jing, J., Wooster, R.F. & Bachman, K.E. Analysis of glutamine dependency in non-small cell lung cancer: GLS1 splice variant GAC is essential for cancer cell growth. *Cancer biology & therapy* **13**, 1185-1194 (2012).

177. Zhang, J. *et al.* Inhibition of GLS suppresses proliferation and promotes apoptosis in prostate cancer. *Bioscience reports* **39** (2019).

178. Saha, S.K. *et al.* Multiomics analysis reveals that GLS and GLS2 differentially modulate the clinical outcomes of cancer. *Journal of clinical medicine* **8**, 355 (2019).

179. Gross, M.I. *et al.* Antitumor activity of the glutaminase inhibitor CB-839 in triple-negative breast cancer. *Molecular cancer therapeutics* **13**, 890-901 (2014).

180. Chakrabarti, G. *et al.* Targeting glutamine metabolism sensitizes pancreatic cancer to PARP-driven metabolic catastrophe induced by ss-lapachone. *Cancer & metabolism* **3**, 1-12 (2015).

181. Meric-Bernstam, F. *et al.* Phase 1 study of CB-839, a small molecule inhibitor of glutaminase (GLS), alone and in combination with everolimus (E) in patients (pts) with renal cell cancer (RCC). American Society of Clinical Oncology; 2016.

182. Wong, R.S. Apoptosis in cancer: from pathogenesis to treatment. *Journal of Experimental & Clinical Cancer Research* **30**, 1-14 (2011).

183. Leverson, J.D. *et al.* Exploiting selective BCL-2 family inhibitors to dissect cell survival dependencies and define improved strategies for cancer therapy. *Science translational medicine* **7**, 279ra240-279ra240 (2015).

184. Oltersdorf, T. *et al.* An inhibitor of Bcl-2 family proteins induces regression of solid tumours. *Nature* **435**, 677-681 (2005).

185. Moore, V.D.G. *et al.* Chronic lymphocytic leukemia requires BCL2 to sequester prodeath BIM, explaining sensitivity to BCL2 antagonist ABT-737. *The Journal of clinical investigation* **117**, 112-121 (2007).

186. Ishizawa, J. *et al.* Mitochondrial profiling of acute myeloid leukemia in the assessment of response to apoptosis modulating drugs. *PLoS One* **10**, e0138377 (2015).

187. Youle, R.J. & Van Der Bliek, A.M. Mitochondrial fission, fusion, and stress. *Science* **337**, 1062-1065 (2012).

188. Chan, D.C. Fusion and fission: interlinked processes critical for mitochondrial health. *Annual review of genetics* **46**, 265-287 (2012).

189. Ramachandran, R. Mitochondrial dynamics: the dynamin superfamily and execution by collusion. Seminars in cell & developmental biology; 2018: Elsevier; 2018. p. 201-212.

190. Berman, S., Pineda, F.J. & Hardwick, J.M. Mitochondrial fission and fusion dynamics: the long and short of it. *Cell Death & Differentiation* **15**, 1147-1152 (2008).

191. Milani, M. *et al.* DRP-1 functions independently of mitochondrial structural perturbations to facilitate BH3 mimetic-mediated apoptosis. *Cell death discovery* **5**, 1-11 (2019).

192. Morita, M. *et al.* mTOR controls mitochondrial dynamics and cell survival via MTFP1. *Molecular cell* **67**, 922-935. e925 (2017).

193. Milani, M. *et al.* DRP-1 is required for BH3 mimetic-mediated mitochondrial fragmentation and apoptosis. *Cell death & disease* **8**, e2552-e2552 (2018).

194. Christian, S. *et al.* The novel dihydroorotate dehydrogenase (DHODH) inhibitor BAY 2402234 triggers differentiation and is effective in the treatment of myeloid malignancies. *Leukemia* **33**, 2403-2415 (2019).

195. Wu, D. *et al.* Pharmacological inhibition of dihydroorotate dehydrogenase induces apoptosis and differentiation in acute myeloid leukemia cells. *Haematologica* **103**, 1472 (2018).

196. Yedida, G., Milani, M., Cohen, G.M. & Varadarajan, S. Apogossypol-mediated reorganisation of the endoplasmic reticulum antagonises mitochondrial fission and apoptosis. *Cell death & disease* **10**, 1-11 (2019).

197. Xu, K., Liu, P. & Wei, W. mTOR signaling in tumorigenesis. *Biochimica et Biophysica Acta (BBA)-Reviews on Cancer* **1846**, 638-654 (2014).

198. Lionello, M. *et al.* High mTOR expression is associated with a worse oncological outcome in laryngeal carcinoma treated with postoperative radiotherapy: a pilot study. *Journal of oral pathology & medicine* **41**, 136-140 (2012).

199. Ohtsu, A. *et al.* everolimus for previously treated advanced gastric cancer: results of the randomized, double-blind, phase III GRANITE-1 study. *Journal of Clinical Oncology* **31**, 3935 (2013).

200. O'Donnell, A. *et al.* Phase I pharmacokinetic and pharmacodynamic study of the oral mammalian target of rapamycin inhibitor everolimus in patients with advanced solid tumors. *Journal of Clinical Oncology* **26**, 1588-1595 (2008).

201. Armstrong, A.J. *et al.* A phase II trial of temsirolimus in men with castration-resistant metastatic prostate cancer. *Clinical genitourinary cancer* **11**, 397-406 (2013).

202. Moschetta, M., Reale, A., Marasco, C., Vacca, A. & Carratù, M. Therapeutic targeting of the mTOR-signalling pathway in cancer: benefits and limitations. *British journal of pharmacology* **171**, 3801-3813 (2014).

203. McCubrey, J.A. *et al.* Mutations and deregulation of Ras/Raf/MEK/ERK and PI3K/PTEN/Akt/mTOR cascades which alter therapy response. *Oncotarget* **3**, 954 (2012).

204. Hou, W. *et al.* Mutation analysis of key genes in RAS/RAF and PI3K/PTEN pathways in Chinese patients with hepatocellular carcinoma. *Oncology letters* **8**, 1249-1254 (2014).

205. Strimpakos, A.S., Karapanagiotou, E.M., Saif, M.W. & Syrigos, K.N. The role of mTOR in the management of solid tumors: an overview. *Cancer treatment reviews* **35**, 148-159 (2009).

206. Rojo, F. *et al.* 4E-binding protein 1, a cell signaling hallmark in breast cancer that correlates with pathologic grade and prognosis. *Clinical Cancer Research* **13**, 81-89 (2007).

207. Gerlinger, M. *et al.* Intratumor heterogeneity and branched evolution revealed by multiregion sequencing. *N Engl j Med* **366**, 883-892 (2012).

208. Xie, J. & Proud, C.G. Signaling crosstalk between the mTOR complexes. *Translation* **2**, e28174 (2014).

209. Li, J., Kim, S.G. & Blenis, J. rapamycin: one drug, many effects. *Cell metabolism* **19**, 373-379 (2014).

210. De, P., Miskimins, K., Dey, N. & Leyland-Jones, B. Promise of rapalogues versus mTOR kinase inhibitors in subset specific breast cancer: old targets new hope. *Cancer treatment reviews* **39**, 403-412 (2013).

211. Kucejova, B. *et al.* Interplay between pVHL and mTORC1 pathways in clear-cell renal cell carcinoma. *Molecular cancer research* **9**, 1255-1265 (2011).

212. Iyer, G. *et al.* Genome sequencing identifies a basis for everolimus sensitivity. *Science* **338**, 221-221 (2012).

213. Motzer, R.J. *et al.* Lenvatinib, everolimus, and the combination in patients with metastatic renal cell carcinoma: a randomised, phase 2, open-label, multicentre trial. *The lancet oncology* **16**, 1473-1482 (2015).

214. Christopoulos, P. *et al.* everolimus with paclitaxel and carboplatin as first-line treatment for metastatic large-cell neuroendocrine lung carcinoma: a multicenter phase II trial. *Annals of Oncology* **28**, 1898-1902 (2017).

215. Barnes, J.A. *et al.* everolimus in combination with rituximab induces complete responses in heavily pretreated diffuse large B-cell lymphoma. *Haematologica* **98**, 615 (2013).

216. Rathkopf, D.E. *et al.* everolimus combined with gefitinib in patients with metastatic castration-resistant prostate cancer: Phase 1/2 results and signaling pathway implications. *Cancer* **121**, 3853-3861 (2015).

217. Davis, I.D. *et al.* EVERSUN: a phase 2 trial of alternating sunitinib and everolimus as first-line therapy for advanced renal cell carcinoma. *Annals of Oncology* **26**, 1118-1123 (2015).

218. Hai, J. *et al.* Synergy of WEE1 and mTOR inhibition in mutant KRAS-driven lung cancers. *Clinical Cancer Research* **23**, 6993-7005 (2017).

219. Hayman, T.J. *et al.* The ATP-competitive mTOR inhibitor INK128 enhances in vitro and in vivo radiosensitivity of pancreatic carcinoma cells. *Clinical Cancer Research* **20**, 110-119 (2014).

220. Gazi, M., Moharram, S.A., Marhäll, A. & Kazi, J.U. The dual specificity PI3K/mTOR inhibitor PKI-587 displays efficacy against T-cell acute lymphoblastic leukemia (T-ALL). *Cancer letters* **392**, 9-16 (2017).

221. Gökmen-Polar, Y. *et al.* Investigational drug MLN0128, a novel TORC1/2 inhibitor, demonstrates potent oral antitumor activity in human breast cancer xenograft models. *Breast cancer research and treatment* **136**, 673-682 (2012).

222. Chen, D. *et al.* Dual PI3K/mTOR inhibitor BEZ235 as a promising therapeutic strategy against paclitaxel-resistant gastric cancer via targeting PI3K/Akt/mTOR pathway. *Cell death & disease* **9**, 1-11 (2018).

223. Lew, S. & Chamberlain, R.S. Risk of metabolic complications in patients with solid tumors treated with mTOR inhibitors: meta-analysis. *Anticancer research* **36**, 1711-1718 (2016).

224. Johnston, P.B., Pinter-Brown, L.C., Warsi, G., White, K. & Ramchandren, R. Phase 2 study of everolimus for relapsed or refractory classical Hodgkin lymphoma. *Experimental hematology & oncology* **7**, 1-10 (2018).

225. Houde, V.P. *et al.* Chronic rapamycin treatment causes glucose intolerance and hyperlipidemia by upregulating hepatic gluconeogenesis and impairing lipid deposition in adipose tissue. *Diabetes* **59**, 1338-1348 (2010).

226. Yu, Z. *et al.* rapamycin and dietary restriction induce metabolically distinctive changes in mouse liver. *Journals of Gerontology Series A: Biomedical Sciences and Medical Sciences* **70**, 410-420 (2015).

227. Graham, L. *et al.* A phase II study of the dual mTOR inhibitor MLN0128 in patients with metastatic castration resistant prostate cancer. *Investigational new drugs* **36**, 458-467 (2018).

228. Geiger, J.L. *et al.* Phase II trial of everolimus in patients with previously treated recurrent or metastatic head and neck squamous cell carcinoma. *Head & neck* **38**, 1759-1764 (2016).

229. Brown, R.E. *et al.* Morphoproteomic and pharmacoproteomic rationale for mTOR effectors as therapeutic targets in head and neck squamous cell carcinoma. *Annals of Clinical & Laboratory Science* **36**, 273-282 (2006).

230. Nathan, C.-A.O. *et al.* Mammalian target of rapamycin inhibitors as possible adjuvant therapy for microscopic residual disease in head and neck squamous cell cancer. *Cancer research* **67**, 2160-2168 (2007).

231. Patel, V. *et al.* Decreased lymphangiogenesis and lymph node metastasis by mTOR inhibition in head and neck cancer. *Cancer research* **71**, 7103-7112 (2011).

232. Shirai, K. *et al.* A pilot, single arm, prospective trial using neoadjuvant rapamycin prior to definitive therapy in head and neck squamous cell carcinoma. American Society of Clinical Oncology; 2015.

233. Grünwald, V. *et al.* TEMHEAD: a single-arm multicentre phase II study of temsirolimus in platin-and cetuximab refractory recurrent and/or metastatic squamous cell carcinoma of the head and neck (SCCHN) of the German SCCHN Group (AIO). *Annals of Oncology* **26**, 561-567 (2015).

234. Faes, S., Demartines, N. & Dormond, O. Resistance to mTORC1 inhibitors in cancer therapy: from kinase mutations to intratumoral heterogeneity of kinase activity. *Oxidative medicine and cellular longevity* **2017** (2017).

235. Ekshyyan, O. *et al.* Comparison of radiosensitizing effects of the mammalian target of rapamycin inhibitor CCI-779 to cisplatin in experimental models of head and neck squamous cell carcinoma. *Molecular Cancer Therapeutics* **8**, 2255-2265 (2009).

236. Fury, M.G. *et al.* A phase I study of temsirolimus plus carboplatin plus paclitaxel for patients with recurrent or metastatic (R/M) head and neck squamous cell cancer (HNSCC). *Cancer chemotherapy and pharmacology* **70**, 121-128 (2012).

237. El Botty, R. *et al.* Inhibition of mTOR downregulates expression of DNA repair proteins and is highly efficient against BRCA2-mutated breast cancer in combination to PARP inhibition. *Oncotarget* **9**, 29587 (2018).

238. Philip, C.-A. *et al.* Inhibition of PI3K-AKT-mTOR pathway sensitizes endometrial cancer cell lines to PARP inhibitors. *BMC cancer* **17**, 1-11 (2017).

239. Jung, Y.-S. *et al.* HPV-associated differential regulation of tumor metabolism in oropharyngeal head and neck cancer. *Oncotarget* **8**, 51530 (2017).

240. Dok, R. *et al.* p16INK4a impairs homologous recombination–mediated DNA repair in human papillomavirus–positive head and neck tumors. *Cancer research* **74**, 1739-1751 (2014).

241. Iacovelli, S. *et al.* Co-targeting of Bcl-2 and mTOR pathway triggers synergistic apoptosis in BH3 mimetics resistant acute lymphoblastic leukemia. *Oncotarget* **6**, 32089 (2015).

242. Li, H., Liu, L., Chang, H., Zou, Z. & Xing, D. Downregulation of MCL-1 and upregulation of PUMA using mTOR inhibitors enhance antitumor efficacy of BH3 mimetics in triple-negative breast cancer. *Cell death & disease* **9**, 1-15 (2018).

243. Seiller, C. *et al.* Dual targeting of BCL2 and MCL1 rescues myeloma cells resistant to BCL2 and MCL1 inhibitors associated with the formation of BAX/BAK hetero-complexes. *Cell death & disease* **11**, 1-14 (2020).

244. Kim, A., Jang, M.H., Lee, S.J. & Bae, Y.K. Mutations of the epidermal growth factor receptor gene in triple-negative breast cancer. *Journal of breast cancer* **20**, 150 (2017).

245. Kalyankrishna, S. & Grandis, J.R. Epidermal growth factor receptor biology in head and neck cancer. *Journal of clinical oncology* **24**, 2666-2672 (2006).

246. Ruvolo, P.P. The broken "Off" switch in cancer signaling: PP2A as a regulator of tumorigenesis, drug resistance, and immune surveillance. *BBA clinical* **6**, 87-99 (2016).

247. Nolt, J.K., Rice, L.M., Gallo-Ebert, C., Bisher, M.E. & Nickels, J.T. PP2ACdc55 is required for multiple events during meiosis I. *Cell Cycle* **10**, 1420-1434 (2011).

248. Lee, H.-J., Hwang, H.-I. & Jang, Y.-J. Mitotic DNA damage response: Polo-like kinase-1 is dephosphorylated through ATM-Chk1 pathway. *Cell cycle* **9**, 2389-2398 (2010).

249. Xu, P. *et al.* CIP2A down regulation enhances the sensitivity of pancreatic cancer cells to gemcitabine. *Oncotarget* **7**, 14831 (2016).

250. Allen-Petersen, B.L. *et al.* Activation of PP2A and inhibition of mTOR synergistically reduce MYC signaling and decrease tumor growth in pancreatic ductal adenocarcinoma. *Cancer research* **79**, 209-219 (2019).

251. Junttila, M.R. *et al.* CIP2A inhibits PP2A in human malignancies. *Cell* **130**, 51-62 (2007).

252. Farrell, A.S. *et al.* Targeting inhibitors of the tumor suppressor PP2A for the treatment of pancreatic cancer. *Molecular Cancer Research* **12**, 924-939 (2014).

253. Chappell, W.H. *et al.* Ras/Raf/MEK/ERK and PI3K/PTEN/Akt/mTOR inhibitors: rationale and importance to inhibiting these pathways in human health. *Oncotarget* **2**, 135 (2011).

254. Stirewalt, D.L. *et al.* FLT3, RAS, and TP53 mutations in elderly patients with acute myeloid leukemia. *Blood, The Journal of the American Society of Hematology* **97**, 3589-3595 (2001).

255. Gupta, S. *et al.* Binding of ras to phosphoinositide 3-kinase p110α is required for ras-driven tumorigenesis in mice. *Cell* **129**, 957-968 (2007).

256. Ma, L., Chen, Z., Erdjument-Bromage, H., Tempst, P. & Pandolfi, P.P. Phosphorylation and functional inactivation of TSC2 by Erk: implications for tuberous sclerosisand cancer pathogenesis. *Cell* **121**, 179-193 (2005).

257. Carracedo, A. *et al.* Inhibition of mTORC1 leads to MAPK pathway activation through a PI3K-dependent feedback loop in human cancer. *The Journal of clinical investigation* **118**, 3065-3074 (2008).

258. Neuzillet, C. *et al.* MEK in cancer and cancer therapy. *Pharmacology & therapeutics* **141**, 160-171 (2014).

259. Peters, S. & Adjei, A.A. MET: a promising anticancer therapeutic target. *Nature reviews Clinical oncology* **9**, 314-326 (2012).

260. Degirmenci, U., Wang, M. & Hu, J. Targeting aberrant RAS/RAF/MEK/ERK signaling for cancer therapy. *Cells* **9**, 198 (2020).

261. Liu, X. *et al.* Combined treatment with MEK and mTOR inhibitors is effective in in vitro and in vivo models of hepatocellular carcinoma. *Cancers* **11**, 930 (2019).

262. Sheppard, K.E. *et al.* Synergistic inhibition of ovarian cancer cell growth by combining selective PI3K/mTOR and RAS/ERK pathway inhibitors. *European journal of cancer* **49**, 3936-3944 (2013).

263. Saini, K.S. *et al.* Targeting the PI3K/AKT/mTOR and Raf/MEK/ERK pathways in the treatment of breast cancer. *Cancer treatment reviews* **39**, 935-946 (2013).

264. Choi, Y.-K. & Park, K.-G. Targeting glutamine metabolism for cancer treatment. *Biomolecules & therapeutics* **26**, 19 (2018).

265. Hassanein, M. *et al.* Targeting SLC1a5-mediated glutamine dependence in non-small cell lung cancer. *International journal of cancer* **137**, 1587-1597 (2015).

266. Chen, L. & Cui, H. Targeting glutamine induces apoptosis: a cancer therapy approach. *International journal of molecular sciences* **16**, 22830-22855 (2015).

267. Xiang, Y. *et al.* Targeted inhibition of tumor-specific glutaminase diminishes cell-autonomous tumorigenesis. *The Journal of clinical investigation* **125**, 2293-2306 (2015).

268. Jacque, N. *et al.* Targeting glutaminolysis has antileukemic activity in acute myeloid leukemia and synergizes with BCL-2 inhibition. *Blood* **126**, 1346-1356 (2015).

269. Khan, M.W., Layden, B.T. & Chakrabarti, P. Inhibition of mTOR complexes protects cancer cells from glutamine starvation induced cell death by restoring Akt stability. *Biochimica et Biophysica Acta (BBA)-Molecular Basis of Disease* **1864**, 2040-2052 (2018).

270. Brix, N. *et al.* The clonogenic assay: robustness of plating efficiency-based analysis is strongly compromised by cellular cooperation. *Radiation Oncology* **15**, 1-12 (2020).

271. Franken, N.A., Rodermond, H.M., Stap, J., Haveman, J. & Van Bree, C. Clonogenic assay of cells in vitro. *Nature protocols* **1**, 2315-2319 (2006).

272. Whitfield, M.L., George, L.K., Grant, G.D. & Perou, C.M. Common markers of proliferation. *Nature Reviews Cancer* **6**, 99-106 (2006).

273. Huch, M. *et al.* In vitro expansion of single Lgr5+ liver stem cells induced by Wnt-driven regeneration. *Nature* **494**, 247-250 (2013).

274. Antonica, F. *et al.* Generation of functional thyroid from embryonic stem cells. *Nature* **491**, 66-71 (2012).

275. Greggio, C. *et al.* Artificial three-dimensional niches deconstruct pancreas development in vitro. *Development* **140**, 4452-4462 (2013).

276. Maltese, W.A. & Overmeyer, J.H. Non-apoptotic cell death associated with perturbations of macropinocytosis. *Frontiers in physiology* **6**, 38 (2015).

277. Swanson, J.A. & Watts, C. Macropinocytosis. *Trends in cell biology* **5**, 424-428 (1995).

278. Karch, A., Koch, A. & Grünwald, V. A phase II trial comparing pazopanib with doxorubicin as first-line treatment in elderly patients with metastatic or advanced soft tissue sarcoma (EPAZ): study protocol for a randomized controlled trial. *Trials* **17**, 1-8 (2016).

279. Zhang, Y.-W., Shi, J., Li, Y.-J. & Wei, L. Cardiomyocyte death in doxorubicin-induced cardiotoxicity. *Archivum immunologiae et therapiae experimentalis* **57**, 435-445 (2009).

280. Aung, L.H., Li, R., Prabhakar, B.S. & Li, P. Knockdown of Mtfp1 can minimize doxorubicin cardiotoxicity by inhibiting Dnm1l-mediated

mitochondrial fission. *Journal of cellular and molecular medicine* **21**, 3394-3404 (2017).